TECHNICAL REPORT STANDARD TITLE PAGE

1. Report No.	2. Government Accession No.	3. Recipient's Catalog No.

4. Title and Subtitle
LINEAR ELASTIC LAYER THEORY AS A MODEL OF DISPLACEMENTS MEASURED WITHIN AND BENEATH FLEXIBLE PAVEMENT STRUCTURES LOADED BY THE DYNAFLECT

5. Report Date
August, 1974

6. Performing Organization Code

7. Author(s)
Frank H. Scrivner and Chester H. Michalak

8. Performing Organization Report No.
Research Report 123-25

9. Performing Organization Name and Address
Texas Transportation Institute
Texas A&M University
College Station, Texas 77843

10. Work Unit No.

11. Contract or Grant No.
Research Study 1-8-69-123

12. Sponsoring Agency Name and Address
Texas Highway Department
11th and Brazos
Austin, Texas 78701

13. Type of Report and Period Covered
Interim - September, 1971
August, 1974

14. Sponsoring Agency Code

15. Supplementary Notes
Research performed in cooperation with DOT, FHWA
Research Study Title: A System Analysis of Pavement Design and Research Implementation

16. Abstract

Presented in this report are the results of an investigation of the capability of linear elastic theory to predict measured displacements on the surface, within, and beneath flexible pavement structures. In measuring predictive capability, the yard stick used was replication error.

Sources of data were an NCHRP project, the AASHO Road Test, and the Texas Transportation Institute's Flexible Pavement Test Facility. Only the Texas source, which employed a vibrating surface load (the Dynaflect) and specially designed transducers lowered into small-diameter measurement holes, furnished both horizontal and vertical displacements. These were measured at various depths ranging from zero to 65 inches beneath the pavement surface, and at horizontal distances ranging from 10 to 216 inches.

An analysis of a selected portion of the Texas data, using the theory of elastic layered systems as a model, yielded prediction errors that were reasonably commensurate with replication error.

17. Key Words	18. Distribution Statement
Theory of layered systems. Flexible pavement design. In situ elastic moduli of road materials. Displacement vector field in pavement structures.	

19. Security Classif. (of this report)	20. Security Classif. (of this page)	21. No. of Pages	22. Price
Unclassified	Unclassified	140	

Form DOT F 1700.7 (8-69)

LINEAR ELASTIC LAYER THEORY AS A MODEL OF DISPLACEMENTS MEASURED WITHIN AND BENEATH FLEXIBLE PAVEMENT STRUCTURES LOADED BY THE DYNAFLECT

by

Frank H. Scrivner
Chester H. Michalak

Research Report No. 123-25

A System Analysis of Pavement Design and Research Implementation

Research Project 1-8-69-123

conducted for

The Texas Highway Department

in cooperation with the
U. S. Department of Transportation
Federal Highway Administration

by the

Highway Design Division
Texas Highway Department

Texas Transportation Institute
Texas A&M University

Center for Highway Research
The University of Texas at Austin

August 1974

DISCLAIMER

The contents of this report reflect the views of the authors who are responsible for the facts and the accuracy of the data presented herein. The contents do not necessarily reflect the official views or policies of the Federal Highway Administration. This report does not constitute a standard, specification, or regulation.

PREFACE

This is the twenty-fifth of a series of reports issued by the staff of Research Study 1-8-69-123, A System Analysis of Pavement Design and Research Implementation, being conducted at the Texas Transportation Institute, the Center for Highway Research at the Univeristy of Texas, and the Texas Highway Department, as part of the cooperative research program with the Texas Highway Department and the Department of Transportation, Federal Highway Administration.

The authors wish to thank the following of their colleagues at the Texas Transportation Institute for their assistance in the preparation of the report: Dr. W. M. Moore, Mr. Gilbert Swift, Mr. Rudell Poehl and Mr. Charles E. Schlieker, for their help in the analysis of the displacement data from the TTI Flexible Pavement Test Facility; Dr. Robert L. Lytton and Dr. Wayne A. Dunlap for advice in the field of soil mechanics; and Dr. Larry J. Ringer for assistance in the field of statistics.

The authors are also grateful to Dr. Paul E. Irick, of the Transportation Research Board, for his advice regarding the AASHO Road Test deflection data used in the report; and to Mr. James L. Brown, of the Texas Highway Department, for his assistance in securing authorization for pursuit of the work.

LIST OF REPORTS

Report No. 123-1, "A Systems Approach Applied to Pavement Design and Research," by W. Ronald Hudson, B. Frank McCullough, F. H. Scrivner, and James L. Brown, describes a long-range comprehensive research program to develop a pavement systems analysis and presents a working systems model for the design of flexible pavements, March 1970.

Report No. 123-2, "A Recommended Texas Highway Department Pavement Design System Users Manual," by James L. Brown, Larry J. Buttler, and Hugo E. Orellana, is a manual of instructions to Texas Highway Department personnel for obtaining and processing data for flexible pavement design system, March 1970.

Report No. 123-3, "Characterization of the Swelling Clay Parameter Used in the Pavement Design System," by Arthur W. Witt, III, and B. Frank McCullough, describes the results of a study of the swelling clays parameter used in pavement design system, August 1970.

Report No. 123-4, "Developing A Pavement Feedback Data System," by R. C. G. Haas, describes the initial planning and development of a pavement feedback data system, February 1971.

Report No. 123-5, "A Systems Analysis of Rigid Pavement Design," by Ramesh K. Kher, W. R. Hudson, and B. F. McCullough, describes the development of a working systems model for the design of rigid pavements, November 1970.

Report No. 123-6, "Calculation of the Elastic Moduli of a Two Layer Pavement System from Measured Surface Deflections," by F. H. Scrivner, C. H. Michalak, and William M. Moore, describes a computer program which will serve as a subsystem of a future Flexible Pavement System founded on linear elastic theory, March 1971.

Report No. 123-6A, "Calculation of the Elastic Moduli of a Two Layer Pavement System from Measured Surface Deflections, Part II," by Frank H. Scrivner, Chester H. Michalak, and William M. Moore, is a supplement to Report No. 123-6 and describes the effect of a change in the specified location of one of the deflection points, December 1971.

Report No. 123-7, "Annual Report on Important 1970-71 Pavement Research Needs," by B. Frank McCullough, James L. Brown, W. Ronald Hudson, and F. H. Scrivner, describes a list of priority research items based on findings from use of the pavement design system, April 1971.

Report No. 123-8, "A Sensitivity Analysis of Flexible Pavement System FPS2," by Ramesh K. Kher, B. Frank McCullough, and W. Ronald Hudson, describes the overall importance of this system, the relative importance of the variables of the system and recommendations for efficient use of the computer program, August 1971.

Report No. 123-9, "Skid Resistance Considerations in the Flexible Pavement Design System," by David C. Steitle and B. Frank McCullough, describes skid resistance consideration in the Flexible Pavement System based on the testing of aggregates in the laboratory to predict field performance and presents a nomograph for the field engineer to use to eliminate aggregates which would not provide adequate skid resistance performance, April 1972.

Report No. 123-10, "Flexible Pavement System - Second Generation, Incorporating Fatigue and Stochastic Concepts," by Surendra Prakash Jain, B. Frank McCullough and W. Ronald Hudson, describes the development of new structural design models for the design of flexible pavement which will replace the empirical relationship used at present in flexible pavement systems to simulate the transformation between the input variables and performance of a pavement, January 1972.

Report No. 123-11, "Flexible Pavement System Computer Program Documentation," by Dale L. Schafer, provides documentation and an easily updated documentation system for the computer program FPS-9, April 1972.

Report No. 123-13, "Benefit Analysis for Pavement Design System," by Frank McFarland, presents a method for relating motorist's costs to the pavement serviceability index and a discussion of several different methods of economic analysis.

Report No. 123-14, "Prediction of Low-Temperature and Thermal-Fatigue Cracking in Flexible Pavements," by Mohamed Y. Shahin and B. Frank McCullough, describes a design system for predicting temperature cracking in asphalt concrete surfaces, August 1972.

Report No. 123-15, "FPS-11 Flexible Pavement System Computer Program Documentation," by Hugo E. Orellana, gives the documentation of the computer program FPS-11, October 1972.

Report No. 123-16, "Fatigue and Stress Analysis Concepts for Modifying the Rigid Pavement Design System," by Piti Yimprasett and B. Frank McCullough, describes the fatigue of concrete and stress analyses of rigid pavement, October 1972.

Report No. 123-17, "The Optimization of a Flexible Pavement System Using Linear Elasticity," by Danny Y. Lu, Chia Shun Shih, and Frank H. Scrivner describes the integration of the current Flexible Pavement System computer program and Shell Oil Company's program BISTRO, for elastic layered systems, with special emphasis on economy of computation and evaluation of structural feasibility of materials, March 1973.

Report No. 123-18, "Probabilistic Design Concepts Applied to Flexible Pavement System Design," by Michael I. Darter and W. Ronald Hudson, describes the development and implementation of the probabilistic design approach and its incorporation into the Texas flexible pavement design system for new construction and asphalt concrete overlay, May 1973.

Report No. 123-19, "The Use of Condition Surveys, Profile Studies, and Maintenance Studies in Relating Pavement Distress to Pavement Performance," by Robert P. Smith and B. Frank McCullough, introduces the area of relating pavement distress to pavement performance, presents work accomplished in this area, and gives recommendations for future research, August 1973.

Report No. 123-20, "Implementation of a Complex Research Development of Flexible Pavement Design System into Texas Highway Department Design Operations," by Larry Butler and Hugo Orellana, describes the step-by-step process used in incorporating the implementation research into the actual working operation.

Report No. 123-21, "Rigid Pavement Design System, Input Guide for Program RPS2 In Use by the Texas Highway Department," by R. Frank Carmichael and B. Frank McCullough, describes the input variables necessary to use the Texas rigid pavement design system program RPS2, January 1974 (subject to approval).

Report No. 123-22, "An Integrated Pavement Design Processor," by Danny Y. Lu, Chia Shun Shih, Frank H. Scrivner, and Robert L. Lytton, provides a comprehensive decision framework with a capacity to drive different pavement design programs at the user's command through interactive queries between the computer and the design engineer.

Report No. 123-23, "Stochastic Study of Design Parameters and Lack-of-Fit of Performance Model in the Texas Flexible Pavement Design System," by Malvin Holsen and W. Ronald Hudson, describes a study of initial serviceability index of flexible pavements and a method for quantifying lack-of-fit of the performance equation.

Report No. 123-24, "The Effect of Varying the Modulus and Thickness of Asphaltic Concrete Surfacing Materials," by Danny Y. Lu and Frank H. Scrivner, investigates the effect on the principal stresses and strains in asphaltic concrete resulting from varying the thickness and modulus of that material when used as the surfacing of a typical flexible pavement.

Report No. 123-25, "Linear Elastic Layer Theory as a Model of Displacements Measured Within and Beneath Flexible Pavement Structures Loaded by the Dynaflect," by Frank H. Scrivner and Chester H. Michalak, compares predictions from linear elasticity with measured values of vertical and horizontal displacements at the surface of flexible pavements, within the pavement structures, within the embankments, and within the foundation material.

ABSTRACT

Presented in this report are the results of an investigation of the capability of linear elastic theory to predict measured displacements on the surface, within, and beneath flexible pavement structures. In measuring predictive capability, the yardstick used was replication error.

Sources of data were an NCHRP project, the AASHO Road Test, and the Texas Transportation Institute's Flexible Pavement Test Facility. Only the Texas source, which employed a vibrating surface load (the Dynaflect) and specially designed transducers lowered into small-diameter measurement holes, furnished both horizontal and vertical displacements. These were measured at various depths ranging from zero to 65 inches beneath the pavement surface, and at horizontal distances ranging from 10 to 216 inches.

An analysis of a selected portion of the Texas data, using the theory of elastic layered systems as a model, yielded prediction errors that were reasonably commensurate with replication error.

Key words: Theory of layered systems. Flexible pavement design. In situ elastic moduli of road materials. Displacement vector field in pavement structures.

SUMMARY

Purpose

The principal purpose of the work described in this report was to investigate the suitability of the theory of linear elastic layered systems for use as a model of dynamic displacements occurring throughout the body of flexible pavement structures as the result of a vibrating load applied to the surface by a Dynaflect.

Loading and Measurements System

The Dynaflect applied an oscillating load varying sinusoidally with time at a frequency of 8 Hz and with a peak-to-peak amplitude of 1000 pounds. The resulting displacements, both horizontal and vertical, were measured at depths ranging from zero to 65 inches, and at horizontal distances from the load ranging from 10 to 216 inches, by means of geophones lowered into 1 3/4 in. diameter holes drilled vertically through the pavement structure, through an embankment, and one foot into the foundation material.

Pavement Test Facility

The pavements tested were a set of 27 statistically designed sections built at Texas A&M University's Research Annex in 1965. Normal Dynaflect surface deflections had been measured in 1966. The vertical and horizontal displacements at surface and subsurface elevations were measured in 1972. Since surface deflections (i.e., vertical displacements at the surface) were measured in both instances, and since only an occasional light vehicle traveled over the sections in the six-year interim, data were available for studying long-term environmental effects on deflections in the absence of traffic.

Environmental Effects

Some discrepancies were discovered between the 1966 and the 1972 deflection data. After considerable study, discrepancies were ascribed to the entrapment of free water in pervious portions of the facility in the years 1966-1971, and the subsequent drainage of the water just prior to the start of the 1972 measurements program.

Also ascribed to the entrapped water was the swelling of a plastic clay embankment included in the facility, and the appearance of longitudinal cracks in sections supported by that embankment.

Side Studies

As a side study in the investigation, published data from other sources (an NCHRP project and the AASHO Road Test) were used to estimate the speed of a 1000-lb. (dead weight) wheel load that would induce the same deflection in a flexible pavement surface as the vibrating 1000-lb. Dynaflect load. The purpose here was to show that Dynaflect loading is clearly related to high-speed traffic loading.

In a second side study, published load-deflection data from the AASHO Road Test were used to establish the degree of linearity of the load-deflection relationship as a test of the hypothesis that the load supporting materials had linear elastic properties. In the analysis use was made of replication error as a practical yard stick for measuring the accuracy required of the linear elastic model.

Analysis of Vertical and Horizontal Displacements

Replication error was used for the same purpose in the analysis of the 1972 displacement data measured at the A&M Pavement Facility. In this analysis it was necessary to find values for the elastic moduli of eight materials that

would satisfy the requirement that the differences between computed and measured displacements were, on the whole, of about the same size as the replication error. Although the time and funds available limited the analysis to a fraction of the data available, it is believed that enough evidence was mustered to support the findings.

Findings

The main report lists a number of findings of which the following are considered the most important.

1. According to an analysis of previously published data the 1000-lb. Dynaflect can be expected to produce a surface deflection of about 45% of the deflection caused by a static load of 1000 lbs., or the same deflection as a dual wheel load of 1000 lbs. dead weight moving at high speed (roughly 50-60 mph).

2. Finding 1 implies that either materials supporting the load possessed visco-elastic properties, or the effect on deflections of the inertia of these materials was greater than has usually been assumed.

3. Results of load-deflection tests made on flexible pavements at the AASHO Road Test a few weeks after construction, but before the first freeze of the winter season, indicated that the load supporting materials behaved, on the average, in a manner in agreement with the assumptions of linear elasticity. Variations from the average behavior were no greater than variations in the behavior of identical designs located in different traffic loops. However, shortly after a severe freeze-thaw cycle, the supporting materials behaved in a manner consistently contrary to the assumptions of linear elasticity.

4. Linear elasticity was found to be an acceptable model for the vertical and horizontal components of the displacement vector measured in 1972 within the body of seven selected sections of the A&M pavement test facility, inasmuch as the combined prediction error in each component was about the same size as

the corresponding combined replication error for the seven sections.

The dynamic in situ moduli determined in the analysis and used in calculating prediction errors are given below in pounds per square inch.

Asphaltic concrete	141,200
Limestone plus cement	469,800
Limestone plus lime	189,300
Limestone	86,000
Sandy gravel	49,200
Sandy clay	31,600
Plastic clay	12,400
Dense clay	47,500

Recommendation

It is recommended that a study be made to determine the feasibility of pre-computing and storing on tape an extensive table of stresses, strains, and displacements for use in accomplishing the double purpose of estimating in situ moduli, and of determining (in FPS) stresses, strains or displacements at critical points in trial designs. Such a table, computed from the theory of linear elastic layered systems, would be costly, but once computed and stored, the values would be available at minimal cost for use by researchers and designers alike.

IMPLEMENTATION STATEMENT

This report presents evidence to show that linear elasticity apparently will, in an environment like that of most of Texas, predict the displacement vector field for flexible pavements with sufficient accuracy to warrant its trial, at an appropriate time, in the Texas Highway Department's Flexible Pavement Design System. How to make that trial is more difficult to define, but it seems fairly clear that one step toward implementation of the theory was made in 1973, with publication of Research Report 123-17, "The Optimization of a Flexible Pavement System Using Linear Elasticity", (12). Another step in this direction, yet to be taken, would be to follow the recommendation, stated in the last chapter herein, to pre-compute and store an extensive table of stresses, strains and displacements for use in accomplishing the double purpose of estimating in situ moduli, and of determining (in FPS) stresses, strains and displacements at critical points in trial designs. A third step toward implementation would be the standardization in Texas of a method for estimating the tensile strength of both water bound and stabilized materials. Finally, if full advantage is to be taken of the theory, the surface curvature index (SCI), would have to be replaced as an indicator of pavement life, by parameters consistent with fatigue theory.

The work involved in fully implementing linear elasticity as a subsystem of FPS may appear formidable, but the authors do not wish to infer that it should not be done.

TABLE OF CONTENTS

LIST OF FIGURES

LIST OF FIGURES (Continued)

LIST OF TABLES

LIST OF TABLES (Continued)

1. INTRODUCTION

General Purpose

The general purpose of the research work described in this report was to investigate, subject to the constraints of available time and funds, the suitability of the theory of linear elastic layered systems for use as a model of dynamic displacements, or particle motions, occurring at points on the surface, within, and beneath a flexible pavement structure as a result of dynamic surface loading.

Sources of Data

Although selected surface deflections measured by the Dynaflect and/or the Benkelman Beam in an NCHRP research project (1) and at the AASHO Road Test (2) will be discussed in Chapters 2 and 3, the source of the vertical and horizontal dynamic displacement data used in the principal analysis reported herein is a recently terminated Texas Transportation Institute project, Study 2-8-69-136, "Design and Evaluation of Flexible Pavements", jointly sponsored by the Texas Highway Department and the Federal Highway Administration (3). A more specific statement of the objective of the research work reported here can be made after a brief review is given of the measurement program followed in the last mentioned project, Study 136 (4).

Measuring Program, Study 136

As a part of the work performed in Study 136 a Dynaflect load oscillating sinusoidally at 8 Hz, with a total peak-to-peak magnitude of 1000 lbs, was applied through two 6.25-sq. in. loaded areas spaced at 20 inches c/c at selected positions on the surfaces of 30-12 ft. x 40 ft. test sections of various designs at the Flexible Pavement Test Facility located at Texas A&M

University's Research Annex (4). The facility, a drawing of which is shown in Figure 1, contains a total of seven types of compacted materials founded on a layer of plastic clay overlying a bed of stiffer clay of unknown thickness. The amplitude of horizontal and vertical harmonic motions of the materials, excited by the oscillating load, were sensed by miniature geophones lowered to pre-selected depths into a small diameter (1 3/4") hole drilled vertically through the pavement structure to depths of 65 inches or more. Two such geophones were required, one sensitive to vertical and the other to horizontal motion.

By lowering into the hole to a selected depth a geophone sensitive to horizontal motion, clamping it to the adjacent material by a specially designed mechanism, and stationing the Dynaflect at selected distances from the hole, horizontal displacements were (in effect) measured in a vertical plane in each section at 117 points on a rectangular grid 9 points deep by 13 points long. Vertical displacements were measured in a similar manner at the same grid points and at 9 additional points (for a total of 126 points) on a vertical line passing midway between the two Dynaflect load wheels. (On this line horizontal displacements excited by the two loads were equal and opposite in direction, with the result that a horizontal displacement could not be measured.) A typical 126-point grid, 9 points deep by 14 points long, is shown in Figure 2.

The measurement procedure followed was essentially equivalent to holding the Dynaflect stationary, and selecting measuring points along a horizontal line that passed through the actual measuring point and paralleled the path actually followed by the Dynaflect.

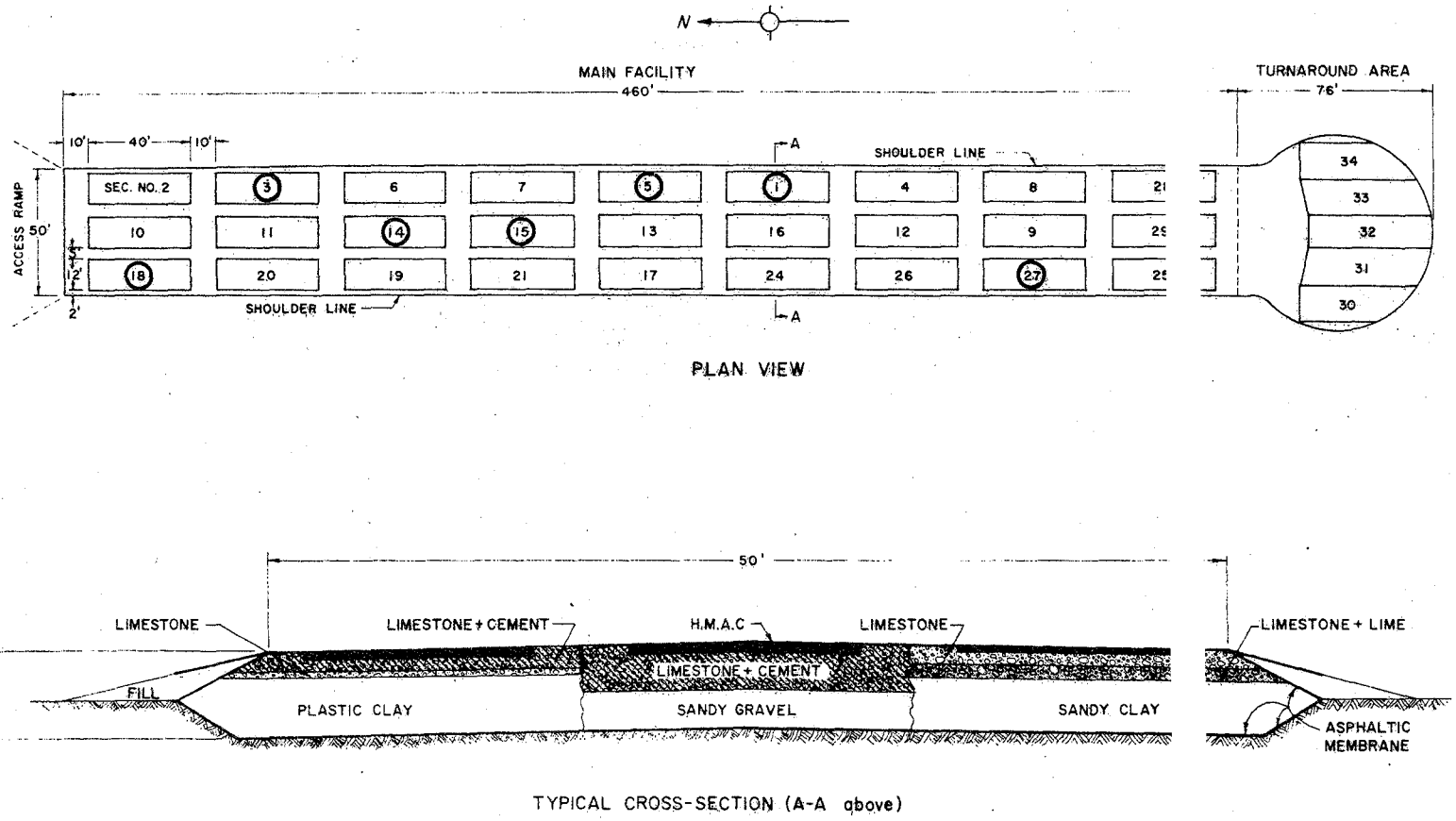

Figure 1: TTI Pavement Test Facility. Selected data from sections with circled numbers were used in testing linear elasticity as a model of measured displacements

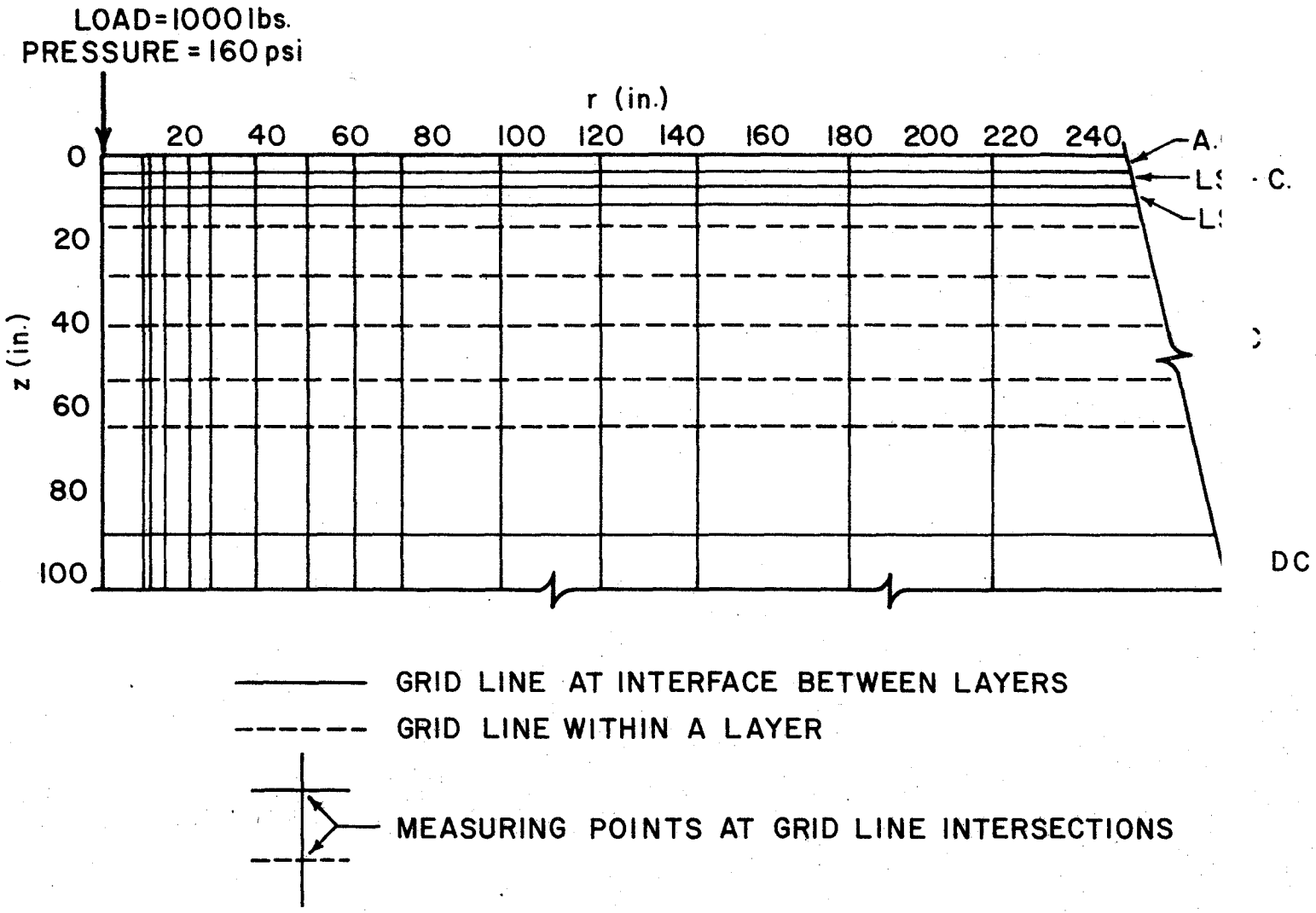

Figure 2: A typical measurement grid 9 points deep by 14 points long. Measurements were taken at interface between layers (except at 90 in. interface), and at points within thicker layers. This grid applies to Section 1. (See Table 14 for material abbreviations.)

The line of travel of the Dynaflect, as it was shifted from one position to the next away from the measurement hole, was parallel to the longitudinal center-line of the test section, so that the 20-inch line connecting the centers of the two loaded areas was perpendicular to--and bisected by--the Dynaflect's line of travel, as shown in Figure 3. The geophones were oriented in the measuring hole so that the measured horizontal component (M_h in Figure 3) of the displacement vector was parallel to the Dynaflect's line of travel, while the measured vertical component was perpendicular to it. Because of this configuration of geophones and load wheels, the Study 136 research team decided to employ the principle of superposition to replace the two 500-lb. loads by a theoretical single 1000-lb. load located at either of the actual application points. Thus, the word "load", when used in connection with Study 136 data, means a 1000-lb. single load (160 psi applied over an area of 6.25 sq. in.), while the term "horizontal (or radial) distance" means the distance labelled r in Figure 3, i.e. the center-to-center slant distance from one of the loaded areas to the measurement hole. Furthermore the term "measured horizontal (or radial) displacement" means the corrected displacement, u, indicated in Figure 3, rather than the displacement actually measured, M_h. The term "vertical displacement", or the symbol w, means the vertical displacement actually measured, since the vertical components due to the two loads were parallel and therefore additive. It is pertinent to the objective of this report to point out that this use of the principle of superposition implies within itself the validity of linear elasticity as a model of the observed displacements.

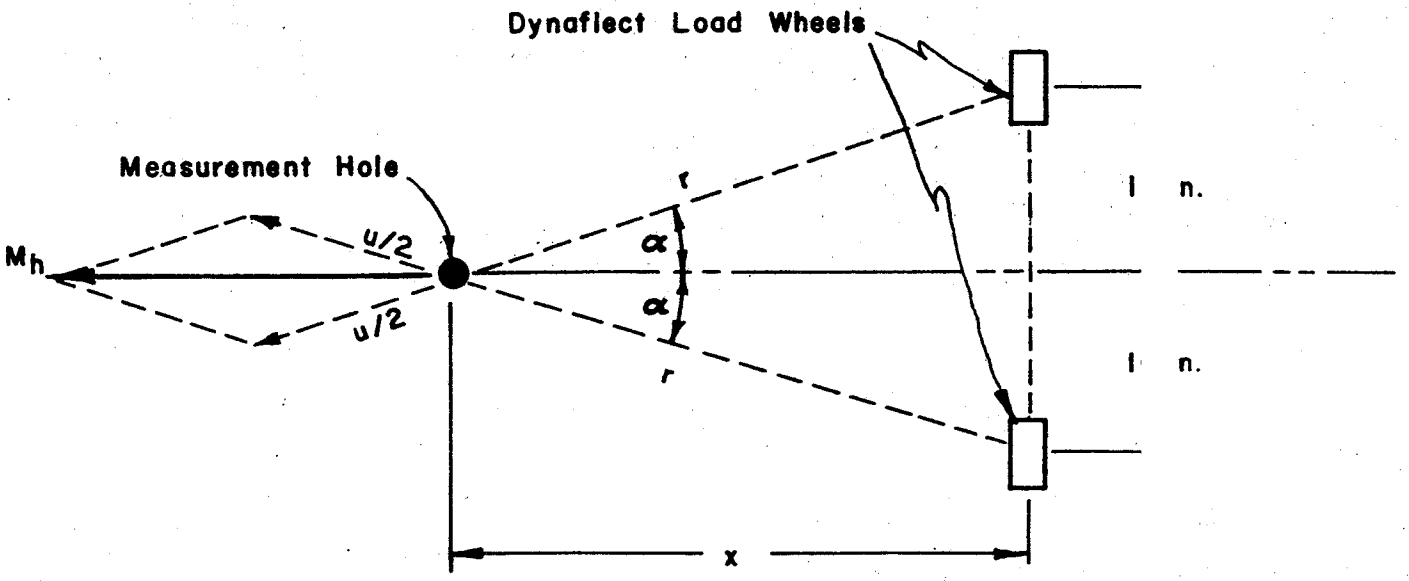

Figure 3: Relation of the measured horizontal displacement, M_h, to the radial displacements, u/2, produced by each Dynaflect wheel. This configuration leads to the equation, $u = M_h \sec \alpha$. (4, pp. 18. 19).

Study 136 Replication Error

One other feature of the Study 136 measurement program needs mentioning, namely, replication of measurements used for evaluating experimental error. In each of the 12-ft. x 40-ft. test sections two measurement holes were drilled, one approximately two feet to the right of center-line near one end of the section, and the other approximately the same distance to the left of center-line near the other end, as indicated in Figure 4. All measurements taken in one hole with the Dynaflect travelling in one direction were repeated in the other hole with the Dynafelct travelling in the other direction. Thus, comparisons could be made between the two sets of measurements and a replication (or experimental) error for each section could be (and was) calculated. The importance of the replication error to the objective of this research is pointed out by Moore and Swift in the following words: "Replication errors observed on a test section reflect not only the variability of the measuring process but also include the effects of variations in the structural properties of the section. The combined variability will define the limiting prediction accuracy for the displacement model being sought. (P. 7 of Reference 4, with emphasis added.)

Specific Objective

With the foregoing serving as background information, it is now possible to state more precisely the original objective of the research effort described in succeeding chapters. The objective, which paraphases statements appearing in the 1973-74 work plan of Study 123, is to provide an answer to the follwoing question:

"Can it be shown that the theory of elastic layered systems is adequate for use as a model of dynamic displacements induced by a Dynaflect and mea-

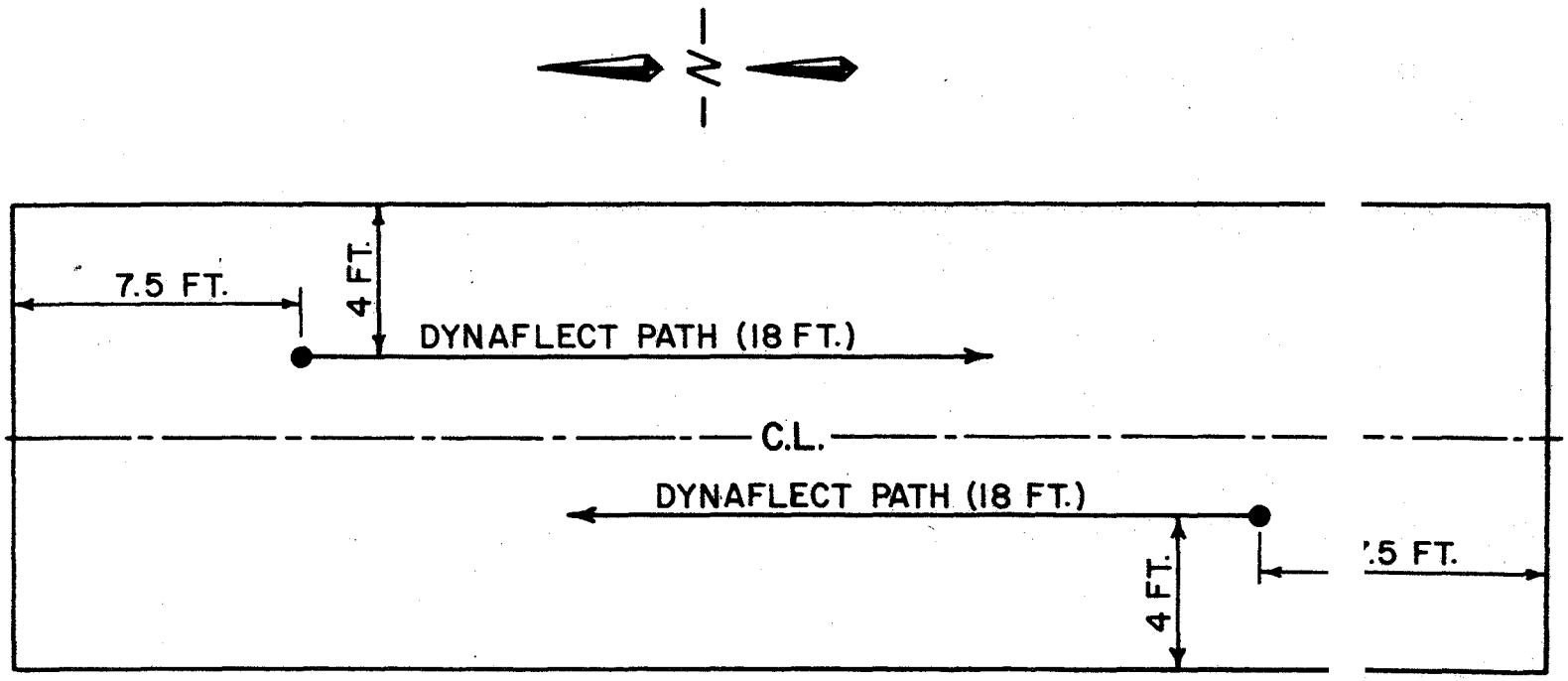

Figure 4: Typical locations of measuring holes for replication. In some cases a different pattern was used due to the presence of holes drilled during the developmental stages of the measurement program.

sured within and beneath the pavements at the TTI Flexible Pavement Test Facility?"

Assuming that it can be extrapolated to Texas highways, the answer to this question could be important to the improvement of the systems approach to the design and management of Texas pavements, a continuing goal of the Texas Highway Department.

The criterion adopted in this report for accepting or rejecting linear elasticity is based primarily on comparisons of prediction error with replication error. In short, the theory is considered acceptable if its prediction error is of approximately the same magnitude as the measured replication error; otherwise, the theory is considered inadequate.

Because of limitations of both time and funds available, only seven of the thirty test sections were analyzed in this study, and only a portion of the voluminous data in these sections were used. It is believed, however, that enough data were analyzed to accomplish the objective. The sections studied are indicated on the plan view of Figure 1 by circles surrounding the section number. Typical grid points at which measured displacements were selected for analysis are shown in Figure 5. By comparing Figure 5 with Figure 2, it can be seen that the amount of data actually analyzed was much less than the total amount of data available in each of the seven sections. The reason for limiting the data has already been stated. One reason for excluding grid points at large horizontal distances from the point of load application was the belief that if some data points must be eliminated, one should retain points where the stresses and strains could be expected to be the highest. Another reason for excluding the more distant points ($r>50$ in.)

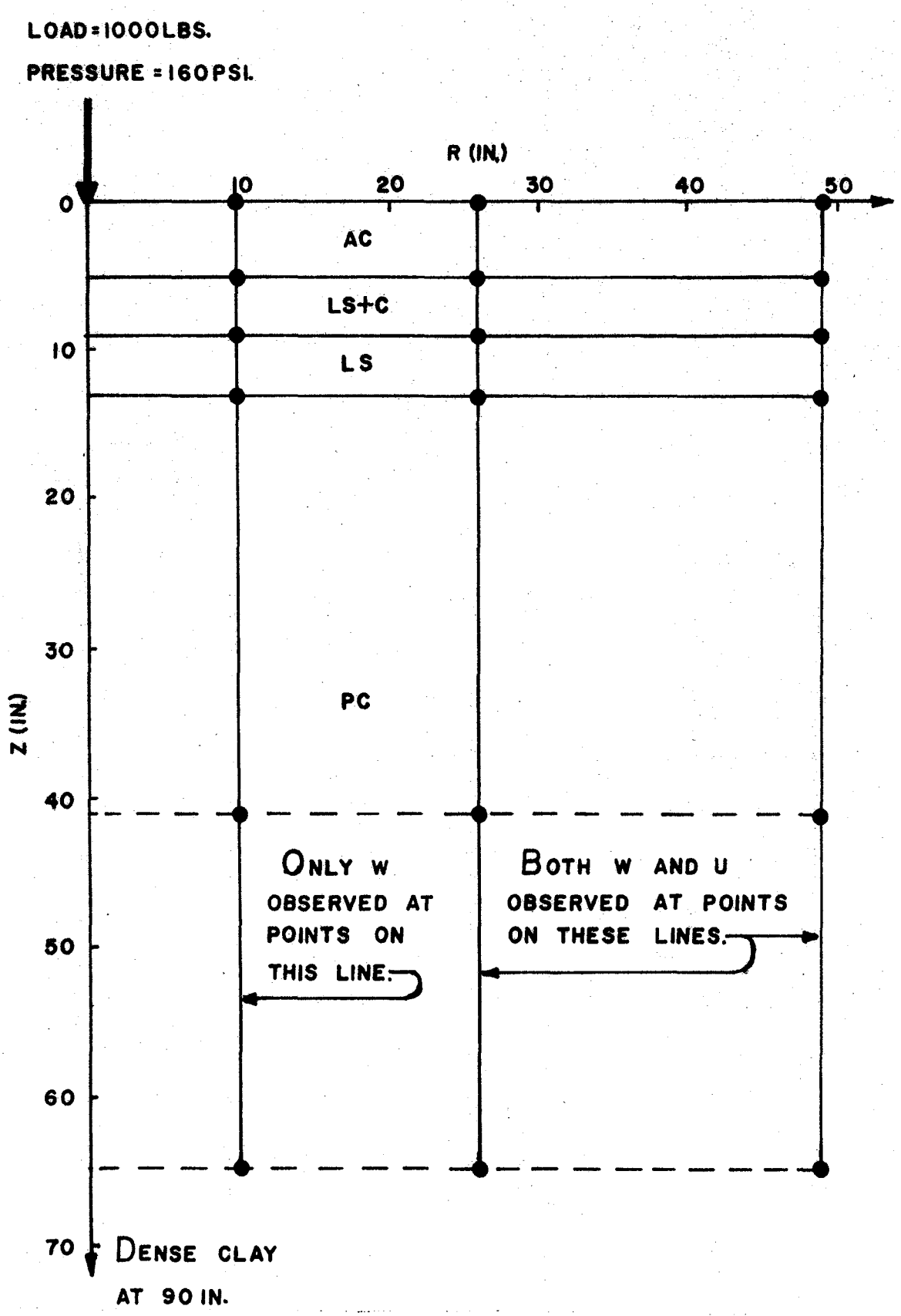

Figure 5: Typical grid points at which measured displacements were selected for analysis. This grid applies to Section 1. Compare with complete grid shown in Figure 2.

was the feeling that the symmetry of the measured data about the z-axis might be destroyed as the Dynaflect moved to positions more distant from the measuring hole than the shortest distance from the hole to an adjacent test section of differing design. The latter distance was about 4 feet.

2. THE PAVEMENT SURFACE DEFLECTION INDUCED BY A DYNAFLECT COMPARED TO THAT PRODUCED BY A STATIC AND A MOVING WHEEL LOAD

Since this report is concerned with the motion of particles within flexible pavements resulting from a loading device (the Dynaflect) that is radically different from the vehicles for which highway pavements are designed, the authors felt constrained to present some evidence from previous research that Dynaflect deflections can be related to surface deflections resulting from "real world" traffic. It is the purpose of this chapter to review briefly a part of such evidence that is readily available from an NCHRP Project Report (1) and an AASHO Road Test Report (2).

Dynaflect Deflections Versus Static Load Deflections

That the answer to the question posed in the objective on page 7 is not merely academic but is actually related to the effect of stationary or slowly moving heavy trucks on highways is borne out by correlation studies made in the field between surface deflections measured between the load wheels of the Dynaflect, and the deflection measured between the dual tires of a 9-kip truck wheel load by means of the Benkelman Beam. One such correlation, displayed in Figure 6, is based upon 240 pairs of observations made on flexible pavements of a variety of designs in Northern Illinois and Minnesota in 1967 as part of an NCHRP project (1). The deflections, measured during a period of deep frost (February), a period of rapid strength

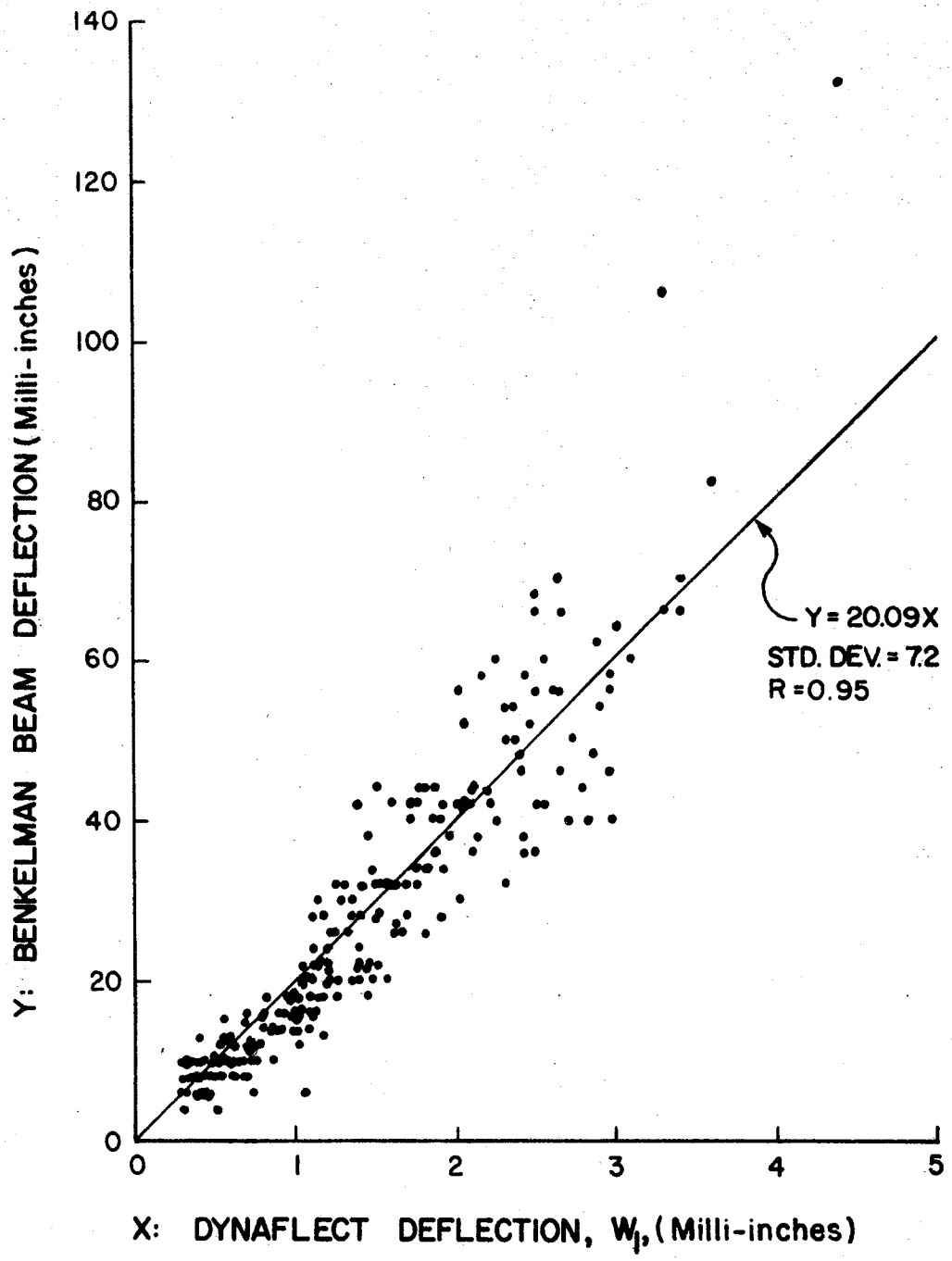

Figure 6: Deflections produced by a 9-kip wheel load and measured by Benkelman Beam, versus Dynaflect deflections. (1, p. 21).

loss (April), and a period of slow strength recovery (August), are believed to be representive of the range of deflections measured on U.S. highway flexible pavements. According to the equation given in Figure 6, an estimate of the surface deflection caused by a 9-kip wheel load (18-kip single axle load) may be obtained by multiplying the corresponding Dynaflect deflection by 20, with a probability of about 2/3 that the error of the estimate will be less than 7/1000 of an inch. While this error may seem large, the squared correlation coefficient was 0.90: i.e., approximately 90% of the variation in the Benkelman Beam deflections could be explained by the Dynaflect Deflections. That two instruments of such widely varying characteristics should correlate this well can be accepted as evidence that both are accomplishing their common purpose - to provide an approximate measurement of the overall stiffness of pavement and subgrade.

Dynaflect Deflections Versus Moving Load Deflections

In the correlation study just described the Dynaflect load was 1-kip, while the truck wheel load was 9-kips: thus, one might expect that the slope of the best-fitting line shown in Figure 6 would be in the neighborhood of 9 instead of 20 even if one makes allowance for the difference in the geometry of the two loads. But since the truck load was essentially static, while the Dynaflect load was vibrating, one is led to the hypothesis that the 1-kip Dynaflect load, applied and released in 1/8 of a second, causes a deflection approximately 9/20, or 45%, of the deflection that a static load of the same magnitude (1-kip) would produce.

Large scale experiments designed to determine the effect of vehicular speed-or rate of load application - on pavement deflections were conducted at the AASHO Road Test near Ottawa, Illinois, in late August, late September

and early December, 1959. Surface deflections, measured electronically, were produced by moving vehicles with single axle loads of 12, 18 and 30 kips (or wheel loads of 6, 9 and 15 kips) travelling at speeds varying from 2 mph to 50 mph on eight flexible pavements of various designs.

The Road Test staff analyzed the data by means of linear regression using the logarithmic form of the following model:

$$d(v) = 10^{A_o + A_1 v} \tag{1}$$

where $d(v)$ = the deflection under the controid of a dual-tired wheel load moving at v mph while A_o and A_1 were contants determined from the regression analysis.

For a static load (v = o), the model reduces to

$$d(o) = 10^{A_o} \tag{2}$$

and the ratio of the deflection produced by a moving wheel load to that caused by the same load at rest is, according to Equations 1 and 2,

$$\frac{d(v)}{d(o)} = 10^{A_1 v} \tag{3}$$

The "speed coefficient", A_1, was negative in all cases, indicating that a reduction in deflection always accompanied a decrease in the time consumed in applying and withdrawing the load. Values of A_1, given in Table 1, were apparently related to load, but to none of the other measured variables (surfacing temperature as well as thickness of surfacing, base and subbase).

As a first approximation let us ignore the apparent decrease of $|A_1|$ in Table 1 that accompanies an increase in load, and accept the average value, $\overline{A_1}$, given at the bottom of the table, as a constant that is independent of load. Then, for any load, we have (from Equation 3) the approximation

TABLE 1: VALUES OF A_1 IN EQUATION 3. DATA FROM AASHO ROAD TEST DEFLECTION-SPEED STUDIES

Surfacing Temperature	Date	Wheel Load	Values of A	
			Loop 4	Loop 6
87°F	Aug. 20, 1959	6	-.0072	-.0070
		9	-.0058	*
		15	*	-.0055
62°F	Sept. 30, 1959	6	-.0070	-.0075
		9	-.0062	*
		15	*	-.0058
40°F	Dec. 2, 1959	6	-.0062	-.0060
		9	-.0058	*
		15	*	-.0058

Average of all values, $\bar{A}_1$ -.0063

Standard deviation .0006

Number of values averaged 12

* No data taken.

$$\frac{d(v)}{d(o)} \approx 10^{-.0063v} \tag{4}$$

From the hypothesis, previously stated, that the vibrating 1-kip Dynaflect load causes a deflection that is 45% of that caused by a 1-kip static load, we have for the Dynaflect

$$\frac{d(v)}{d(o)} = 0.45 \tag{5}$$

where v is taken to mean the speed at which a 1-kip wheel load would have to travel to produce the same deflection as a 1-kip load vibrating at 8 cps.

Remembering that Equation 4 has been assumed to hold for any load, we find from Equations 4 and 5 that

$$0.45 \approx 10^{-.0063v} \tag{6}$$

which, when solved for v yields

$$v \approx 55 \text{ mph} \tag{7}$$

Thus, by a round about way, we have arrived at the conclusion that a 1-kip load applied to, and released from, a small area of a pavement surface in 1/8 of a second, apparently produces approximately the same deflection as a 1-kip wheel load moving at 55 mph.

It is not the intention of the authors to claim much precision in these calculations, not enough data being available to support such a claim, but merely to point out that full scale deflection - speed tests tend to confirm the following inequality observed in the field correlation study, previously mentioned, between Dynaflect and a 9-kip static load deflections:

$$\frac{\text{Dynaflect deflection}}{\text{Static load deflection}} < \frac{\text{Dynaflect load}}{\text{Static load}}$$

or, in round numbers

$$\frac{1}{20} < \frac{1}{9}$$

This type of inequality, apparently arising from differences in the rate of load application, has been ascribed by a growing number of researchers to visco-elastic properties possessed by pavement and subgrade materials. It also is possible that inertial effects on deflections are greater than has usually been assumed.

3. THE QUESTION OF LINEARITY BETWEEN STATIC OR SLOWLY MOVING WHEEL LOADS AND PAVEMENT SURFACE DEFLECTIONS

Stress-Dependent Moduli

The use of linear elastic layered theory in flexible pavement design involves a commitment to the assumption that the material within each horizontal layer, including layers in the underlying subgrade soils, has - at least momentarily - a constant modulus of elasticity, E, and a constant Poissons ratio, μ, at every point in the layer. Of these two constants, the one of greater importance is E. Thus, the results of the analysis of Study 136 data to be described later depends, to a large extent, upon the stability of the value of E, at least for short periods of time. It therefore is appropriate to examine some of the previous research that might throw some light on this question.

The literature on the subject seems to be replete with evidence, mostly from laboratory tests, that the modulus, E, is not constant for the kinds of materials found in road structures and their foundations. For example as early as 1962 Dunlap (5), and as late as 1973 Barker, Brabston and Townsend (6), reported that, in effect, a laboratory specimen of granular material subjected to repetitive loading does not exhibit a constant modulus as required by linear elastic theory: instead, the modulus of such a specimen usually increases when compressive stresses applied to the boundaries of the specimen increase. By mentally extrapolating these results to field conditions one is led to the conclusion that as the distance from a moving wheel load to any selected point within or beneath a flexible pavement structure continuously changes, the modulus of the material immediately surrounding the point also continuously changes. Hence, at a given instant during the passage of a

vehicle along a pavement, the modulus at different points within and beneath the pavement structure apparently would differ, depending upon their distance and direction from the load.

By the same token, it might be inferred that the increment of surface deflection of a pavement resulting from changing a static wheel load from, say, 6 to 9 kips, would be greater than the deflection increment caused by changing the load from 9 to 12 kips, or from 12 to 15 kips, because of the accompanying increases in compressive stresses acting on the materials within and beneath the pavement structure under the load. (The surface deflection spoken of here is intended, as in Chapter 2, to mean the deflection of a point on the surface of the pavement directly beneath the centroid of a dual-tire truck wheel load). Figure 7 compares the kind of load-deflection curve one would expect from the reported laboratory tests (curve A) with the straight line predicted by linear elastic theory (curve B).

That linear elasticity cannot faithfully represent the response of full-scale airfield flexible pavements was concluded by Barker, et. al (6) in the report previously mentioned. Their conclusion was based on some comparisons of measured surface deflections, stresses and strains, with values computed from linear elastic theory. The report also presents some evidence that if the concept of a stress-dependent modulus is taken into account through the use of a finite-element computer program, the behavior of airfield flexible pavements, heavily loaded with a single tire, can be simulated with better accuracy.

In another recent report (1973) of experiments on airfield pavements, Ahlvin, Chou and Hutchinson (7) found that the principle of superposition, denied by the concept of a stress-dependent modulus, held with reasonable

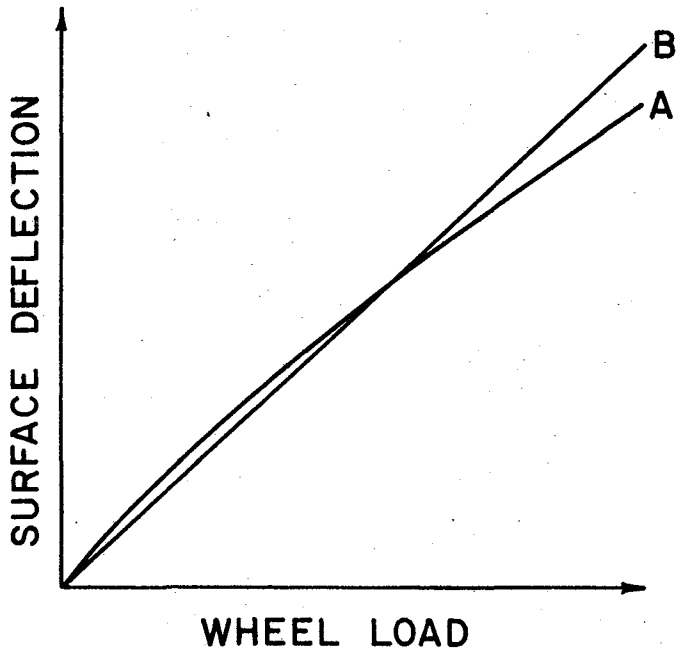

Figure 7: The shape of load-deflection curves as an indicator of the existence of stress-dependent moduli. Curve A apparently indicates stress-dependent moduli. Curve B, a straight line, indicates constant moduli.

accuracy when measured effects produced by separately applied loads were added. "Evidently," the report says, "there is a strong contradiction between prototype field measurements and laboratory findings in material behavior". Nevertheless, according to the same report, surface deflection basins computed from linear elasticity departed radically from the measured basins.

Evidence will be presented in this chapter, based on a report from the AASHO Road Test (2), that while considerable variability in the shape of load-deflection curves exists, the concept of a stress-dependent modulus appears to be supported by load-deflection data gathered shortly after a period during which the pavement and subgrade materials had been subjected to the disruptive action of a severe freeze-thaw cycle. On the other hand, other data from the same source will also be presented, and will tend to show that the same materials that appeared to have a stress-dependent modulus shortly after the spring thaw, were, on the average, behaving as if each had a constant (or nearly constant) modulus in the preceeding fall.

Portions of the AASHO Road Test Facilities Used as Sources of Deflection Data

It will be assumed that the reader is generally familiar with the AASHO Road Test, but a few explanatory remarks are necessary prior to presenting the data treated in this chapter.

Traffic at the Road Test consisted of both single-axle and tandem -axle vehicles, but only single axle trucks will be considered here because only these were used to generate the deflection data to be studied.

The portion of the AASHO Road Test facility considered here consisted of three numbered loops, each of which was a segment of a four-lane divided East-West highway whose parallel roadways were connected by turn-arounds

at each end. The flexible pavement sections considered were 100-ft. segments of the 12-feet wide lanes (designated as Lane 1) of the north tangents of Loops 4, 5 and 6. Each tangent within a loop was 6,800 feet (1.3 miles) in length, and the three loops, arranged in tandem, spanned a total distance of approximately 5 1/2 miles. Of this distance, after excluding the turnarounds, 20,400 feet (approximately 3.9 miles) were flexible pavement tangents.

Only load-deflection data from the "main factorial experiment", designated "Design 1", will be analyzed in this chapter. Within each loop Design 1 consisted of 27 test sections, all differing in thickness design, plus three replicate sections provided for measuring within-loop experimental error. Here we shall pay only passing attention to within-loop replication error, and instead will rely on across-loop error, using data from several designs that were common to all three loops. It is believed that the latter (i.e., differences in the shape of the load-deflection curves of supposedly indentical test sections located in different loops), rather than differences encountered at shorter distances within loops, are not only more appropriate for testing models fitted to data from all three loops, but are also more representative of unexplained differences that would occur in a normal highway project.

The materials used for surfacing, base, subbase, and embankment were, respectively, a hot-mix asphaltic concrete, a crushed limestone, a cohesionless uncrushed gravel, and a clay taken from three borrow pits along the right-of way.

The thicknesses of surfacing, base and subbase were varied between test sections, but the thickness of the embankment was constant for all sections-three feet. Although there was some overlap of designs, the average within-

loop design thickness increased in the same order as the loop numbers, 4, 5 and 6.

Unusually rigid moisture and density controls were excercised in constructing the facility. The achievement of uniformity, rather than unusually high strengths, was the principal goal in construction.

Shape of Load-Deflection Curves in the Fall of 1958 at the AASHO Road Test

On October 8 and again on November 19, 1958, shortly after construction, the AASHO Road Test staff measured, by means of the Benkelman Beam, the surface deflections produced by two different single-axle loads moving at creep speed (about 2 mph) in Lane 1 of Loops 4,5 and 6. Averages of the deflections taken on the two days are given in Appendix C of Reference 2, and are repeated in Tables 2, 3 and 4 herein.

These tables also show, section by section, the values of the quantities a and b appearing in the model

$$d = e^{a}L^{b} \tag{8}$$

where

d = deflection (mils) observed on a section,

e = the base of Napierian logarithms,

L = axle load (kips),

a = a section constant supposedly dependent upon the design of the section and the properties of the materials, including materials in the foundation to an undetermined depth, and

b = a section constant which, for the purposes of this study, is regarded simply as an indicator of the distance and direction of departure of the load-deflection curve from a straight line through the origin. Of the two section constants, only b is of concern here.

TABLE 2: FALL 1958 CREEP SPEED DEFLECTION DATA LOOP 4, LANE 1, AASHO ROAD TEST WITH CONSTANTS COMPUTED FROM DEFLECTIONS AND LOADS

Thickness (inches) of the Materials Indicated	Deflection d(mils) Caused By The Axle Load, L(kips) Indicated		Computed Constants in Model, $d=e^{a}L^{b}$	
AC-LS-GR	12	18	a	b
3-0-4	69	121	.792	1.385
3-0-8	46	72	1.083	1.105
3-0-12	26	47	-.370	1.460
3-3-4	39	62	.823	1.143
3-3-8	29	43	.953	.971
3-3-12	20	30	.511	1.000
3-6-4	46	72	1.083	1.105
3-6-8	32	47	1.110	.948
3-6-12	22	32	.795	.924
4-0-4	39	77	-.505	1.678
4-0-8	23	37	.222	1.173
4-0-12	22	32	.795	.924
4-3-4	32	53	.374	1.244
4-3-8	28	42	.847	1.000
4-3-12	19	31	-.056	1.207
4-6-4	34	57	.360	1.274
4-6-8	25	37	.816	.967
4-6-12	23	31	1.306	.736
5-0-4	45	74	.758	1.227
5-0-8	29	50	.029	1.343
5-0-12	20	32	.115	1.159
5-3-4	25	36	.984	.899
5-3-8	24	34	1.043	.859
5-3-12	24	32	1.415	.710
5-6-4	25	38	.653	1.033
5-6-8	19	33	-.439	1.362
5-6-12	19	30	.145	1.127

Mean Value of b: 1.110
Standard deviation, σ: .222
No. test sections: 27

Note: AC = asphaltic concrete
LS = crushed limestone
GR = uncrushed sandy gravel
d = base of Napierian logarithims
Other symbols as defined in column headings

TABLE 3: FALL 1958 CREEP SPEED DEFLECTION DATA LOOP 5, LANE 1, AASHO ROAD TEST WITH CONSTANTS COMPUTED FROM DEFLECTIONS AND LOADS

Thickness (inches) of the Materials Indicated	Deflections d(mils) Caused By The Axle Load, L(kips), Indicated		Computed Constants in Model, $d=e^{a}L^{b}$	
AC-LS-GR	12	22.4	a	b
3-3-4	47	99	.884	1.194
3-3-8	44	64	2.292	.600
3-3-12	23	35	1.464	.673
3-6-4	44	67	2.110	.674
3-6-8	30	54	1.061	.942
3-6-12	24	33	1.910	.510
3-9-4	40	61	2.009	.676
3-9-8	33	51	1.763	.697
3-9-12	26	42	1.349	.768
4-3-4	65	130	1.415	1.111
4-3-8	24	47	.502	1.077
4-3-12	27	43	1.443	.746
4-6-4	28	44	1.533	.724
4-6-8	29	50	1.199	.873
4-6-12	24	36	1.564	.650
4-9-4	34	57	1.469	.828
4-9-8	28	45	1.443	.760
4-9-12	19	30	1.126	.732
5-3-4	38	63	1.625	.810
5-3-8	28	49	1.104	.897
5-3-12	20	31	1.251	.702
5-6-4	35	66	1.030	1.016
5-6-8	26	48	.817	.982
5-6-12	21	33	1.245	.724
5-9-4	23	41	.834	.926
5-9-8	23	35	1.464	.673
5-9-12	23	35	1.464	.673

Mean Value of b: .801
Standard deviation, σ: .167
No. Test Sections: 27

Note: AC = asphaltic concrete
LS = Crushed limestone
GR = uncrushed sandy gravel
e = base of Napierian logarithims
Other symbols are as defined in column headings

TABLE 4: FALL 1958 CREEP SPEED DEFLECTION DATA LOOP 6, LANE 1, AASHO ROAD TEST WITH CONSTANTS COMPUTED FROM DEFLECTIONS AND LOADS

Thickness (inches) of the Materials Indicated	Deflection d(mils) Caused By The Axle Load, L(kips), Indicated		Computed Constants in Model $d=e^{a}L^{b}$	
AC-LS-GR	12	30	a	b
4-3-8	30	86	.545	1.149
4-3-12	13	33	.039	1.017
4-3-16	16	46	-.091	1.153
4-6-8	18	47	.288	1.047
4-6-12	21	58	.289	1.109
4-6-16	16	37	.499	.915
4-9-8	22	63	.238	1.148
4-9-12	18	57	-.236	1.258
4-9-16	14	40	-.208	1.146
5-3-8	18	58	-.283	1.277
5-3-12	15	42	-.084	1.124
5-3-16	15	41	-.019	1.097
5-6-8	19	55	.062	1.160
5-6-12	11	35	-.741	1.263
5-6-16	15	35	.410	.925
5-9-8	15	44	-.210	1.174
5-9-12	16	39	.356	.972
5-9-16	14	39	-.139	1.118
6-3-8	13	40	-.483	1.227
6-3-12	14	36	.078	1.031
6-3-16	13	36	-.197	1.112
6-6-8	14	50	-.813	1.389
6-6-12	12	38	-.641	1.258
6-6-16	10	30	-.677	1.199
6-9-8	15	47	-.389	1.246
6-9-12	12	35	-.418	1.168
6-9-16	14	35	.154	1.000

Mean Value of b: 1.136
Standard deviation, σ: .113
No. test sections: 27

Note: AC = asphaltic concrete
LS = crushed limestone
GR = uncrushed sandy gravel
e = base of Napierian logarithims
Other symbols as defined in column headings

Values of a and b in Equation 8 were found for each section from the logarithmic form of the model, which can be written as follows:

$$a + b \ln L_j = d_j \quad (j= 1, 2) \tag{9}$$

The two values of L and the two corresponding values of d (given in Table 2, 3 or 4) were substituted in Equation 9 for each section, resulting in two simultaneous equations in two unknowns. These were then solved for the unknowns, a and b.

Figure 8 illustrates how the value of b, referred to hereafter as the "shape factor", influences the shape of the load-deflection curve. Regardless of the value of the constant a, if $b>1$ the slope of the curve increases as the load L increases; if $b=1$, the slope is constant: if $b<1$, the slope decreases as L increases.

The cases of $b=1$ and $b<1$ have already been discussed in the context of stress-dependent moduli (see Figure 7). The authors are not prepared to speculate on the physical inference of $b>1$ beyond saying that this case seems to indicate that a significant thickness of the materials supporting the load loses stiffness as the load is increased.

By scanning the last column of Tables 2,3 and 4, one can observe considerable variation in the shape factor, b, as he glances down the column from one design to the next. At the bottom of the column in each table he will find the mean value of b, and the standard deviation, a measure of within-loop variation of the shape factor.

The same statistics (the mean and standard deviation), together with the range of variation of b within each loop, are shown graphically in Figure 9. Also displayed in this figure are similar statistics when the data from all loops are considered to belong to the same data set.

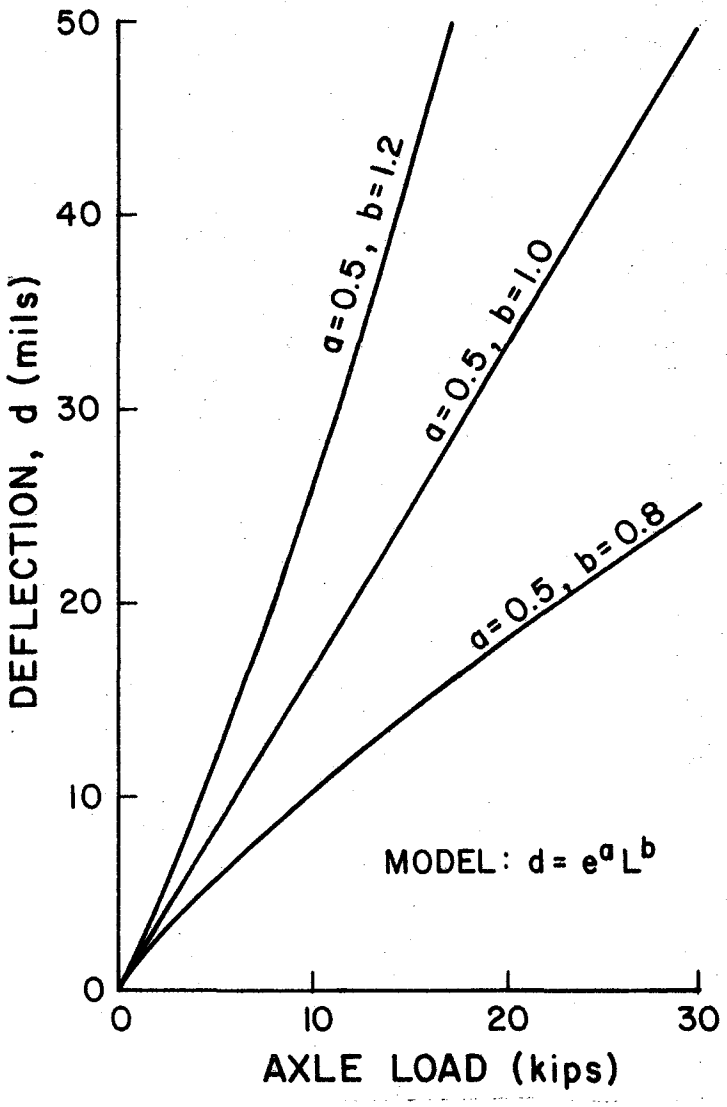

Figure 8: An indication of the influence of the value of b on the shape of load-deflection curves computed from Equation 8.

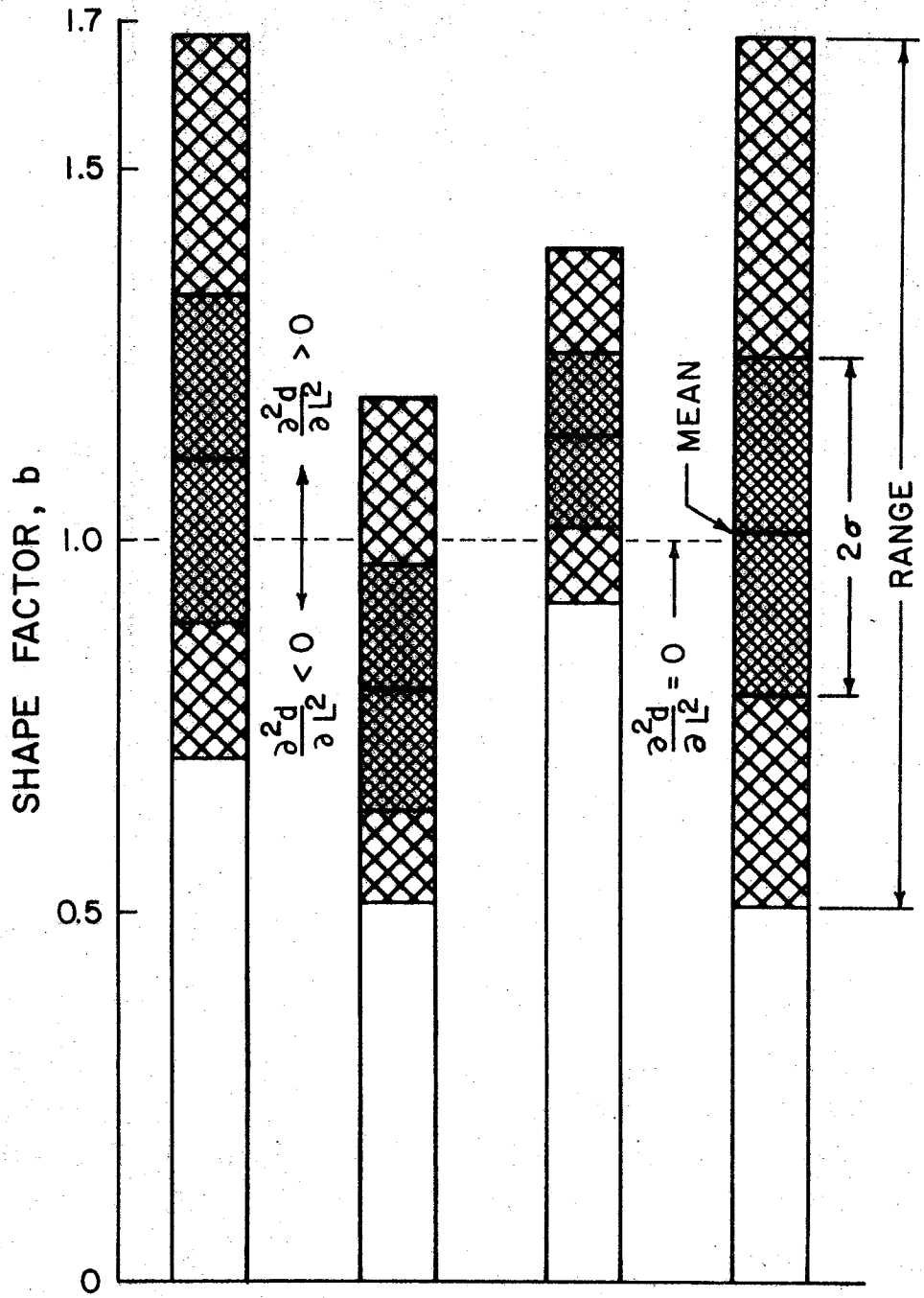

LOOP	4	5	6	ALL DATA
LANE	1	1	1	
AXLE LOADS (kips)	12,18	12,22.4	12,30	
NO. SECTIONS	27	27	27	81
DESIGNS				
WEAKEST	3-0-4	3-3-4	4-3-8	3-0-4
STRONGEST	5-6-12	5-9-12	6-9-16	6-9-16

Figure 9: Data from Tables 2, 3 and 4, for fall of 1958, AASHO Road Test.

That the shape factors of Loops 4 and 6 belong to the same data set seems obvious from Figure 9, and can be inferred from an analysis of variance that indicates no significant difference in their means. On the other hand, analyses of variance indicate that the mean of Loop 5 is significantly less than that of both Loop 4 and Loop 6. Thus, from the statistical point of view, the bar graph in Figure 9 grouping all data in one set cannot be justified. From a practical point of view, however, the authors justify the combining of all data on the grounds of necessity: no data are available to explain the difference between loops. Moreover, the existence of unexplained spatial variability in the behavior and performance of highway pavements is a matter of common knowledge in the profession, so that the variation of the mean values of the shape factors for the three loops shown in Figure 9 should surprise no one conversant with highway behavior.

The mean value of b for the 81 sections studied was 1.02, tending to indicate linearity of the load-deflection curve, but the standard deviation was large (0.23) and the range was quite large (from 0.51 to 1.68). Although large unexplained variations were expected, it was decided nevertheless to investigate the possibility that the known pavement design variables, D_1, (surfacing thickness), D_2 (base thickness), and D_3 (subbase thickness) might significantly influence the value of the shape factor, b. For this purpose a "select regression" computer program, developed at Texas A&M University by Lamotte and Hocking (8) , was employed, using as a model a second degree surface made up of squares and two-factor interactions of the three design variables. Thus, the full model contained the dependent variable, b, nine independent variables with their constant coefficients, and one constant term.

The select regression program operates as follows: it first uses the full model with N independent variables, printing out the coefficients of the variable terms, the constant term, the squared correlation coefficient, the standard error, and the probability of a Type 1 error for each independent variable. It then finds the optimum model containing N-1 independent variables, and prints out similar statistics for the reduced model. The process of identifying the optimum reduced model and performing a regression is continued, until the last model used contains one independent variable and a constant term. Models other than the optimum, as well as additional statistics for each model, are also chosen by the program and the results printed, but only the full model with 9 independent variables, and the remaining 8 optimum models containing fewer terms, will be considered here. The results are given in Table 5.

Table 5 presents information based on a model which, though having no roots in mechanistic theory, nevertheless appears to be sufficiently flexible to warrant the following conclusion.

No model based on the assumption that the physical properties of each of the five materials involved are constant for all test sections, can be expected to predict the shape factor, b, of the 81 sections analyzed, with an error much less than the standard deviation of b about its mean value. (The five materials referred to above are those composing the surfacing, base, subbase, embankment and foundation). This is tantamount to saying that the authors accept 1.0 as the best estimate of b, and ascribe deviations from 1.0 as a combination of the effects of instrumental error and of unknown, unmeasured variations in the properties of all the materials that yielded under load and thus contributed to the measured deflections.

TABLE 5: RESULTS OF SELECT REGRESSION OF b ON PAVEMENT DESIGN VARAIBLES (FALL 1958 DEFLECTIONS, ALL LOOPS)

One dependent variable: Shape factor, b.
Nine independent variables: D_1, D_2, D_3, D_1^2, D_2^2, D_3^2, $D_1 x D_2$, $D_1 x D_3$, $D_2 x D_3$

Independent Variables In Optimum Model				
	Prob. of Type 1 Error < 0.1			
No. in Model	No.	Variables	R^2	Standard Error
9(all)	2	D_2, $D_1 x D_2$	.32	.20
8	2	D_2, $D_1 x D_2$	.32	.20
7	2	D_2, $D_1 x D_2$	.31	.20
6	2	D_2, $D_1 x D_2$	.31	.20
5	3	D_2, D_3, $D_1 x D_2$	.31	.20
4	4	D_2, D_3, $D_1 x D_2$, $D_2 x D_3$	.29	.20
3	3	D_2, D_2^2, $D_1 x D_2$	.27	.20
2	2	D_2, $D_1 x D_2$	.24	.20
1	1	D_2	.10	.22
0	0	----------	---	.23*

*Standard deviation of the dependent variable, b, about its mean value of 1.02

As another, and perhaps more convincing means of arriving at the conclusion that the best estimate of b is 1.0, consider the eight designs, shown in Table 6, that were common to all three loops. Each value of b given in the columns headed Loop 4, Loop 5 and Loop 6, represents the response of one test section. Ideally, the set of three numbers representing three test sections of the same design, would be identical. But they are not, thus furnishing another example of unexplained spatial variability of highway pavements.

The variability of the shape factor b, evident in Table 6, was quantified by computing the across-loop replication error from the following formula applicable to n sets of replicate designs, where each set has three members (test sections):

$$Re = \left\{\frac{2}{9n}\left[\sum_{1}^{n}\left(b_{1i}^{2} + b_{2i}^{2} + b_{3i}^{2}\right) - \left(\sum_{1}^{n} b_{1i}b_{2i} + \sum_{1}^{n} b_{2i}b_{3i} + \sum_{1}^{n} b_{1i}b_{3i}\right)\right]\right\}^{1/2} \qquad (10)$$

wherein b_{1i}, b_{2i} and b_{3i} are the three values of b given in Table 6 for the ith design, and Re is the across-loop replication error. As shown at the bottom of Table 6, Re = 0.17.

The across-loop replication error of 0.17 can be compared directly with the standard errors of the models indicated in Table 5, including the standard deviation of 0.23, shown in the last line of the table and associated with the model

$$b = \bar{b} \qquad (11)$$

where $\bar{b}$ represents the mean value of b for the 81 test sections. If all the errors of Table 5, as well as the across-loops replication error of Table 6,

TABLE 6: VALUES OF b FOR THE EIGHT DESIGNS COMMON TO ALL LOOPS (FALL 1958 DEFLECTIONS)

Design Index, i	Design Thickness (in.)			b		
	Surface	Base	Subbase	Loop 4	Loop 5	Loop 6
1	4	3	8	1.000	1.077	1.149
2	4	3	12	1.207	0.746	1.017
3	4	6	8	0.967	0.873	1.047
4	4	6	12	0.736	0.650	1.109
5	5	3	8	0.859	0.897	1.277
6	5	3	12	0.710	0.702	1.124
7	5	6	8	1.362	0.982	1.160
8	5	6	12	1.127	0.724	1.263

Across-loop replication error = 0.17
(Computed from Equation 10)

Mean value of b = 0.99
Standard Deviation (24 values) = 0.21

are rounded to one decimal, it can be seen that all have the value 0.2. Under these conditions, and bearing in mind that any model selected to represent the shape factor, b, cannot fit all the data with an error much less than the across-loop replication error, it appears that the mean value of b is a reasonable estimate for design purposes, i.e., $b \approx 1.0$. This is the same conclusion previously drawn from the results of the select regression program.

Putting 1.0 for b in Equation 8, and recognizing the approximation involved, we have

$$d \approx e^{a}L \tag{12}$$

or stated in words, the shape of the load-deflection curves observed in the fall of 1958 at the AASHO Road Test tended toward linearity. Moreover, while many of the observed curves were concave downward - apparently an indication of stress-dependent moduli - many others were concave upward. Thus, there appeared to be no consistent support, when all available data were considered, for complicating a model of pavement behavior with the concept of a stress-dependent modulus.

Before passing to the next section, it should be repeated that Equation 11 was accepted mainly on the basis that its associated error of 0.2 was of the same order of magnitude as the across-loops replication error. The within-loops error, which is given at the bottom of Table 7, was smaller, as might be expected, being (to one decimal), 0.1. The reason for not using within-loop replication error as a measure of the suitability of a model fitted to the data from all three loops has already been discussed.

The formula used for computing within-loop replication error is given below:

$$Re = \left\{ \frac{1}{4n} \sum_{1}^{n} (b_{1i} - b_{2i})^2 \right\}^{1/2} \tag{13}$$

TABLE 7: VALUES OF b FOR DESIGNS THAT OCCURRED TWICE IN EACH LOOP

Loop No.	Design No., i	Design Thickness (in.)			b
		Surface	Base	Subbase	
4	1	3	0	12	1.460
		3	0	12R*	.916
	2	4	3	8	1.000
		4	3	8R	1.367
	3	5	6	4	1.033
		5	6	4R	1.033
5	4	3	3	12	0.673
		3	3	12R	0.715
	5	4	6	8	0.873
		4	6	8R	0.685
	6	5	9	4	0.926
		5	9	4R	0.818
6	7	4	3	16	1.153
		4	3	16R	1.011
	8	5	6	12	1.263
		5	6	12R	1.112
	n=9	6	9	8	1.246
		6	9	8R	1.199

Within-loop replication error = 0.12
(Computed from Equation 13)

*R designates the second of a pair of replicate sections appearing in the same loop. Its companion is listed in the line immediately above.

where b_{1i} and b_{2i} are the two values of b given in Table 7 for the ith design, and n is the total number of pairs of replicate sections in all loops (in this case, 9).

Shape of Load-Deflection Curves in the Spring of 1959 at the AASHO Road Test

On March 9 and again on March 31, 1959, deflection tests were repeated on those sections in the main factorial experiment that had survived the "spring breakup" period. Like the fall 1958 deflections, the spring data, averaged over the two testing days, were tabulated in Appendix C of Reference 2. These data, with the exception of some that had been labelled "estimated", are repeated in Tables 8, 9 and 10 in the same format as Tables 2, 3 and 4 previously discussed. Unlike the data shown in Tables 2, 3 and 4, replicate sections were included in Tables 8, 9 and 10 in order to make available for study as much of the spring 1959 deflections as possible, inasmuch as loss of test sections had already unbalanced the loop factorial experiments.

The mean values of the shape factor, b, for Loops 4, 5 and 6, and for all data combined, together with standard deviations and ranges, are displayed graphically in Figure 10. It seems obvious from Figure 10 that the mean values of b for Loops 5 and 6 are not significantly different, while the mean for Loop 4 is significantly smaller than the means of both Loop 5 and Loop 6: these conclusions were borne out by analyses of variance. As in the case of the fall 1958 deflections, and for the same reason - lack of information as to why the loop means should vary in this way-the authors decided to pool all the data, as had been done in the case of the fall deflections, and investigate the possibility that the pavement design variables, D_1, D_2 and D_3, could be used in a second-degree statistical model to predict the values of the shape factor b with a standard error substantially less than

TABLE 8: SPRING 1959 CREEP SPEED DEFLECTION DATA LOOP 4, LANE 1, AASHO ROAD TEST WITH CONSTANTS COMPUTED FROM DEFLECTIONS AND LOADS

Thickness (inches) of the Materials Indicated	Deflection d(mils) Caused By The Axle Load, L(kips) Indicated		Computed Constants in Model, $d=e^{a}L^{b}$	
AC-LS-GR	12	18	a	b
3-0-12	52	77	1.545	.968
3-0-12R	48	56	2.926	.380
3-3-8	70	86	2.987	.508
3-3-12	36	45	2.216	.550
3-6-8	57	66	3.145	.362
3-6-12	34	48	1.413	.850
4-0-4	74	83	3.601	.283
4-0-8	32	44	1.514	.785
4-0-12	34	38	2.845	.274
4-3-4	65	79	2.979	.481
4-3-8	49	62	2.450	.580
4-3-8R	44	53	2.644	.459
4-3-12	35	42	2.438	.450
4-6-4	60	63	3.795	.120
4-6-8	36	47	1.949	.658
4-6-12	31	40	1.872	.629
5-0-4	48	58	2.711	.467
5-0-8	38	41	3.172	.187
5-0-12	26	34	1.614	.662
5-3-4	38	44	2.739	.362
5-3-8	29	44	.812	1.028
5-3-12	28	36	1.792	.620
5-6-4	30	42	1.339	.830
5-6-4R	30	38	1.952	.583
5-6-8	30	36	2.284	.450
5-6-12	28	32	2.514	.329

Mean value of b: .533
Standard deviation: .229
No. test sections: 26

Note: AC = asphaltic concrete
LS = crushed limestone
GR = uncrushed sandy gravel
e = base of Napierian logarithims
Other symbols as defined in column headings

TABLE 9: SPRING 1959 CREEP SPEED DEFLECTION DATA LOOP 5, LANE 1, AASHO ROAD TEST WITH CONSTANTS COMPUTED FROM DEFLECTIONS AND LOADS

Thickness (inches) of the Materials Indicated	Deflection d(mils) Caused By The Axle Load, L(kips) Indicated		Computed Constants in Model, $d=e^{a}L^{b}$	
AC-LS-GR	12	22.4	a	b
4-3-8	50	80	2.041	.753
4-3-12	40	76	1.134	1.028
4-6-4	71	90	3.310	.380
4-6-8	44	78	1.505	.917
4-6-8R	40	62	1.944	.702
4-6-12	32	50	1.689	.715
4-9-4	54	97	1.657	.938
4-9-8	40	71	1.404	.919
4-9-12	28	44	1.533	.724
5-3-4	51	95	1.455	.997
5-3-8	40	60	2.075	.650
5-3-12	29	48	1.361	.807
5-6-4	46	72	2.045	.718
5-6-8	29	57	.677	1.083
5-6-12	24	43	.856	.934
5-9-4	31	54	1.224	.889
5-9-4R	33	60	1.116	.958
5-9-8	21	47	-.162	1.291
5-9-12	24	36	1.564	.650

Mean value of b: .845
Standard deviation: .201
No. test sections: 19

Note: AC = asphaltic concrete
LS = crushed limestone
GR = uncrushed sandy gravel
e = base of Napierian logarithims
Other symbols as defined in column headings

TABLE 10: SPRING 1959 CREEP SPEED DEFLECTION DATA LOOP 6, LANE 1, AASHO ROAD TEST WITH CONSTANTS COMPUTED FROM DEFLECTIONS AND LOADS

Thickness (inches) of the Materials Indicated	Deflection d(mils) Caused By The Axle Load, L(kips) Indicated		Computed Constants in Model, $d=e^{a}L^{b}$	
AC-LS-GR	12	30	a	b
4-3-12	28	60	1.265	.832
4-3-16	42	92	1.611	.856
4-3-16R	46	97	1.805	.814
4-6-12	62	141	1.899	.897
4-6-16	37	59	2.345	.509
4-9-12	40	82	1.742	.783
4-9-16	27	56	1.317	.796
5-3-8	52	96	2.289	.669
5-3-12	37	76	1.659	.786
5-3-16	30	65	1.304	.844
5-6-8	44	87	1.935	.744
5-6-12	32	64	1.586	.756
5-6-12R	30	64	1.346	.827
5-6-16	22	47	1.032	.828
5-9-8	38	72	1.904	.697
5-9-12	28	54	1.551	.717
5-9-16	26	54	1.276	.798
6-3-8	25	56	1.032	.880
6-3-12	30	62	1.433	.792
6-3-16	24	58	.785	.963
6-6-8	33	78	1.164	.939
6-6-12	25	54	1.130	.840
6-6-16	18	36	1.011	.756
6-9-8	31	66	1.385	.825
6-9-8R	26	65	.773	1.000
6-9-12	23	51	.976	.869
6-9-16	17	40	.513	.934

Mean value of b: .813
Standard deviation: .099
No. test sections: 27

Note: AC = asphaltic concrete
LS = crushed limestone
GR = uncrushed sandy gravel
e = base of Napierian logarithims
Other symbols as defined in column headings

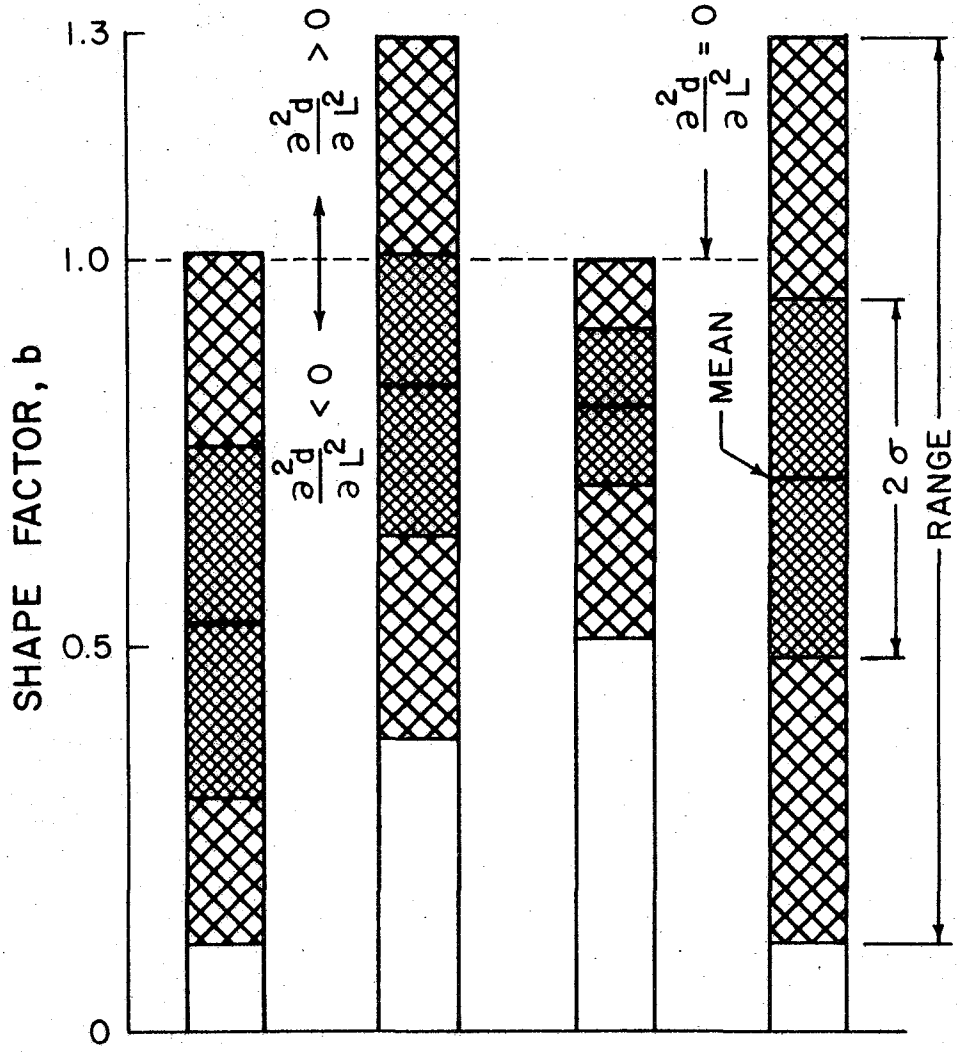

LOOP	4	5	6	ALL
LANE	1	1	1	DATA
AXLE LOADS (kips)	12,18	12,22.4	12,30	
NO. SECTIONS	26	19	27	72
DESIGNS				
WEAKEST	3-0-12	4-3-8	4-3-12	3-0-12
STRONGEST	5-6-12	5-9-12	6-9-16	6-9-16

Figure 10: Data from Tables 8, 9 and 10, for spring of 1959, AASHO Road Test.

the standard deviation of b about its own mean. For this purpose the select regression computer program (8) described in the preceeding section was used. The results are given in Table 11.

The error column of Table 11, derived from the spring 1959 data, and that of Table 5, derived for the fall 1958 data, are almost identical. When rounded to one decimal, all the errors given in Table 11, including the standard deviation of b about its mean value, and (as will be shown later) the across loops replication error, are 0.2: This statement applies equally well to Table 5, as was pointed out in previous discussion. Thus, as in the case of the fall deflections, we are led to the conclusion that a satisfactory estimate of b for the spring deflections is its mean value, $\bar{b}$.

It is in the values of $\bar{b}$ that Tables 5 and 11 differ sufficiently to be highly significant (according to an analysis of variance, $F = 63.2$). The difference is visible when one compares the "all data" bar graph of Figure 9 with the corresponding bar graph of Figure 10. This comparison can be made by inspecting Figure 11, where the two bar graphs have been plotted side-by-side.

The values of $\bar{b}$, rounded to one decimal, were 1.0 for the fall and 0.7 for the spring. If the premise stated earlier in this report and illustrated in Figure 7 is correct (the premise being that if $b < 1$, some or all of the materials supporting the load have stress-dependent moduli), one must conclude that in the spring of 1959 there was evidence to support the concept of stress-dependent moduli. Not only was the average of b less than 1, but also-according to Tables 8, 9 and 10 - in only 5 cases out of the 72 studied was $b \geq 1$.

TABLE 11: RESULTS OF SELECT REGRESSION OF b ON PAVEMENT DESIGN VARIABLES (SPRING 1959 DEFLECTIONS, ALL LOOPS)

One dependent variable: Shape factor, b
Nine independent variables: D_1, D_2, D_3, D_1^2, D_2^2, D_3^2, $D_1 x D_2$, $D_1 x D_3$, $D_2 x D_3$

Independent Variables In Optimum Model				
	Prob. of Type I Error < 0.1			
No. in Model	No.	Variables	R^2	Standard Error
9(all)	2	D_3, $D_2 x D_3$	.31	.20
8	2	D_3, $D_2 x D_3$	.31	.20
7	3	D_3, D_2, $D_2 x D_3$	.31	.20
6	4	D_3, D_2, D_1^2, $D_2 x D_3$	.31	.20
5	4	D_1^2, D_2, D_3, $D_2 x D_3$	.31	.20
4	4	D_1^2, D_2, D_3, $D_2 x D_3$	.29	.20
3	3	D_1^2, $D_2 x D_3$, D_3	.27	.20
2	2	$D_1 x D_2$, $D_1 x D_3$	.22	.21
1	1	$D_1 x D_2$	.18	.21
0	-	----------	---	.23*

*Standard deviation of the dependent variable, b, about its own mean of 0.72.

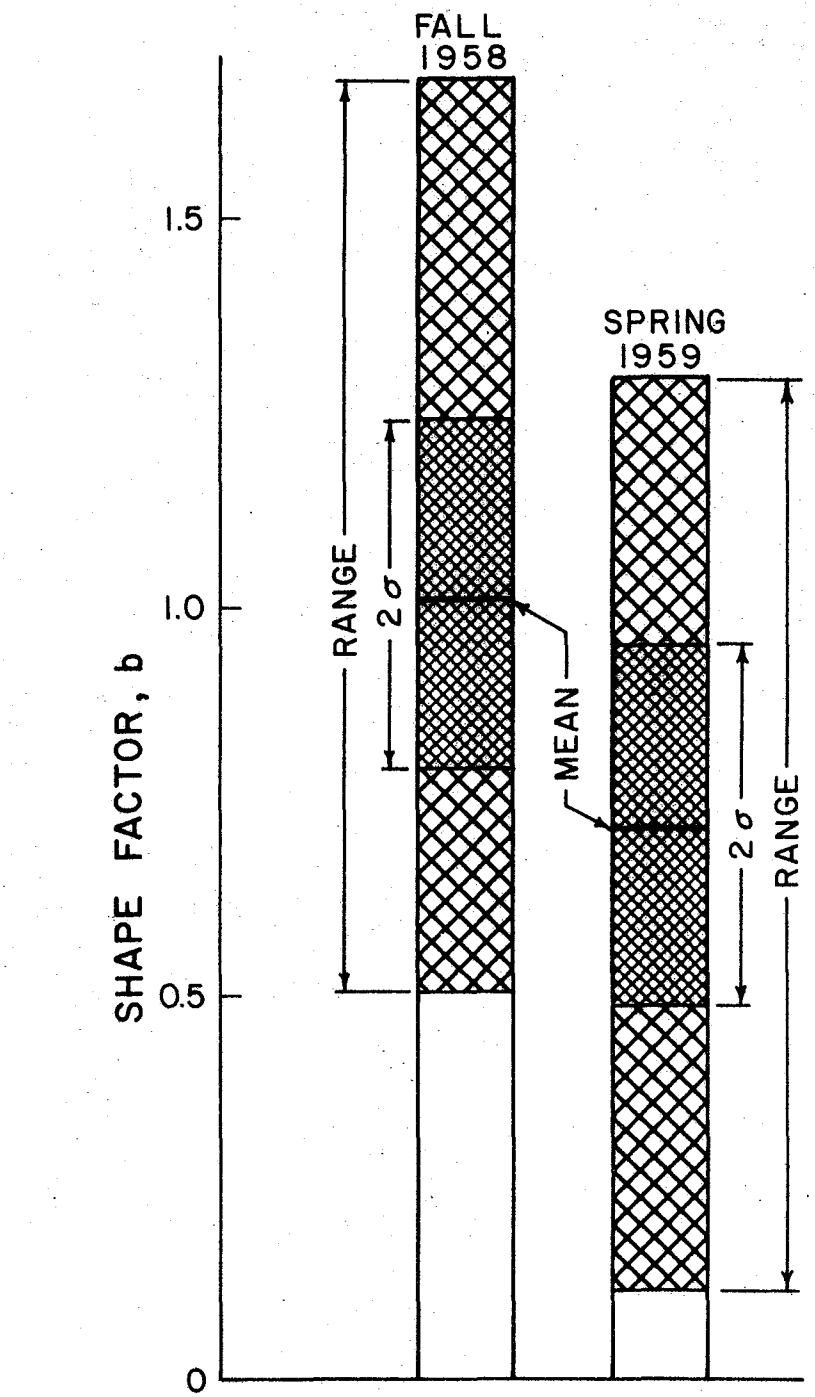

NO. SECTIONS	81	72
DESIGNS		
WEAKEST	3-0-4	3-0-12
STRONGEST	6-9-16	6-9-16

Figure 11: Mean values of b and other statistics for the fall of 1958 compared with similar data for the spring of 1959, AASHO Road Test. Data from Figures 9 and 10.

But if stress-dependent moduli did, in fact, exist during the spring testing period, one is led to another conclusion, namely that disruption of the materials - including the 36-inch embankment - by a freeze-thaw cycle that ended a few days before the gathering of the spring deflection data began, was somehow responsible for significant increases in the degree to which material stiffness was increased by load-induced stress. How this could have happened - if in fact it did- the authors are not prepared to say.

To complete the description of the differences between fall and spring deflections it should be mentioned that the latter were much greater than the former. This can most easily be demonstrated by examining the response of the six designs that were common to all loops in both the fall and the spring, to the one load - a 12-kip single axle load - that was also common to all loops in both seasons. The designs and the response data for each of the 18 test sections involved are given in Table 12.

In Table 12 the across-loops mean value for each design is selected for further attention, rather than individual section values, because - as has been emphasized previously - no data are available for explaining across-loop variability. The across loop means are plotted in Figure 12. In that figure a straight line has been drawn through the origin and the mean of the data, to roughly quantify the ratio of spring to fall deflections. This ratio, as indicated by the slope of the line, is 5/3, or 1.8.

The approximate ratio of 1.8 was confirmed 8 years later by Dynaflect measurements made in the spring and fall of 1967 on sections of highways located near the site of the AAHSO Road Test. In this experiment the

TABLE 12: COMPARISON OF FALL 1958 AND SPRING 1959
12-KIP SINGLE AXLE LOAD DEFLECTIONS

Design Thickness (in.)			Loop	Fall Defl. (mils)		Spring Defl. (mils)	
Surface	Base	Subbase		Section Values	Across-Loops Mean	Section Values	Across-Loops Mean
4	3	12	4	19	20	35	34
			5	27		40	
			6	13		28	
4	6	12	4	23	23	31	42
			5	24		32	
			6	21		62	
5	3	8	4	24	23	29	40
			5	28		40	
			6	18		52	
5	3	12	4	24	20	28	31
			5	20		29	
			6	15		37	
5	6	8	4	19	21	30	34
			5	26		29	
			6	19		44	
5	6	12	4	19	17	28	28
			5	21		24	
			6	11		32	
			Overall Average		21		35

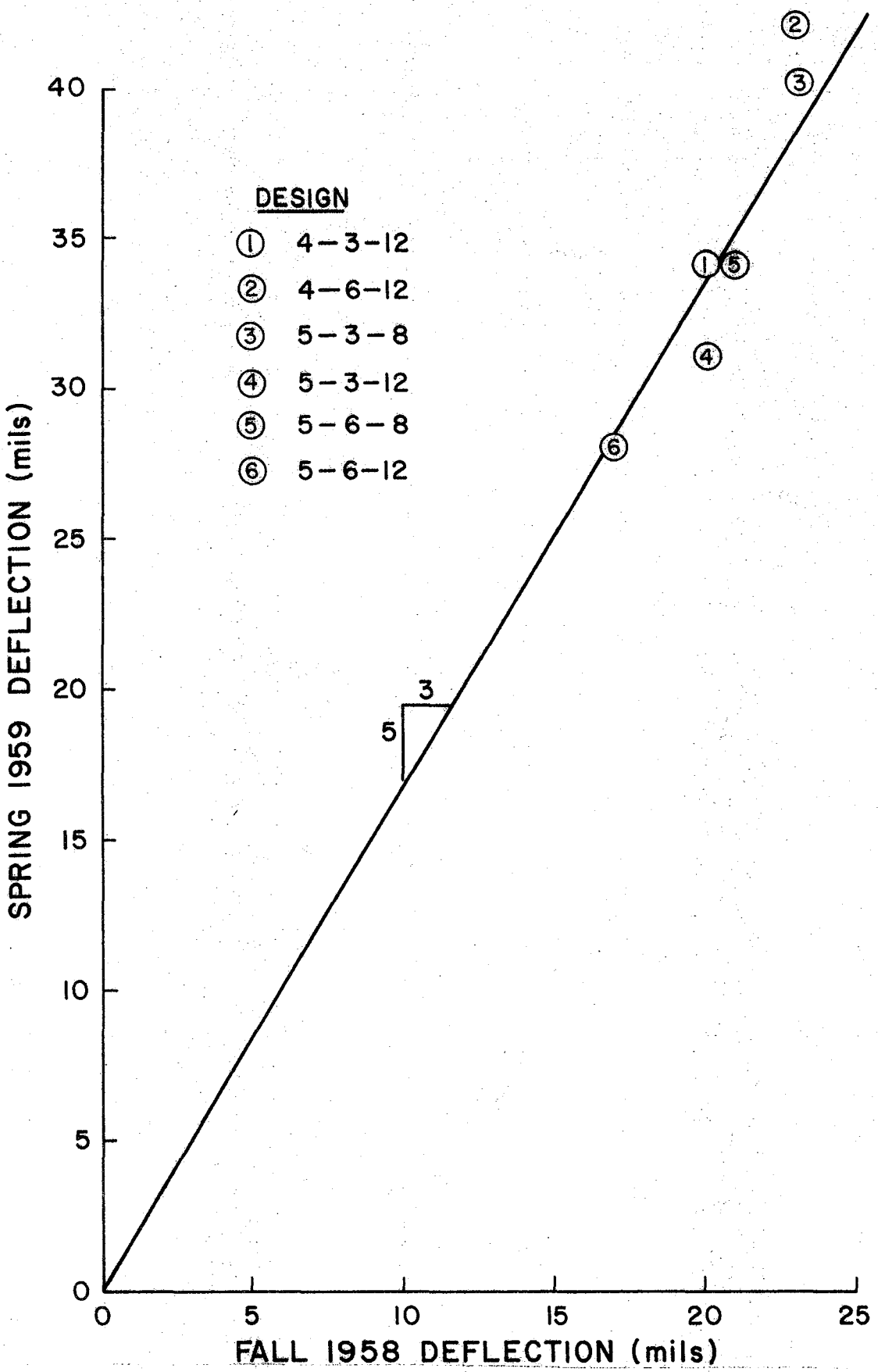

Figure 12: Twelve-kip single axle load deflections in the fall of 1958 compared with similar deflections in the spring of 1959, AASHO Road Test. Data from Table 12.

ratios varied from 1.7 to 2.0 on 5 out of 6 sections tested. The single exception was a pavement constructed on a sand fill; in this case spring and fall deflections were about equal. The remaining 5 sections had subgrades described as silty clay (1, Fig. B-7 through B-12).

In this chapter it remains only to document the statement made earlier (page 42) that the across-loop replication error in the shape factor, b, for the spring 1959 load-deflection curves was approximately 0.2. Table 13 is the necessary documentation. As noted at the bottom of the table only 6 of the original 8 designs that appeared in all loops were available in the spring due to the destruction of some sections by the test traffic.

TABLE 13: VALUES OF b FOR THE SIX SURVIVING SECTIONS COMMON TO ALL LOOPS (SPRING 1959 DEFLECTIONS)

Design No., i	Design Thickness (in.)			b		
	Surface	Base	Subbase	Loop 4	Loop 5	Loop 6
1	4	3	12	0.450	1.028	0.832
2	4	6	12	0.629	0.715	0.897
3	5	3	8	1.028	0.650	0.669
4	5	3	12	0.620	0.807	0.786
5	5	6	8	0.450	1.083	0.744
6	5	6	12	0.329	0.934	0.756

Across-Loop replication error = 0.199
(Computed from Equation 10)

Mean value of b = 0.745
Standard Deviation (18 values) = 0.208

Note: Spring deflection data from only 6 of the original 8 designs common to all loops were available due to destruction of sections by test traffic

4. ENVIRONMENTAL EFFECTS AT THE TTI PAVEMENT TEST FACILITY

Discussed in the preceeding chapter were certain effects of local weather on the magnitude of pavement deflections and the shape of load-deflection curves at the AASHO Road Test. It was assumed that these effects were caused by a disturbance of the structure of the load-bearing materials by deep frost penetration and subsequent thawing, and that immediately following the spring thaw linear elasticity was not applicable, even when replication error was considered.

Entrapment of Water in The TTI Facility

A disturbance of some of the construction materials is known to have also occurred at the TTI Pavement Test Facility, but by a different mechanism, namely, the unforseen entrance of large quantities of water into the embankment materials, followed by the removal of a portion of the water by installation of a drainage system. The resulting changes, if any, in the shapes of load-deflection curves were not measured, but there can be no doubt, as will be shown, that radical changes from the "as-built" condition did occur in some of the materials. In view of their possible bearing on the applicability of linear elasticity to the Study 136 data, these changes, and their effect on surface deflections, are described in this chapter in considerable detail.

Materials and Test Section Designs

The materials composing the 460' x 50' x 53" main facility, a statistically designed experiment, are described briefly in Table 14. The design thickness of the materials, and their vertical position in the structure of each test section, are given in Table 15. As indicated in Figure 1 of the

TABLE 14: MATERIALS USED IN EMBANKMENT, SUBBASE, BASE AND SURFACING OF TEST SECTIONS

Description	Abbreviation Used In Table 15	AASHO Class	Unified Soil Class	Texas Triaxial Class	Compressive Strength (psi)*
Plastic Clay	PC	A-7-6(20)	CH	5.0	22
Sandy Clay	SC	A-2-6(1)	SC	4.0	40
Sandy Gravel	GR	A-1-6	SW	3.6	43
Crushed Limestone	LS	A-1-a	GS-GM	1.7	165
Crushed Limestone + 2% Lime	LS+L	A-1-a	GW-GM	1.0	430
Crushed Limestone + 4% Cement	LS+C	A-1-a	GW-GM	1.0	2270
Hot Mix Asphalt Concrete	AC				

*By Texas triaxial procedure, at a lateral pressure of 5 psi .

Note: The natural material below the embankments was plastic clay similar to that described above, changing to a denser clay at a depth of about 90 inches below the surface of the pavement. The dense clay is abbreviated DC; its properties were not determined in the laboratory.

TABLE 15: TEST SECTION DESIGNS, MAIN FACILITY

Sec.	Thickness (In.)				Material Type (see also Table 14)			
	Surf.	Base	Subb.	Emb.	Surf.	Base	Subb.	Emb.
1	5	4	4	40	AC	LS+C	LS	PC
2	1	12	4	36	AC	LS+C	LS	PC
3	1	4	12	36	AC	LS+C	LS	PC
4	5	12	12	24	AC	LS+C	LS	PC
5	5	4	4	40	AC	LS	LS+C	PC
6	1	12	4	36	AC	LS	LS+C	PC
7	1	4	12	36	AC	LS	LS+C	PC
8	5	12	12	24	AC	LS	LS+C	PC
9	5	4	4	40	AC	LS	LS	GR
10	1	12	4	36	AC	LS	LS	GR
11	1	4	12	36	AC	LS	LS	GR
12	5	12	12	24	AC	LS	LS	GR
13	5	4	4	40	AC	LS+C	LS+C	GR
14	1	12	4	36	AC	LS+C	LS+C	GR
15	1	4	12	36	AC	LS+C	LS+C	GR
16	5	12	12	24	AC	LS+C	LS+C	GR
17	3	8	8	34	AC	LS+L	LS+L	SC
18	1	8	8	36	AC	LS+L	LS+L	SC
19	5	8	8	32	AC	LS+L	LS+L	SC
20	3	4	8	38	AC	LS+L	LS+L	SC
21	3	12	8	30	AC	LS+L	LS+L	SC
24	3	8	8	34	AC	LS	LS+L	SC
25	3	8	8	34	AC	LS+C	LS+L	SC
26	3	8	8	34	AC	LS+L	LS	SC
27	3	8	8	34	AC	LS+L	LS+C	SC
28	3	8	8	34	AC	LS+L	LS+L	PC
29	3	8	8	34	AC	LS+L	LS+L	GR

introductory chapter, three embankments were built side by side, and the entire main facility was enveloped in an asphalt membrane intended to maintain the as-built moisture content.

The protective membranes at the ends of the facility were installed after construction of the end ramps by digging a transverse ditch at each end, spraying its inner wall with liquid asphalt, and then backfilling. Since the ditch walls were vertical, these membranes were thinner than desired, and may have been disturbed by the backfilling operation, permitting the entrance of water. In any event, water did enter the embankments somehow, as evidenced by the following series of events.

Events Prior to Collection of Study 136 Data

The test facility was constructed in the spring and summer of 1965 (9, p. 3). In 1966, during the period from March 9 to March 14, inclusive, Dynaflect deflections were taken at six locations on each of the 27 test sections, and the results averaged to represent the deflection basins of the section (9, p. 13). At that time there were no outward signs that moisture changes had occurred in any of the materials encased in the membrane. But on the other hand, no samples were taken, and there is no guarantee that water had not already entered the facility when the 1966 deflection tests were made seven months after construction.

However, about a year later it was discovered that wide, longitudinal cracks had penetrated through the surface, base and subbase of several of the nine test sections constructed on the plastic clay embankment. These were sealed soon after their discovery, but new cracks, some of which were transverse, subsequently appeared and these, too, were sealed. In addition, cracks paralleling the pavement edge on the plastic clay embankment side

appeared in the shoulder for nearly the entire length of the 460 ft. facility, and a few cracks occurred in sections constructed over the sandy gravel and sandy clay embankments, though the latter cracking was less severe than that associated with the plastic clay embankment.

Eventually the appearance of new cracks seemed to have ceased, and in the early fall of 1971 preparations were made for measuring displacements within the body of the facility as a part of Research Study 136. The work plan required that 1 3/4" - diameter vertical holes be drilled completely through the facility and 12 inches into the foundation beneath the embankments. Many of the holes collapsed before the desired depth could be reached, and free water could be seen flowing into some of them. It quickly became apparent that free water was entrapped in the two pervious embankments and that the plastic clay embankment was much wetter than at the time of construction.

Installation of Drainage System

As a result of the discovery of entrapped water, the measurements program was temporarily halted and a drainage system, designed by Dr. Robert L. Lytton, was installed in the fall of 1971 (10). Lateral drains (3 in. - diameter slotted plastic pipes) were laid just below the bottom of the sandy gravel and sandy clay embankments. Surrounded by a graded filter that penetrated upward through the asphalt membrane, the lateral drains carried water from the two relatively permeable embankments to a longitudinal pipe and thence to a man hole and storm sewer near the north-west corner of the facility. Plan and cross-section views of the system are shown in Figure 13.

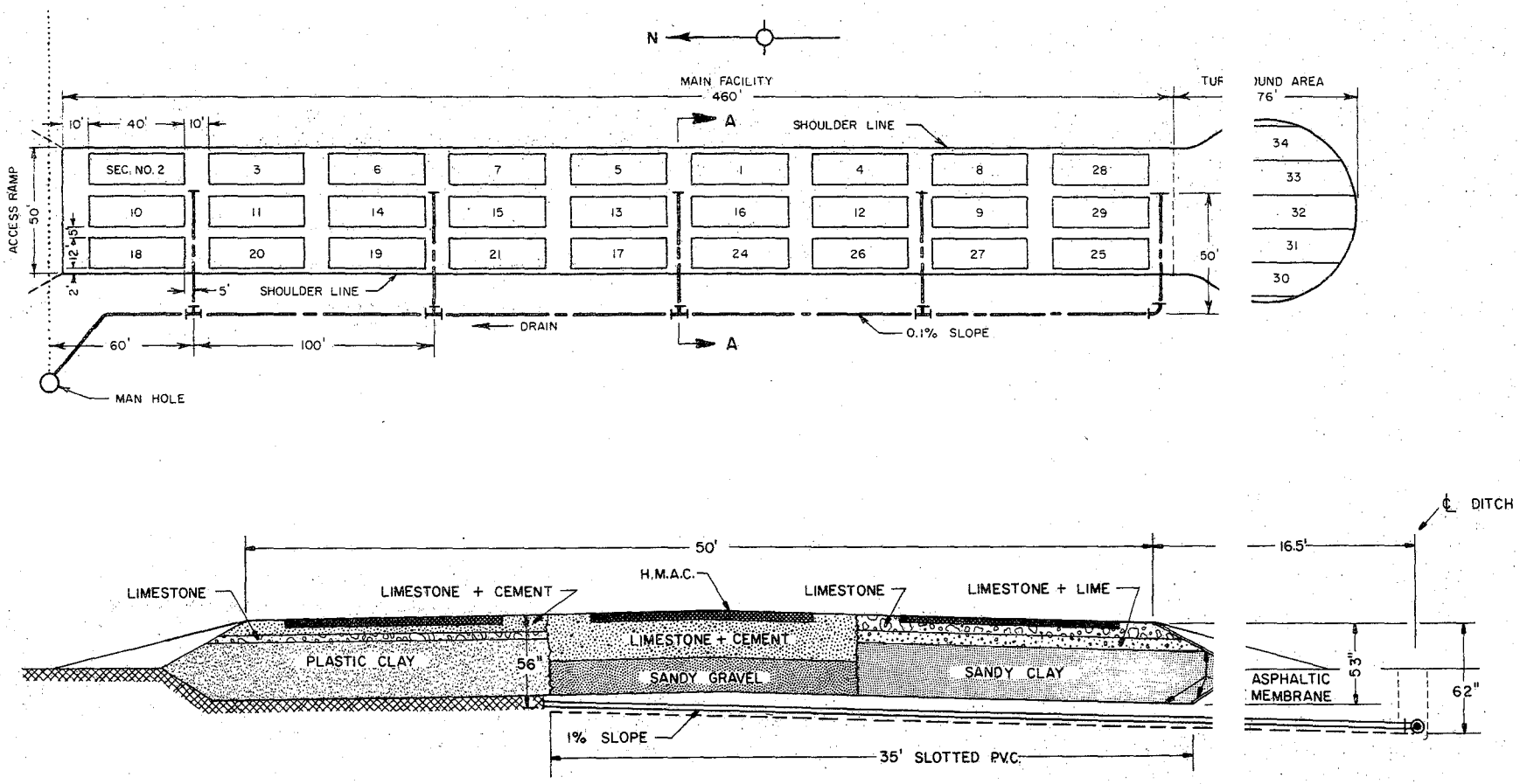

Figure 13: Plan and cross-section views of the TTI Pavement Test cility after installation of drainage system in the fall of 1 l, five years after construction of the facility.

During construction of the drainage system in August and September 1971, a considerable amount of clear water drained out of the facility, but flow rate measurements could not be made until after installation was complete. During the first 40 days (October 10 - November 20, 1971) after completion, it was observed that clear water flowed into the manhole at rates varying from about 100 to 1200 gallons per day, apparently depending upon current rainfall intensity. From late 1971 to May, 1974, inspections made at random intervals have indicated that water continues to drain from the facility. A measurement made on June 17, 1974 indicated a rate of flow of 60 gallons per day. Evidently water is still entering the facility, the source, as previously mentioned, possibly being rain water somehow making its way through defective membranes at the north and/or south ends.

Volume Changes

Whatever the source of the water, its effect on the clay embankment was observable over 2 1/2 years after the drainage system had been installed. Surface elevations measured at the center point of each test section on May 3, 1974, showed that points over the clay embankment were consistently higher (0.14 ft. or 1.7 in. on the average) than those on the sandy clay embankment, although the construction plans called for all 18 points (9 on each of the two outer embankments) to be built to the same elevation.

Individual elevations, the mean elevation, the standard deviation, and the observed range of elevations measured over each embankment are given in Table 16. The last column shows similar statistics for the difference between the points over the two outer embankments. An analysis of variance indicated that the probability that the mean elevation of the plastic clay

TABLE 16: RELATIVE ELEVATIONS TAKEN MAY 3, 1974 ON A&M PAVEMENT TEST FACILITY SHOWING SWELLING OF CLAY EMBANKMENT SINCE CONSTRUCTION IN SUMMER OF 1965.

Station	Test Sections (Left to Right)	Line A (17' Left) Plastic Clay	Line B (C.L. of Facility) Gravel	Line C (17' Right) Sandy Clay	Swell (ft.)* of Clay Emb. (Line A -Line C)
0+30	2, 10, 18	6.05	6.22	5.90	0.15
0+80	3, 11, 20	6.05	6.19	5.89	0.16
1+30	6, 14, 19	5.97	6.20	5.91	0.06
1+80	7, 15, 21	6.07	6.17	5.93	0.14
2+30	5, 13, 17	5.96	6.20	5.90	0.06
2+80	1, 16, 24	5.99	6.20	5.80	0.19
3+30	4, 12, 26	5.99	6.19	5.81	0.18
3+80	8, 9, 27	5.99	6.19	5.78	0.21
4+30	28, 29, 25	5.97	6.24	5.85	0.12
Mean elevation		6.00	6.20	5.86	0.14
Standard Deviation		0.04	0.02	0.05	0.05
Range		5.96-6.07	6.17-6.24	5.78-5.90	0.06-0.21

Note: Each elevation shown in body of table was taken on the surface of the pavement at the central point of a test section. Station 0+00 is at north end of Main Facility and elevation zero is axis of drain pipe outfall in manhole.

* - Assumed

embankment differred from that of the sandy clay embankment through pure chance, was negligible (F=38.3).

While the plastic clay embankment underwent a volume increase that persists to this date, the water entrapped in the sandy gravel and sandy clay embankments apparently had no effect on their volume, as evidenced by the information given below.

The pavements were built with a transverse grade of -2% each way from the center-line of the facility, which was also the center-line of the gravel embankment. Thus, in the 17 feet from the center-line of the gravel embankment (line B in Table 16) to the center-line of the sandy clay embankment (line C in Table 16) there was, at the time of construction, an average change in elevation of about -.02 x 17 = -0.34 ft. According to Table 16, eight years after construction, and in spite of water entrapment and subsequent partial drainage, the mean difference between line C and line B elevations was precisely -0.34 ft., as required by the original plans. We conclude that these two structures, (the sandy clay and the sandy gravel embankments), and the foundation beneath them, probably did not change in volume by any significant amount from the fall of 1965 to May 1974.

Probable Causes of Longitudinal Cracking

After the rolling of the test sections just prior to the 1966 deflection testing, only light test vehicles have travelled the pavements, and these only at infrequent intervals. As a result it seems practically certain that after March 1966, the asphaltic concrete surfacing, lacking the kneading action of regular traffic to keep it "alive", gradually became brittle and subject to cracking as the result of any differential vertical movements that might have occurred in the material beneath it. Differential vertical movements are believed to have occurred in the plastic clay embankment.

The conclusion that vertical differential movements did occur in the plastic clay embankment during its period of expansion rests on the reasonable assumption that spatial variations in the time rate of expansion must have existed throughout the mass of the plastic clay during the expansion period, producing distortions in the shape of the top surface of the embankment and leading eventually to the cracking observed in the overlying subbase, base and surfacing.

Another phenomenon that must have contributed to the longitudinal cracking was the tendency of the plastic clay embankment to expand outward, toward the adjacent shoulder and side slope. (Movement in the opposite direction would have been partially if not completely blocked by the greater mass of sandy gravel and sandy clay). The tensile stresses in the overlying materials, induced by lateral motion of the swelling clay embankment on which they lay, must have contributed to the wide opening of the deep longitudinal cracks first observed.

Distribution of Cracking

The distribution, as of March 1974, of surface cracking throughout the 460 ft. x 50 ft. main facility, is shown schematically in Figure 14. The diagram indicates whether visible cracking had, or had not, occurred within each of four types of areas: (1) a 12 ft. x 40 ft. test section, surfaced with asphaltic concrete; (2) a 10 ft. x 12 ft. longitudinal transition between two sections, also surfaced with asphaltic concrete; (3) a 5 ft. x 40 ft. surface-treated transverse transition between two sections; and (4) a 2 ft. x 40 ft. surface treated shoulder adjacent to a section.

The frequency of cracking within the four area types defined in the preceeding paragraph is given in Table 17, principally for the purpose of

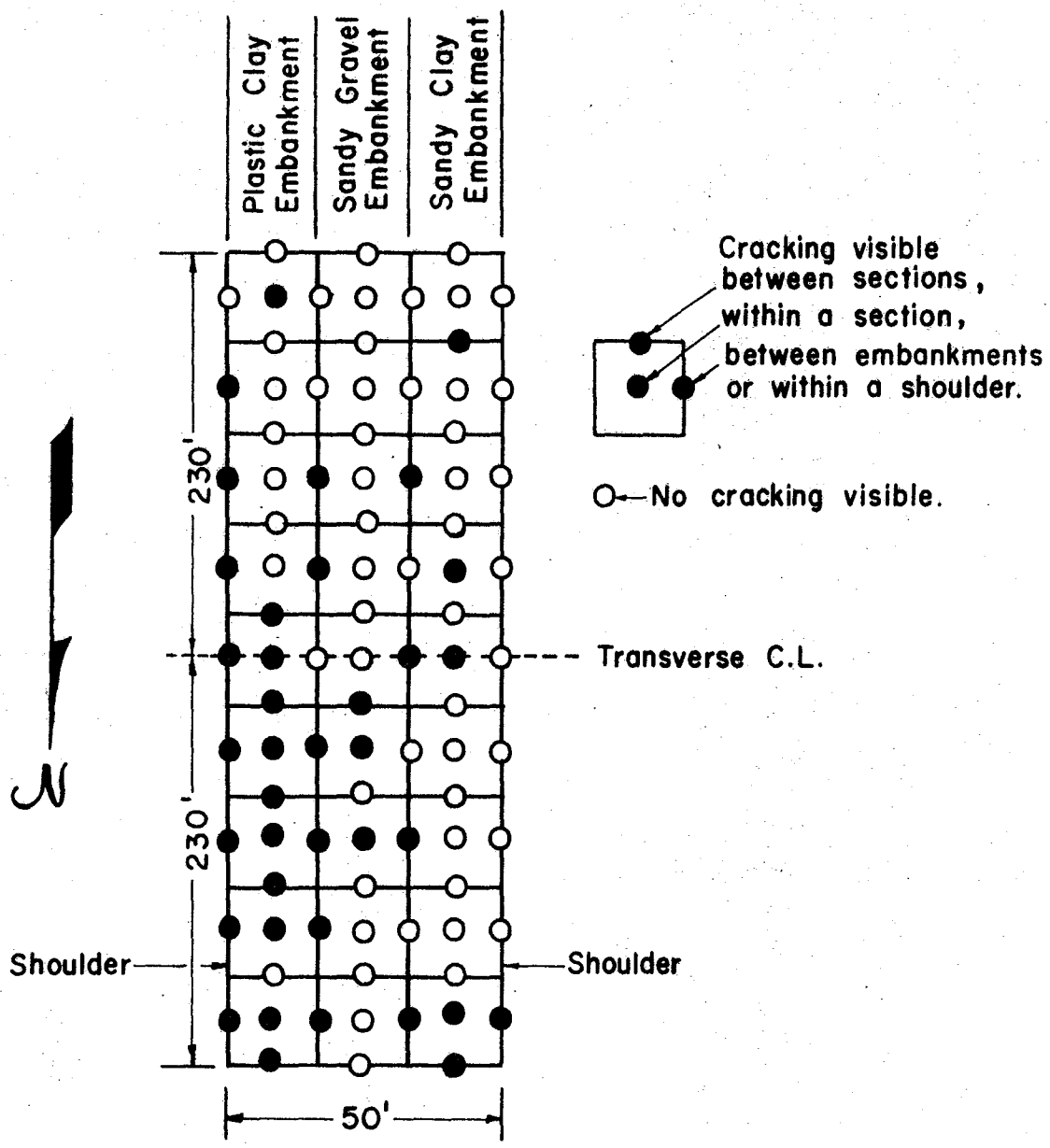

Figure 14: Schematic plan view of TTI Pavement Test Facility showing location of cracking.

TABLE 17: CRACKING WITHIN AND BETWEEN SECTIONS, BETWEEN EMBANKMENTS, AND IN SHOULDERS (MARCH 1972)

Type of Area	Frequency of Cracking				
	PC Emb.	PC and GR Emb.	GR Emb.	GR and SC Emb.	SC Emb.
Test Section	.67	---	.22	---	.33
Long. Transition	.50	---	.10	---	.20
Trans. Transition	---	.67	---	.40	---
Shoulder	.89	---	---	---	.11
Embankment	.68		.16		.21

comparing cracking associated with the expansive clay embankment with that associated with the two embankments composed of non-expansive materials. The frequency of cracking was calculated from Figure 14 simply by counting the number of black circles occurring within a selected area type, and dividing the result by the total number of areas of the given type. Thus, a frequency of 1.0 for a given area type would mean that every area of that type exhibited some cracking. As will be readily apparent from examination of Table 17, each frequency calculation was confined to an area type on a specified embankment, except in the case of transverse transition areas. In the latter case, the areas lay over two adjacent embankments, as indicated in the table.

To clarify the method of frequency determination, a sample calculation follows: according to Figure 14, there are 9 test sections on the plastic clay embankment, of which 6 contain a black circle indicating cracking; hence, 6/9, or 0.67 is the frequency of occurrence of cracking within sections on the plastic clay embankment. This result appears in the upper left corner of Table 17.

The first four lines of data in Table 17 show that cracking frequency was greatest in each of the previously defined area types where these areas occurred over the swelling-clay embankment.

The frequency of cracking within embankments (which includes cracking within sections, within longitudinal transitions, and-for the two outer embankments - within shoulders as well) appears in the last line of Table 17. It shows that the frequency of cracking of materials on the plastic clay embankment exceeded that of materials on the other two by a factor of 3 or 4.

Bearing in mind that this difference in behavior occurred practically in the absence of traffic, that nearly all the cracking was longitudinal, and that the plastic clay embankment underwent a significant increase in volume, there is at least an inference that the swelling of clay subgrades on regular highways may contribute to the formation of longitudinal cracks. A mathematical study of the mechanism involved is beyond the scope of this report, but it is recommended that such a study be made.

Before terminating the discussion of crack distribution, it should be pointed out that the cracking frequency in the north half of the facility was more than twice that in the south half, as may be verified by inspection of Figure 14. This fact may be an indication that water entered the facility at its north end.

Changes of Material Stiffness with Time

Mentioned earlier in this chapter was a series of surface deflections measured by the Dynaflect in March 1966, on each of the 27 test sections composing the main facility (9, p. 15-17). On the same sections, both surface and internal displacements induced by the Dynaflect were measured in the period from mid-November 1971 to late March 1972; these measurements will be referred to hereafter as "Replication A" data. A similar set of measurements, hereafter called "Replication B" data, was taken in the period from early June to late December 1972. Thus, it is possible, and even necessary to the proper documentation of this report, to compare the maximum surface deflection (i.e., the vertical displacement measured between the load wheels of the Dynaflect) on three (averaged) dates: March 1966, February 1972, and July 1972.

The comparison is presented graphically in Figure 15, wherein data from the nine test sections on each embankment have arbitrarily been arranged from left to right in descending order of their March 1966 deflection. (To assist the reader in interpreting this figure, it is pointed out that the vertical scale of the graph at the top of the figure is double that of the other two, while the three horizontal scales are the same).

For sections on the plastic clay embankment, it can be seen in Figure 15 that Replication B deflections, in 8 out of 9 cases, were less than the Replication A deflections measured earlier in the year, while for sections on the other two embankments the differences between the two sets of 1972 data appear to be somewhat random, with the glaring exception of 3 of the 9 sections on the sandy gravel embankment.

Also apparent in Figure 15 is the fact that the deflections measured in 1972 on sections constructed on the plastic and sandy clay embankments were, with few exceptions, smaller than those measured approximately six years earlier (1966), while the 6-year differences in the case of sections on the sandy gravel embankment apparently were random.

That the 1972 maximum surface deflections were, in the main, smaller for the two finer grained embankments is shown more clearly in Figure 16, where Replication A and B data have been averaged and plotted as a single dashed line. It is equally clear from this figure that, with one exception, the nine sections on the sandy gravel embankment deflected (on the average) about the same amount in 1972 as they did six years earlier.

Values of the differences in deflections visible in Figures 15 and 16 are tabulated in Tables 18 and 19, respectively. A negative sign in the

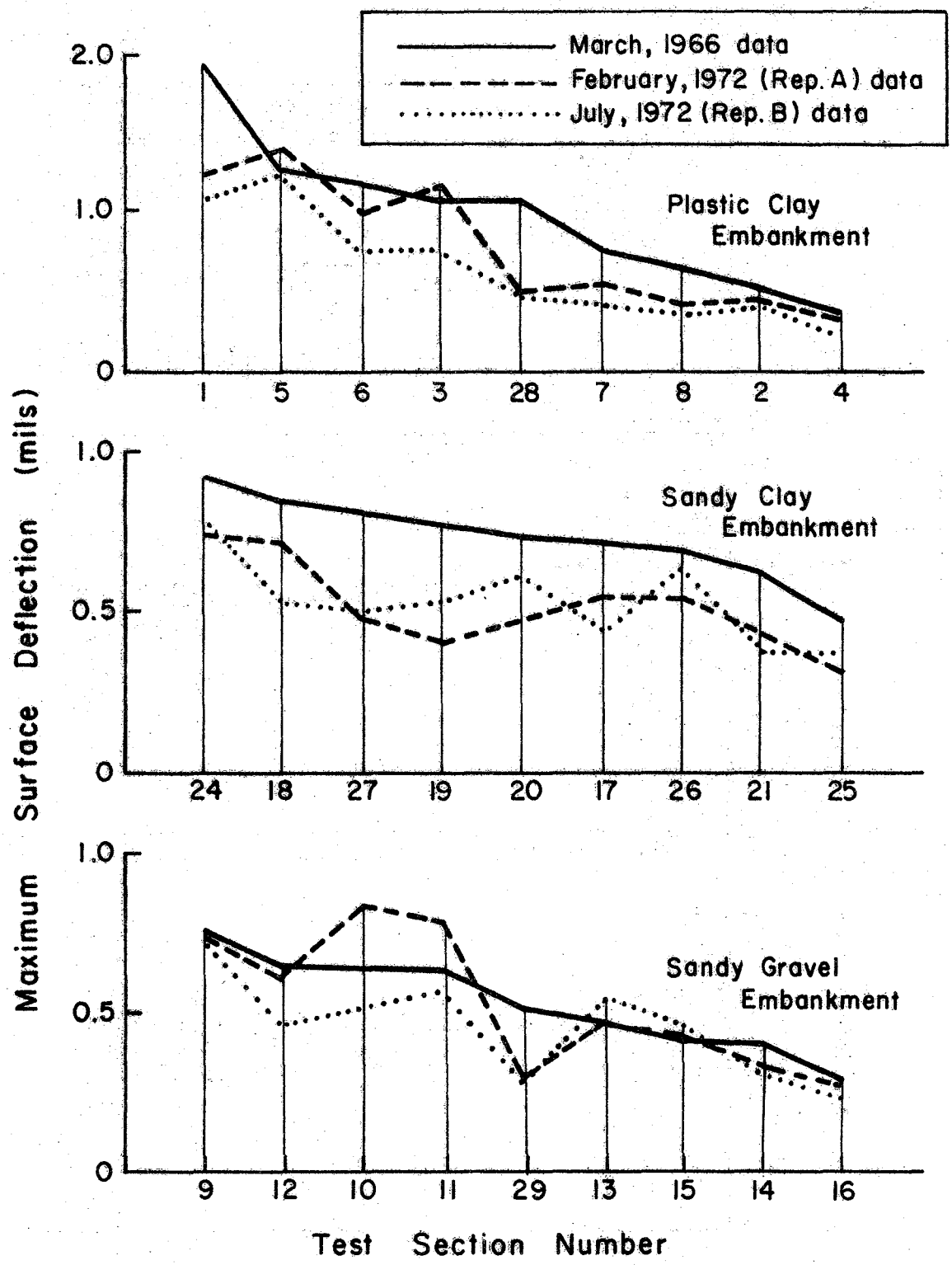

Figure 15: Short- and long-term changes in maximum surface deflections, by embankment type. Months shown for 1972 data are averages of measurement dates extending over several months.

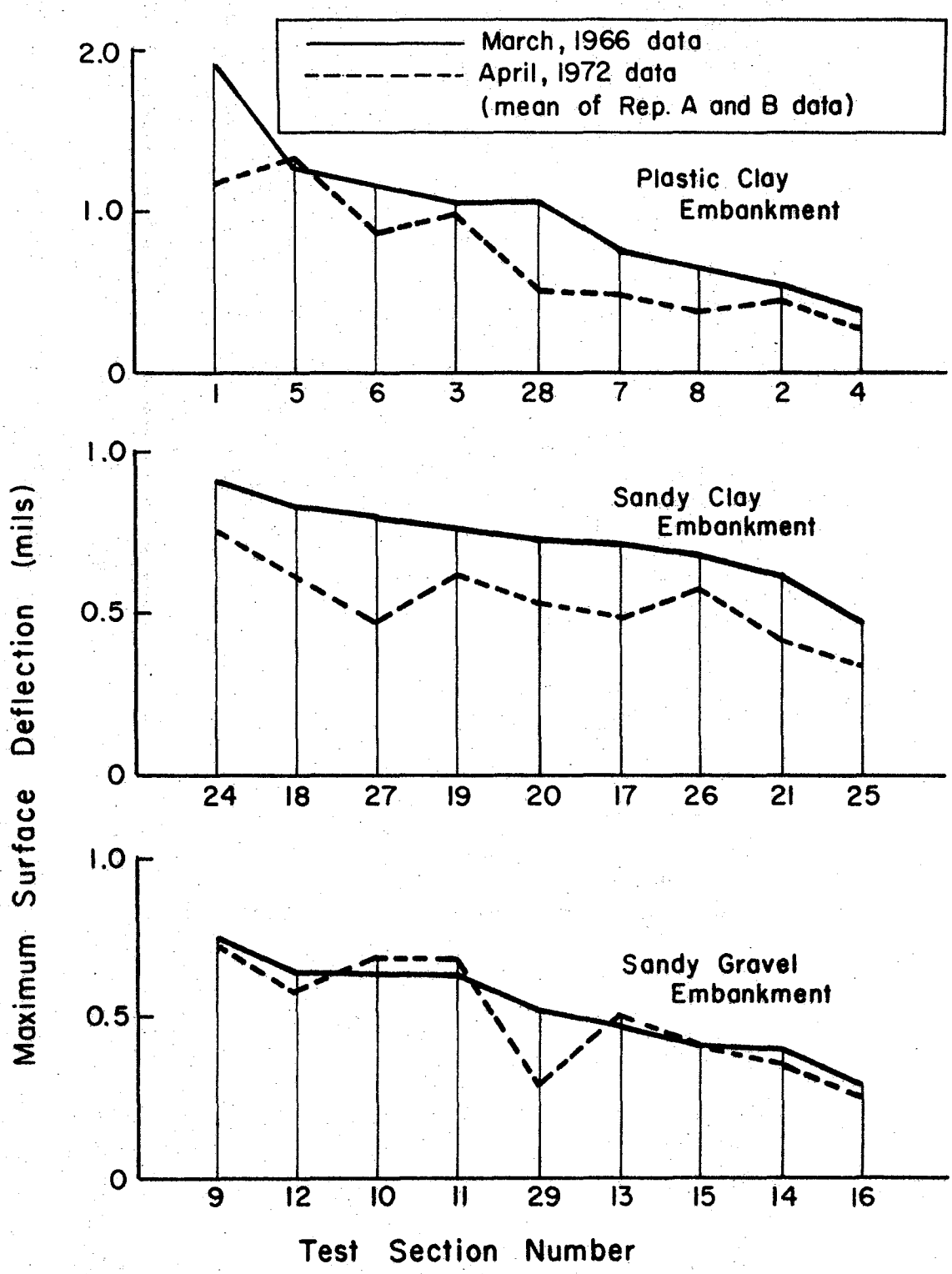

Figure 16: Long-term changes in maximum surface deflections, by embankment type. Month shown for 1972 data is an average of measurement dates extending over approximately one year.

TABLE 18: SHORT-TERM CHANGES IN MAXIMUM SURFACE DEFLECTION AS A FUNCTION OF TIME AND EMBANKMENT MATERIAL

Data Set	Embankment Material	Test Section	Date Tested		Algebraic Difference (Rep. B - Rep. A)	
			Rep. A	Rep. B	Time(days)	Defl. (mils)
1	PC	1	2-28-72	8- 9-72	163	-.14
		2	11-16-71	8-11-72	270	-.05
		3	3- 9-72	8-11-72	155	-.40
		4	3- 3-72	8- 8-72	158	-.12
		5	11-30-71	8- 9-72	254	-.18
		6	11-18-71	8-10-72	267	-.27
		7	3- 8-72	8-10-72	155	-.12
		8	12-13-71	8- 7-72	239	-.06
		28	12-20-71	7-21-72	215	.00
		Mean	1-12-72	8- 7-72	208	-.15
2	SC	17	1-21-72	6- 5-72	136	-.10
		18	2- 9-72	6-18-72	130	-.18
		19	2- 8-72	6-29-72	142	+.03
		20	2-10-72	6-16-72	127	+.14
		21	1-25-72	7- 3-72	160	-.07
		24	1-20-72	6- 6-72	138	+.05
		25	3-10-72	7-20-72	132	+.06
		26	1-17-72	7- 7-72	172	+.12
		27	1-13-72	7-12-72	181	+.02
		Mean	2- 1-72	6-25-72	146	+.01
3	GR	9	3-30-72	9-25-72	179	-.02
		10	3-23-72	8-14-72	144	-.33
		11	3-22-72	8-14-72	145	-.22
		12	3-29-72	9-22-72	177	-.26
		13	3-16-72	8-22-72	159	+.08
		14	3-21-72	8-21-72	153	+.04
		15	3-17-72	8-21-72	157	-.03
		16	3-29-72	8-22-72	146	-.04
		29	1-12-72	7-14-72	184	-.03
		Mean	3-15-72	8-23-72	161	-.09
	Overall Mean		2- 8-72	7-29-72	172	-.08
	Overall Range					
		From	11-16-71	6- 5-72	127	-.40
		To	3-30-72	9-25-72	270	+.14

TABLE 19: SIX-YEAR CHANGES IN MAXIMUM SURFACE DEFLECTIONS AS A FUNCTION OF EMBANKMENT MATERIAL

Date Set	Embankment Material	Test Section	Change In Defl. (mils)
1	PC	1	-.77
		2	-.10
		3	-.09
		4	-.10
		5	+.04
		6	-.30
		7	-.27
		8	-.23
		28	-.57
		Mean	-.26
2	SC	17	-.23
		18	-.23
		19	-.34
		20	-.19
		21	-.22
		24	-.15
		25	-.13
		26	-.10
		27	-.33
		Mean	-.21
3	GR	9	-.01
		10	+.05
		11	+.04
		12	-.06
		13	+.03
		14	-.05
		15	.00
		16	-.04
		29	-.24
		Mean	-.03

last column of either table denotes a decrease in deflection with time, while a positive sign indicates an increase.

In Table 18, as in Figure 15, there may be noted a rather consistent decrease during 1972 that is associated with the plastic clay embankment, a tendency toward no change associated with the sandy clay embankment, and an apparent decrease associated with the sandy gravel embankment. However, in the last case, as already mentioned in the discussion of Figure 15, only three sections (10, 11 and 12) of the nine sections on the sandy gravel embankment exhibited a significant decrease in deflection: in fact, the changes of the remaining six sections were small, and their net change was nil.

Two other significant features of the 1972 testing program are brought out by the testing dates displayed in Table 18, the first being the long time required to complete each of the two sets of replicate measurements, and the second being the considerable variability in the elapsed time between replicate measurements given in the next to last column of the table. As shown in the last line of this column, the time between two replicate measurements on a section ranged from 127 to 270 days, while there was a lapse of 67 days (March 30 to June 5) between the last Replication A measurement and the first Replication B measurement. The mean times of the two sets of measurements differed by 172 days. Thus, the replication error, an important decision criterion to be used in judging the applicability of linear elasticity later in this report, lumps together not only measurement error and spatial variability in material properties, but also temporal variability as well.

In Table 19, which presents long-range changes, each number in the column, "change in Deflection (mils)", was computed for the indicated section by subtracting the mean value of Replication A and B measurements, from the March, 1966 deflection (itself the mean of 6 observations): thus, as in Table 18, a negative sign in Table 19 denotes a decrease in deflection occurring over a period of time.

The average 6-year change in deflection associated with each embankment shown in Table 19 was compared with the average for each of the other two embankments by performing analyses of variance. Results are shown below.

Embankments	F	Probability, P, that Mean Deflection Changes are NOT Different
PC and SC	0.34	$P > 0.500$
PC and GR	6.70	$P < 0.025$
SC and GR	20.56	$P < 0.001$

Thus, even when variations within each of the three sets of data given in Table 19 are considered, it may be concluded with little risk, that the average stiffness of the plastic clay and sandy clay embankments increased by approximately the same amount between 1966 and 1972, while the average change in stiffness of the sandy gravel was significantly less than that of the other finer grained materials, being practically zero.

It is believed that the clearer distinction between the deflection behavior of the three groups of pavements achieved after averaging the Replication A and B data, resulted from "averaging out" the temporal component of the replication error.

If the character of the embankment material is disregarded, the 1966 and 1972 maximum deflections can be compared section-by-section on a single plot, as shown in Figure 17. When the earlier deflections are used to predict the later ones, the following equation, obtained by simple linear regression, results:

$$y = 0.0024 + 0.7848x \tag{14}$$

where x = the average of six observations made in 1966, and

y = the average of two observations made in 1972.

The squared correlation coefficient, R^2, was 0.66 and the standard error, σ, was 0.14. The constant term, 0.0024, is obviously not significantly different from zero, so that the equation may be written as follows:

$$y = 0.785x \tag{14a}$$

with negligible change in the predicted value. Thus, we conclude that when the type of embankment material is ignored, the average 1972 deflections were approximately 78% of the 1966 deflections. Why?

Possible Explanation of Changes of Deflection with Time

The question can be narrowed, according to the previous discussion of Figure 16 and Table 19, to include only sections on the plastic clay and sandy clay embankments, since the average 6-year stiffness change of the gravel embankment was near zero. Why, then, did the finer grained embankment materials stiffen, while the gravel embankment did not? The authors cannot be sure of the answer, because the materials were not examined in 1966, but if water had entered the facility between completion of construction in August, 1965, and the beginning of the first deflection measurements program in March 1966, an answer to the question posed above is possible. The increase in stiffness observed in 1972 may have been caused by the rapid drainage of the facility just before the 1972 measurements program began, which could

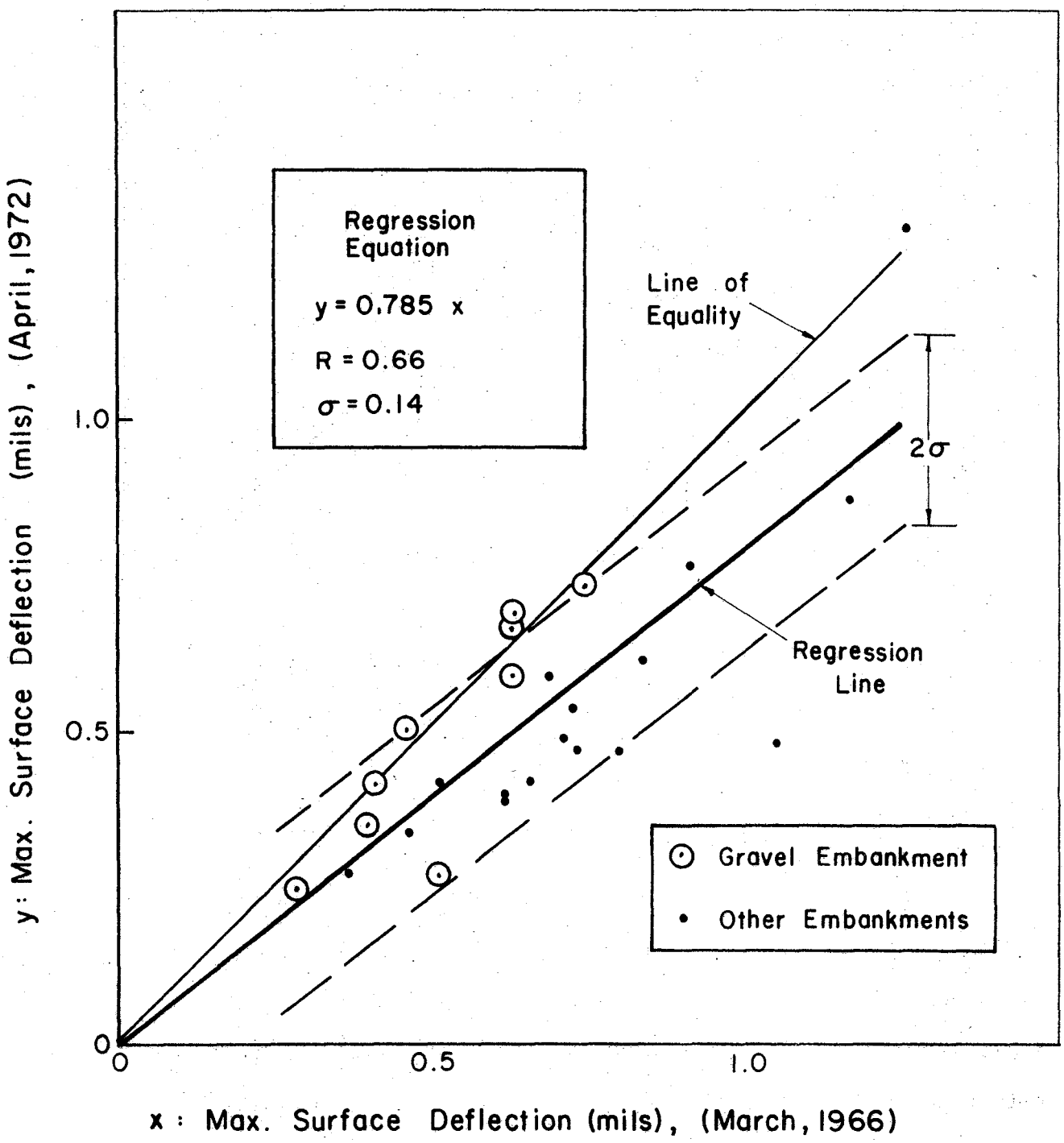

Figure 17: Mean of 1972 maximum deflection data compared with 1966 data. In the regression analysis differences in embankment materials were ingored. Section 1 data were omitted because the 1966 measurement was apparently in error (Reference 9, Fig. 14A).

have resulted in a sudden stiffness increase in both of the finer grained embankments, similar to the quick increase in shear strength of an earth dam resulting from a "rapid drawdown". This sudden stiffness increase was followed by a further, gradual increase in the case of the plastic clay material during the long 1972 testing period. Such a sequence of events could explain the deflection behavior displayed in Figures 15 and 16.

Remaining to be answered is the question: if free water were present in March, 1966, in the previous embankments, and had already softened the plastic clay embankment, why had the swelling of this embankment not produced visible cracking in March, 1966? The authors can only surmise that cracking had begun in the subbase, and perhaps also in the base, but had not yet penetrated the surfacing material which, as previously mentioned, was an unusually "tender" mix that had been rolled just prior to the start of the 1966 testing program. Such a mix could have yielded to larger lateral strains without cracking than a harder mix: furthermore, if cracking were present at the bottom of the mat, the rolling could have closed them. Later, after sufficient exposure to air and actinic radiation from the sun had hardened the asphalt binder, and after some further shifting of the plastic clay embankment had presumably further increased the width of cracks in the underlying subbase and base, the longitudinal cracking of the surfacing material occurred.

The theory that excess water was present in the embankments as of March, 1966, requires that an ample supply of water was available from rainfall in the months of September, 1965, through February, 1966, i.e., in the period following completion of construction to the beginning of the 1966 testing.

Weather records show that 30.6 inches of rain fell in the vicinity of the pavement testing facility during this 6-month period, as opposed to a normal rainfall of 18.2 inches for the same period. Thus, actual rainfall was 12.4 inches, or 69% , above normal. Nearby roadway drainage ditches across the north end and along the east edge of the facility could have been a major source of the water that, according to the theory proposed above, entered the gravel embankment, which then served as an aquafer to carry water to the adjacent materials.

An alternate theory might be advanced, namely, that the measurements system read deflections that were too high in 1966, or too low in 1972, through an error in calibration. This explanation seems to be ruled out by the fact that 8 of the 9 sections on the embankment composed of sandy gravel - the one embankment material that would be least affected by water - had average deflections in 1972 that were nearly the same as in 1966. This is clearly demonstrated in Figure 17, where 8 of the 9 circled points appear to cluster about the line of equality drawn on the graph.

5. LINEAR ELASTICITY APPLIED TO STUDY 136 DISPLACEMENT DATA

Before launching an attack upon the problem of how to analyze the displacement data of Study 136 in the context of linear elasticity, it seems pertinent to review briefly the background information previously presented.

Summary of Background Information

In preceeding chapters the specially developed measurement system and the Dynaflect loading method used in Study 136 were described. An argument based on published data was presented with the intention of showing that the vibrating, 1,000-lb. peak-to-peak Dynaflect load was equivalent to a fast-moving wheel load of 1000 pounds dead weight, a result suggesting that the supporting materials must have possessed visco-elastic rather than linear-elastic properties, or that the effect of inertia on the deflections was greater than is usually assumed. The rejection of linear elasticity in favor of visco-elasticity and/or non-linear elasticity by a number of pavement researchers, was reported. In favor of the use of linear elasticity, special analyses of AASHO Road Test published data were presented which indicated that in full scale experiments, pavement surface deflections can be regarded as directly proportional to load if replication error is accurately known, if this error is used as a practical decision criterion, and if the materials have not recently been subjected to the disruptive action of a severe freeze-thaw cycle.

Also reported were disruptive forces acting on the materials in the TTI Pavement Test Facility as evidenced by the following series of events: the early discovery of longitudinal cracking, the later discovery of free water in the more pervious materials, the swelling of the plastic clay embankment resulting from the presence of the free water, and the subsequent drainage of the facility prior to collection of the Study 136 data. Based in part on these events, a theory was proposed (with some misgivings because of lack of certain

essential data) intended to explain certain large discrepancies between surface deflections measured on the TTI facility in 1966 and those measured in 1972. Because some of these 1972 surface deflections form a small but important subset of the displacement data to be analyzed in this chapter, the discrepancies noted above--as well as the post-construction changes in the materials--seemed to point toward failure of linear elasticity as a model. Such, however, was not the case, at least in the opinion of the authors.

Decisions Required Prior to Analysis

The following decisions had to be made prior to performing the analysis.

1. Selection of a Decision Criterion For Acceptance or Rejection of the Model: As stated in the introductory chapter, replication error was selected to define the allowable prediction error of the model.

2. Choice of Type of Data (Rep. A, Rep. B, or The Mean of The Replicated Measurements): It was decided to use the mean of the Replication A and Replication B data for the analysis. This decision automatically required that the replication error at a point be defined as one-half the algebraic difference between the values measured in the Replication A and the Replication B measurement programs.

The use of the mean of replicate measurements of the displacements, u and w, also led to use of the mean of replicate measurements of layer thickness, rather than the planned thickness.

3. Choice of Data Points: Data points selected were located at the interfaces (excepting the interface at 90" between the plastic and the dense clay where measurements were not available), and in addition within the embankment at z=41 in., and within the plastic clay foundation at z=65 in. The r coordinates were 10 in., 26 in., and 49 in. Figure 5 shows a typical grid of data points (page 10).

4. Choice of the Dependent Variable (u or w): A prior study of the displacements indicated that measurements of w were larger and more reliable than measurements of u (p.29, Ref. 3). It was therefore decided to use the prediction error in w, rather than u, as the error to be minimized, although prediction errors in both variables would be used in making the decision to accept or reject linear elasticity as a model.

5. Choice of Layered System Computer Program: While a number of linear elastic layered system computer programs were available, the authors' familiarity with and confidence in BISTRO* led to the use of this program in the analysis (11).

6. Choice of Poisson's Ratio: Poisson's ratio was taken as 0.40 for the plastic clay (PC), the dense clay (DC), and the sandy clay (SC), and as 0.25 for the remaining five materials (AC, LS, LS+L, LS+C, and GR).

7. Choice of Trial Values of Moduli: The analysis plan, an iterative process, required initial estimates of the moduli of eight materials. Estimates were made on the basis of past experience in the use of the Dynaflect for estimating the moduli of similar materials in two-layer systems (11),and on the advice of Mr. Gilbert Swift, who had previously made estimates of the moduli of the materials in the test facility. It is reiterated here that these were dynamic moduli of materials in situ, and were greater than would be measured by some current laboratory procedures.

8. Selection of Sections: The following restrictions were placed on the choice of sections.

   a. The number of sections had to be limited to a fraction of the 27 available in the statistically designed experiment, for reasons of economy already given. Seven were selected.

---

* - Koninklijke/Shell-Laboratorium, Amsterdam.

b. Among the seven designs selected, each of the seven compacted materials above the natural foundation had to appear at least twice (i.e., in two different sections) so that the expected spatial variation in the properties of each material could contribute to the prediction error of the model. Otherwise there would exist the possibility of bias in favor of the model.

c. The seven designs had to be capable of being placed in an ordered array, such that any design in the array, except the first, contained at the most two materials not previously appearing in the array. This requirement would permit temporary values of the moduli of the first design to be established by iteration. These values could then be carried forward to the second design, the analysis of which would require only one iteration if the materials were the same as those in the first design, or a relatively few iterations if the second design contained one or two new materials. By the same token, it would be possible to pass from the second to the third design, etc., until all seven designs had been processed. Precise details of the analysis plan will be presented later.

d. Finally, the seven selected sections had to have replication errors covering approximately the range observed on the full experiment of 27 sections. This restriction would prevent the inadvertant selection of a decision criterion that was either unduly restrictive or unrealistically liberal.

Treatment of Thin Surfacing Layers

Seven sections meeting the above-mentioned requirements, their planned designs, and the order in which they were arranged for analysis, are shown in Table 20. Indicated by foot-note in that table is the fact that in the case

Table 20: Design Data and Order in Which Analyses Were Performed

	Layer	Identification and Design Data						
Section Index, j	-	1*	2	3	4*	5*	6*	7
Section Number	-	3	1	5	14	15	18	27
Materials:	1	AC	AC	AC	AC	AC	AC	AC
	2	LS+C	LS+C	LS	LS+C	LS+C	LS+L	LS+L
	3	LS	LS	LS+C	GR	GR	SC	LS+C
	4	PC	PC	PC	PC	PC	PC	SC
	5	DC	DC	DC	DC	DC	DC	PC
	6	--	--	--	--	--	--	DC
Design Thickness (in.):	1	1	5	5	1	1	1	3
	2	4	4	4	16	16	16	8
	3	12	4	4	36	36	36	8
	4	73	77	77	37	37	37	34
	5	∞	∞	∞	∞	∞	∞	37
	6	--	--	--	--	--	--	∞
No. New Materials:		4	1	0	1	0	2	0
No. Iterations, 1st Run		1	1	1	2	1	1	1
No. Iterations, 2nd Run		1	1	1	1	1	1	1

* - Layers 1 and 2 were treated as a single material in this section. The modulus found for the combination was assigned to the material in the second layer (LS+C or LS+L). See text for explanation.

of a section having a design thickness of only one inch of asphaltic concrete surfacing, the thickness of the surfacing was added to that of the material beneath it, and the combined thickness was treated as a single material in the analysis. In each such case (j=1, 4, 5 and 6), the composite modulus of the two materials was assigned to the underlying material, which was from 4 to 16 times as thick as the asphaltic concrete. The decision to combine layers was based on past studies which indicated that modular values of thin surfacing layers could be only vaguely estimated from Dynaflect data.

With sections having a one-inch surfacing eliminated, only sections with 3-in. and 5-in. surfacings (j=2, 3 and 7 in Table 20) remained for estimating a modulus for asphaltic concrete.

(The data shown in the last two lines of Table 20 will be discussed in connection with the detailed analysis plan and the results.)

Symbols Appearing in Analysis Plan

Symbols used in the analysis plan are defined below in the order in which they appear in the plan.

j=an index number assigned to a test section (See Table 20). It designates the order in which the sections are analyzed, (j=1, 2, ..., 7).

E_i'=a trial value of the modulus of the material constituting the ith layer of a selected section.

$u_{jk}\ (E_1', E_2', \ldots)$ or $w_{jk}\ (E_1', E_2', \ldots)$ = the value of u (or w) computed by BISTRO at the K^{th} nodal point of the j^{th} section, using the trial values, $E_1', E_2', \cdots$. $(k=1,2, \cdots, N_j)$.

u_{jk} (or w_{jk})= the value of u (or w) measured at the k^{th} nodal point of the j^{th} section.

A_j and B_j= regression constants applying to the j^{th} section.

E_i="the adjusted moduli" corresponding to E_i' for a selected section. In general, $E_i=E_i'/B_j$.

$\bar{E}$=the average of all the adjusted moduli of a selected material determined in one "run" through the first 16 steps of the analysis plan. One run provides 8 values of $\bar{E}$.

$u_{jk}(\bar{E}_1, \bar{E}_2, \cdots)$ or $w_{jk}(\bar{E}_1, \bar{E}_2, \cdots)$ = the value of u (or w) computed by BISTRO at the k^{th} nodal point of the j^{th} section, using the appropriate values of $\bar{E}$ as noduli in the j^{th} section.

$PE_j(u)$ or $PE_j(w)$= prediction error in u (or w) of the linear elastic model for the j^{th} section. These errors can be compared with the corresponding replication errors. Computing formulas are given in Step 11 of the analysis plan.

$RE_j(u)$ or $RE_j(w)$=replication error in u (or w) associated with the j^{th} section. Computing formulas are given in Step 12 of the analysis plan.

PE(u), PE(w), RE(u), and RE(w) are the combined prediction and replication errors in u and w for all seven sections included in the analysis. The combined prediction errors can be compared directly with the corresponding combined replication errors.

Analysis Plan

A step-by-step presentation of the analysis plan is given below. Though written in the style of a preliminary outline of a computer program, the plan was not computerized because at some points in the procedure it was felt that intuitive decisions would have to be made, particularly at points requiring changes in moduli to secure better agreement with the measured data.

One pass through the 16 sequential steps of the plan is designated as one "run." Only two runs were made, as indicated at the bottom of Table 20, and

in only one case (Run 1, j=4) was more than one iteration per section necessary. There was some indication, however, as will be evident later, that had funds been available, at least one more run might have resulted in smaller prediction errors in some sections.

The sixteen-step analysis plan follows.

1. Select for analysis the j^{th} section of the seven shown in Table 20. (The initial value of j is 1). If all the materials in the j^{th} section have appeared in sections previously analyzed, go to Step 3. Otherwise go to next step.

2. Estimate the modulus of the material (or materials), E_1', where i is the index of the layer in which a new material occurs.

3. Using BISTRO, compute values of $u_{jk}(E_1', E_2', \cdots)$ and $w_{jk}(E_1', E_2', \cdots)$ at the N_j nodes of the measurement grid of the j^{th} section.

4. Regress the observed values, w_{jk}, of the vertical displacement, on the computed values $w_{jk}(E_1', E_2', \cdots)$, obtaining the linear equation for estimating w_{jk}:

$$w_{jk}=A_j + B_j\, w_{jk}(E_1', E_2', \cdots),$$

where A_j and B_j are constants associated with the j^{th} section only. Compute the statistics, R^2 and standard error, associated with the above equation applying to the j^{th} section. If no new material has been included in the j^{th} section, go to Step 6. Otherwise, go to the next step. (The number of new materials in each section is shown in Table 20.)

5. If the results obtained from the regression analyses performed in Step 4 are unsatisfactory ($R^2 < 0.80$, standard error much greater than the replication error of the j^{th} section), return to Step 2: otherwise, go to the next step. (The number of iterations required for each section is shown in Table 20.)

6. Compute a set of adjusted moduli, E_i for the j^{th} section from the equation, $E_i=E_i'/B_j$. (The reason for making this adjustment will be explained later.)

7. Increment j, and return to Step 1, repeating the cycle Steps 1 through 7, until all seven sections have been processed. Then go to the next step.

8. Select any one of the eight materials. Average the several values of the adjusted moduli of the selected material. Represent the average adjusted modulus of the material by the symbol $\bar{E}$.

9. Repeat Step 8 for the remaining seven materials, thus obtaining an average adjusted modulus, $\bar{E}$, for each of the eight materials.

10. Using BISTRO, and values of $\bar{E}$ instead of the values of E' used in Step 3, compute $u_{jk}(\bar{E}_1, \bar{E}_2, \cdots)$ and $w_{jk}(\bar{E}_1, \bar{E}_2, \cdots)$ at the nodal points of all seven sections.

11. Compute $PE_j(u)$ and $PE_j(w)$, the prediction errors in u and w, respectively, for the j^{th} section, from the following equations:

$$PE_j(u)= \{(1/N_j) \sum_{K=1}^{N_j} [u_{jk}-u_{jk}(\bar{E}_1, \bar{E}_2, \cdots)]^2\}^{1/2}$$

$$PE_j(w)= \{(1/N_j) \sum_{K=1}^{N_j} [w_{jk}-w_{jk}(\bar{E}_1, \bar{E}_2, \cdots)]^2\}^{1/2}$$

Repeat for all seven sections.

12. Compute $RE_j(u)$ and $RE_j(w)$, the replication errors in u and w, respectively, for the j^{th} section, from the following equations:

$$RE_j(u)=\{(0.25/N_j) \sum_{K=1}^{N_j} [u_{jk}(\text{Rep.A}) - u_{jk}(\text{Rep. B})]^2\}^{1/2}$$

$$RE_j(w)=\{(0.25/N_j) \sum_{K=1}^{N_j} [w_{jk}(\text{Rep. A}) - w_{jk}(\text{Rep. B})]^2\}^{1/2}$$

where the abbreviations, "Rep. A" and "Rep. B" indicate the source, Replication A

or Replication B, of the measured displacements, u_{jk} and w_{jk}. Repeat for all seven sections.

13. Compute PE(u), the overall prediction error for the group of seven sections, from the formula

$$PE(u)= \{(1/M) \sum_{j=1}^{M} N_j[PE_j(u)]^2\}^{1/2},$$

where $M= \sum_{j=1}^{7} N_j$.

14. Compute the overall errors PE(w), RE(u), and RE(w) by substituting, in turn, $PE_j(w)$, $RE_j(u)$, and $RE_j(w)$, for $PE_j(u)$ in the formula given in Step 13.

15. Compare the prediction errors with the replication errors, section by section.

16. Compare the overall prediction errors with the overall replication errors. Steps 1 through 16 constitute one "run." If the results of Step 16 are not satisfactory, use the values of $\bar{E}$ computed in Steps 8 and 9 as starting values and perform another run, excepting the computation of replication errors in Steps 12 and 14, which need be computed only once. If the results of Step 16 are satisfactory, stop.

The Adjusted Moduli, E_i

The analysis plan ends with Step 16. Remaining to be explained is why the adjustment, made in Step 6, of the modulus, E_i', is necessary. We begin by recalling that in Step 4, a simple linear regression analysis is performed, with observed value, w_{jk}, as the dependent variable, and the BISTRO value, $w_{jk}(E_1', E_2', \cdots)$ as the independent variable. The resulting equation is

$$\hat{w}_{jk}=A_j + B_j\, w_{jk}(E_1', E_2', \cdots). \qquad (a)$$

Ideally, A_j would be zero, and B_j would be unity in Equation (a),

but this never happens: instead, $A_j \neq 0$ and $B_j \neq 1$, though both may, in some cases, be near their ideal values.

Now a fundamental consequence of linear elastic theory can be expressed as follows:

$$w_{jk}(E_1'/B_j, E_2'/B_j, \cdots) = B_j w_{jk}(E_1', E_2', \cdots) \qquad (b)$$

(For example, if one halves the modulus of every material in a linear elastic layered system without changing any other parameter, he will surely double the displacement at every point in the structure. For this example, $B_j=2$).

In view of Equation (b), we may write Equation (a) in the following form:

$$\hat{w}_{jk} = A_j + w_{jk}(E_1'/B_j, E_2'/B_j, \cdots), \qquad (c)$$

or, since E_i is, by definition, equivalent to E_i'/B_j, Equation (c) becomes

$$\hat{w}_{jk} = A_j + w_{jk}(E_1, E_2, \cdots). \qquad (d)$$

where $E_1, E_2, \cdots$ are the adjusted moduli of the j^{th} section. Furthermore, because of the equivalence of E_i and E_i'/B_j, Equation (b) can be written as follows:

$$w_{jk}(E_1, E_2, \cdots) = B_j w_{jk}(E_1', E_2', \cdots) \qquad (e)$$

From Equation (e) one could compute N_j values of $w_{jk}(E_1, E_2, \cdots)$, once Steps 4 and 5 are completed, since the quantities on the right side of the equation would be available. If one should then plot the N_j observed values, w_{jk}, as ordinates, versus the N_j computed values, $w_{jk}(E_1, E_2, \cdots)$, as abscissas, he would find that the points would tend to scatter about a line with a slope of 1.0 (or 45°), with an intercept of A_j. Clearly, then, $w_{jk}(E_1, E_2, \cdots)$ is a better estimate of the measured value, w_{jk}, than $w_{jk}(E_1', E_2', \cdots)$. Therefore, the adjusted moduli, E_i, are better estimates than the trial moduli, E_i'. It was for this reason that the adjusted moduli were calculated in Step 6,

and later (in Steps 8 and 9) averaged to obtain a modulus, $\bar{E}$, to represent each of the eight materials involved in the analysis.

With regard to the hypothetical plot mentioned in the preceeding paragraph, it can be shown that if the least-squares, best fitting line through these data were determined by regression, the equation for the regression line would be Equation (d). Furthermore, the statistics, R^2 and standard error, associated with Equation (d), would have precisely the same values as the R^2 and standard error associated with Equation (a) and available from Step 4. These relationships between Equations (a) and (d) insure that if good agreement between observed and BISTRO-computed values is obtained in Step 4, using the trial moduli, E_i', then an equally good fit would have been achieved if the adjusted (and more accurate) moduli, E_i, had been used in BISTRO. This fact justifies the use of the R^2 and the standard error computed in Step 4, as decision criteria in Step 5.

Results of the Analysis

As indicated in the last two lines of Table 20, only two runs through the 16-step analysis plan were completed. Trial values of moduli used in the first run are shown in the second column of Table 21, and the values of $\bar{E}$ resulting from the first run are given in the third column. The latter (third column) values were used as trial values for a second run. The second run, in turn, resulted in a new set of values of $\bar{E}$, given in the fourth column of Table 21, which could have been used as starting values for a third run. However, after comparing the overall prediction errors of the second run with the corresponding replication errors, and after noting the rather slow convergence of the moduli (as demonstrated in Table 21), it was decided not to expend further funds in continuing the analysis.

Table 21: Trial Moduli, E', and Mean

Adjusted Moduli, $\bar{E}$, in Pounds per Sq. In.

Material	Trial Modulus, E', For First Run	Mean Adjusted Modulus, $\bar{E}$, for First Run, and Trial Modulus, E', for Second Run	Mean Adjusted Modulus, $\bar{E}$, for Second Run, and Trial Modulus, E', for Third Run*
AC	150,000	141,200	138,100
LS+C	500,000	469,800	462,700
LS+L	180,000	189,300	194,800
LS	100,000	86,000	79,500
GR	50,000	49,200	50,500
SC	30,000	31,600	32,500
PC	13,000	12,400	12,200
DC	50,000	47,500	46,700

* - Third run was not made because of slow convergence of $\bar{E}$, indicated by this table. The first run values of $\bar{E}$ were used to compute the reported prediction errors (Figure 18).

Given in Table 22 are the results of the regression analyses of observed values of w on values computed from BISTRO in Step 4 of the second (and final) run. The values of R^2 are generally high, as judged by ordinary standards. The absolute value of A (which may be considered a part of the prediction error), and the value of the standard error, are less than the section replication error (computed in Step 12) in 4 cases and greater in 3, the latter being the cases, j=4, 5 and 7. The average values of A and B are near their ideal values of zero and one, respectively, an apparent indication that the analysis plan is capable of seeking out the set of eight moduli that result in the best agreement between computed and measured values of w in all the sections analyzed.

For example, in Figure 18, which is a general summary of the analysis results, it may be seen that the combined prediction errors, listed in the "All Sections" column of the error tables, are not very different from the combined replication errors shown in the same column. We therefore conclude that, in accordance with the decision criterion adopted from the beginning of this report, linear elesticity is acceptable as a model of the displacements measured in the seven-section sample of the 27 sections making up the statistically designed experiment of the TTI Pavement Test Facility.

Each of the overall errors, expressed in mils in the "All Sections" column of Figure 18, can be expressed in another, and perhaps more meaningful way, namely, as a percentage of the average absolute value of the appropriate measured displacement appearing in the box at the bottom of the "All Sections" column. The percentage errors are given below.

Rep. Error in w=16% of average absolute measured value.

Pred. Error in w=18% of average absolute measured value.

Rep. Error in u=28% of average absolute measured value.

Pred. Error in u=40% of average absolute measured value.

Table 22: Results of regressions of observed values of w on values computed from BISTRO in Step 4 of Run 2. Replication error is given for comparing with standard error and |A|.

Section Index, j	No.	A	B	R^2	Standard Error (Mils)	Replication Error (Mils)
1	3	-.046	1.084	0.997	0.015	0.098
2	1	.025	0.940	0.982	0.052	0.078
3	5	-.028	1.272	0.984	0.057	0.097
4	14	.033	0.846	0.913	0.021	0.012
5	15	-.014	1.147	0.875	0.043	0.023
6	18	.026	1.025	0.924	0.043	0.045
7	27	.029	0.924	0.837	0.050	0.009
Average		.004	1.034	0.930	0.040	0.052

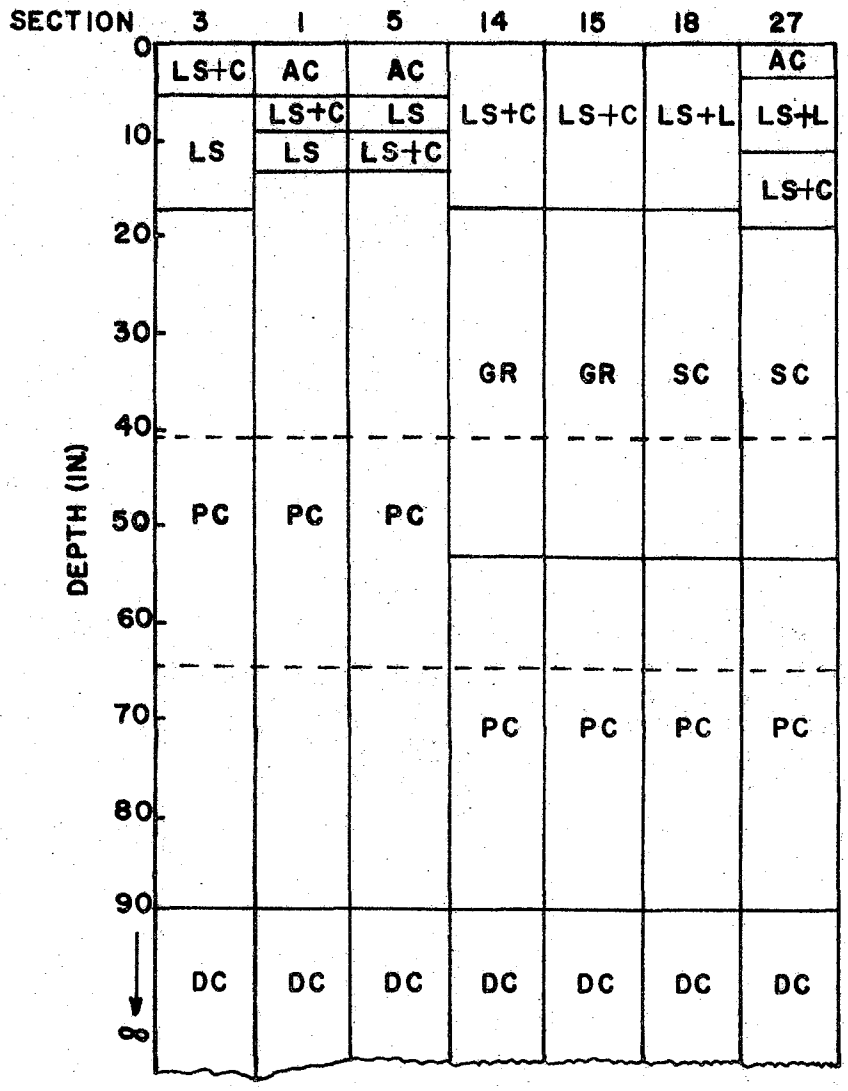

MATERIAL	MODULUS (PSI)
AC	141200
LS+C	469800
LS+L	189300
LS	86000
GR	49200
SC	31600
PC	12400
DC	47500

ERRORS (MILS)

W DATA

	3	1	5	14	15	18	27	ALL SECTIONS
REP.	.10	.08	.10	.01	.02	.05	.01	.063
PRED.	.03	.06	.16	.02	.05	.05	.05	.071

U DATA

	3	1	5	14	15	18	27	ALL SECTIONS
REP.	.01	.02	.02	.01	.01	.01	.01	.012
PRED.	.02	.02	.02	.02	.02	.02	.02	.017

MEASURED AVERAGE ABSOLUTE VALUES (MILS)

	3	1	5	14	15	18	27	ALL SECTIONS
W	.46	.56	.65	.23	.25	.34	.30	.398
U	.06	.08	.06	.02	.02	.04	.03	.043

Figure 18: Section designs, moduli used in BISTRO, prediction errors, replication errors, and average absolute measured values.

The fact that the percentage replication error in w is smaller than in u is attributed to the fact, mentioned earlier in connection with the decision to use w as the dependent variable, that measured values of u were less reliable than measured values of w.

The fact that better agreement was achieved between the percentage prediction error and the percentage replication error in w than in u is attributed both to the greater reliability of measured values of w and to the fact that w was used as the dependent variable in the analysis: that is, the analysis was aimed at minimizing the difference between measured and BISTRO-computed values of w, rather than of u.

Use of Subjective Criteria For Judging The Results of The Analysis

Readers who would rather base an opinion of the suitability of the model on plots of the measured and predicted values of u and w, are referred to Figures 19 through 29.

Plotted values of u appear in Figures 19 through 22, section by section: plotted values of w are shown in Figures 23 through 29.

In each section graph the measured displacement u (or w), and the corresponding BISTRO-computed value of the displacement, both expressed in micro-inches, are plotted against the depth, z, in inches. Points having the same coordinate, r, are joined by straight lines.

Also shown in each graph is a distance, in micro-inches, equal to the measured replication error in u (or w), for visual comparison with differences between measured and computed points.

Tabulated Data

Table 23, in the Appendix, contains the basic measured data, i.e. the Replication A and Replication B data. For use in the analysis, these data were

averaged, and the averaged values were recorded in Table 24, also located in the Appendix. Table 24, in addition to showing the measured mean values, likewise gives the corresponding BISTRO-computed values.

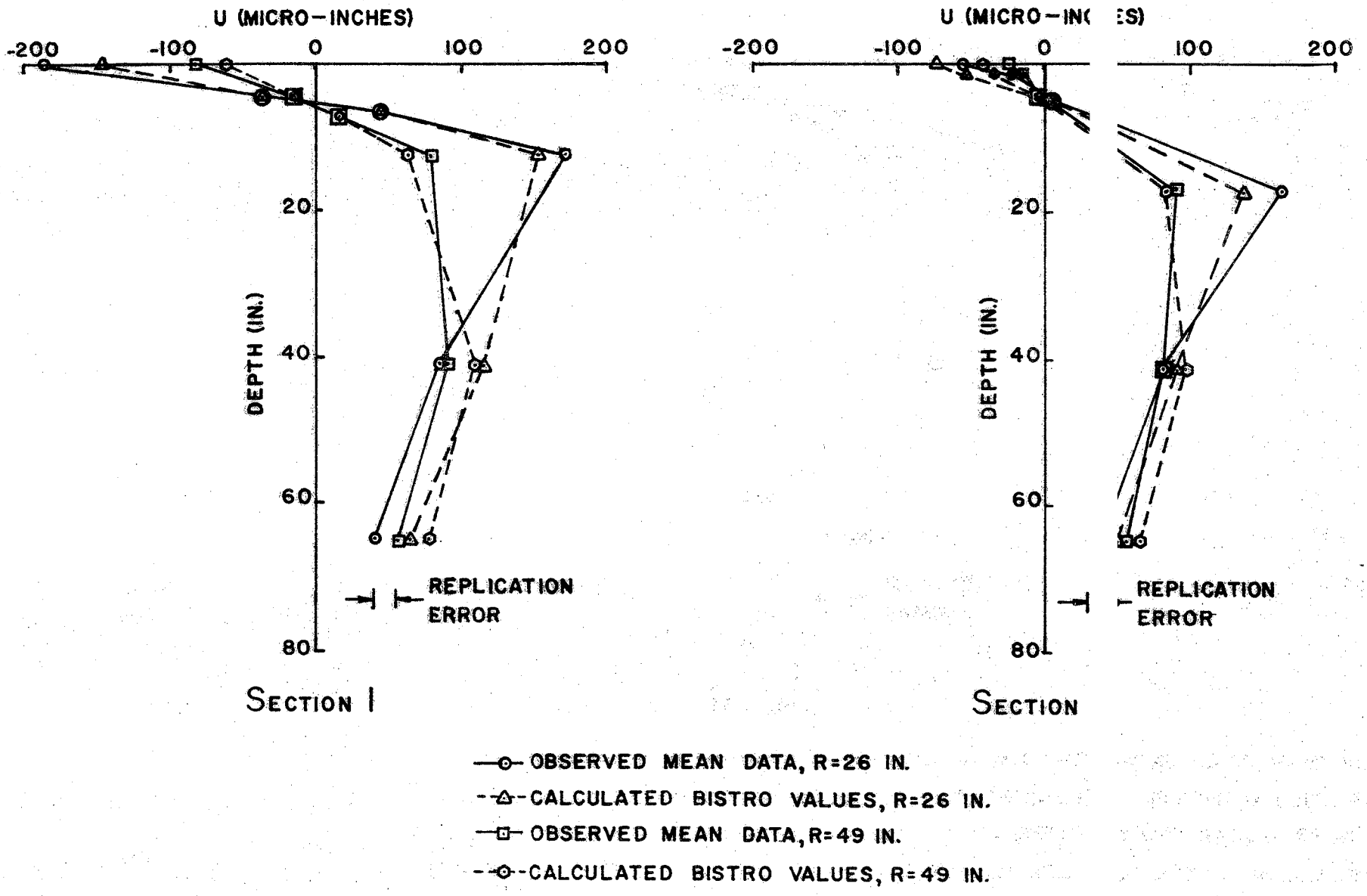

Figure 19: Observed and computed values of u, Sections 1 and 3, plotted versus depth.

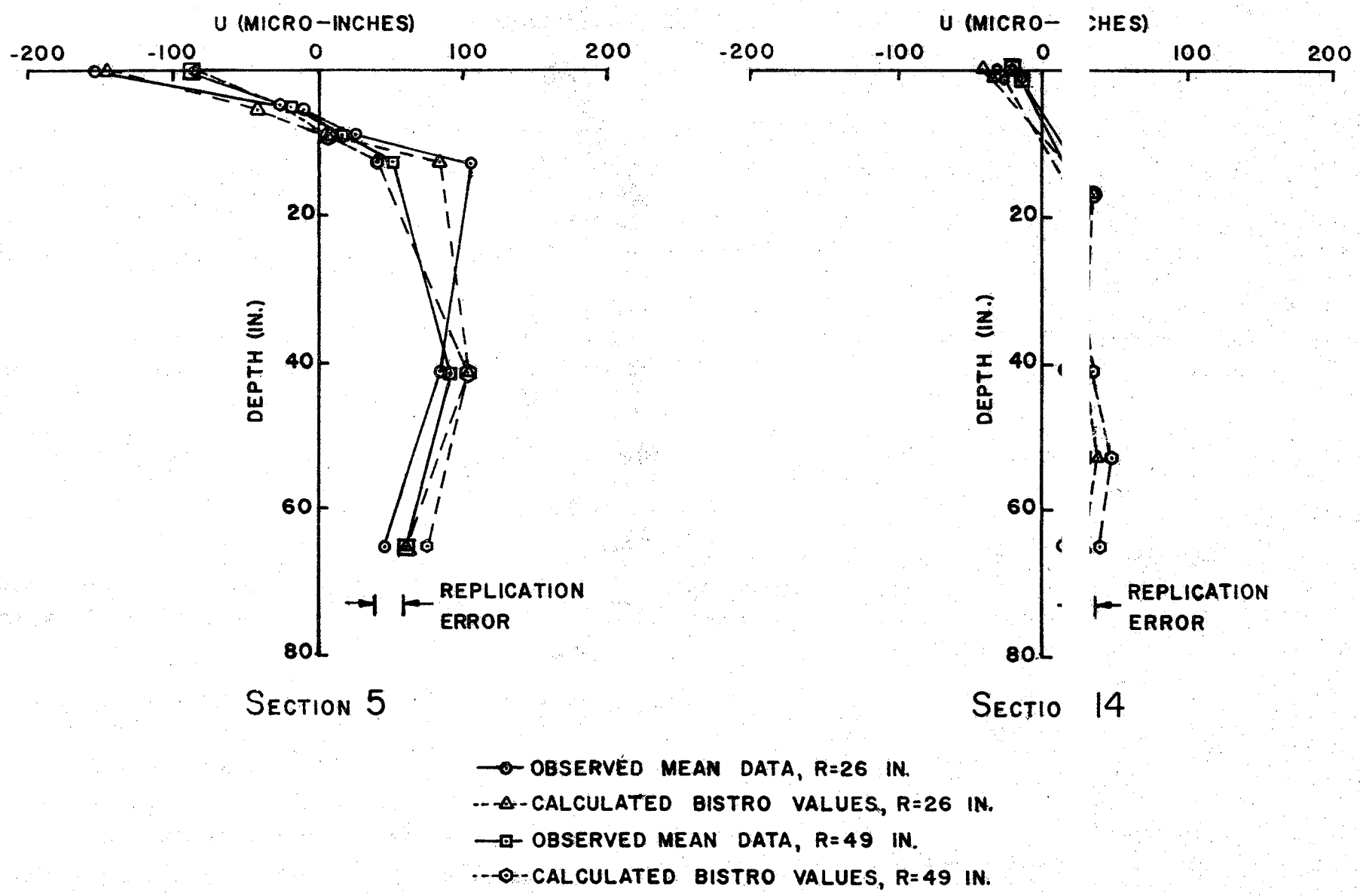

Figure 20: Observed and computed values of u, Sections 5 and 4, plotted versus depth.

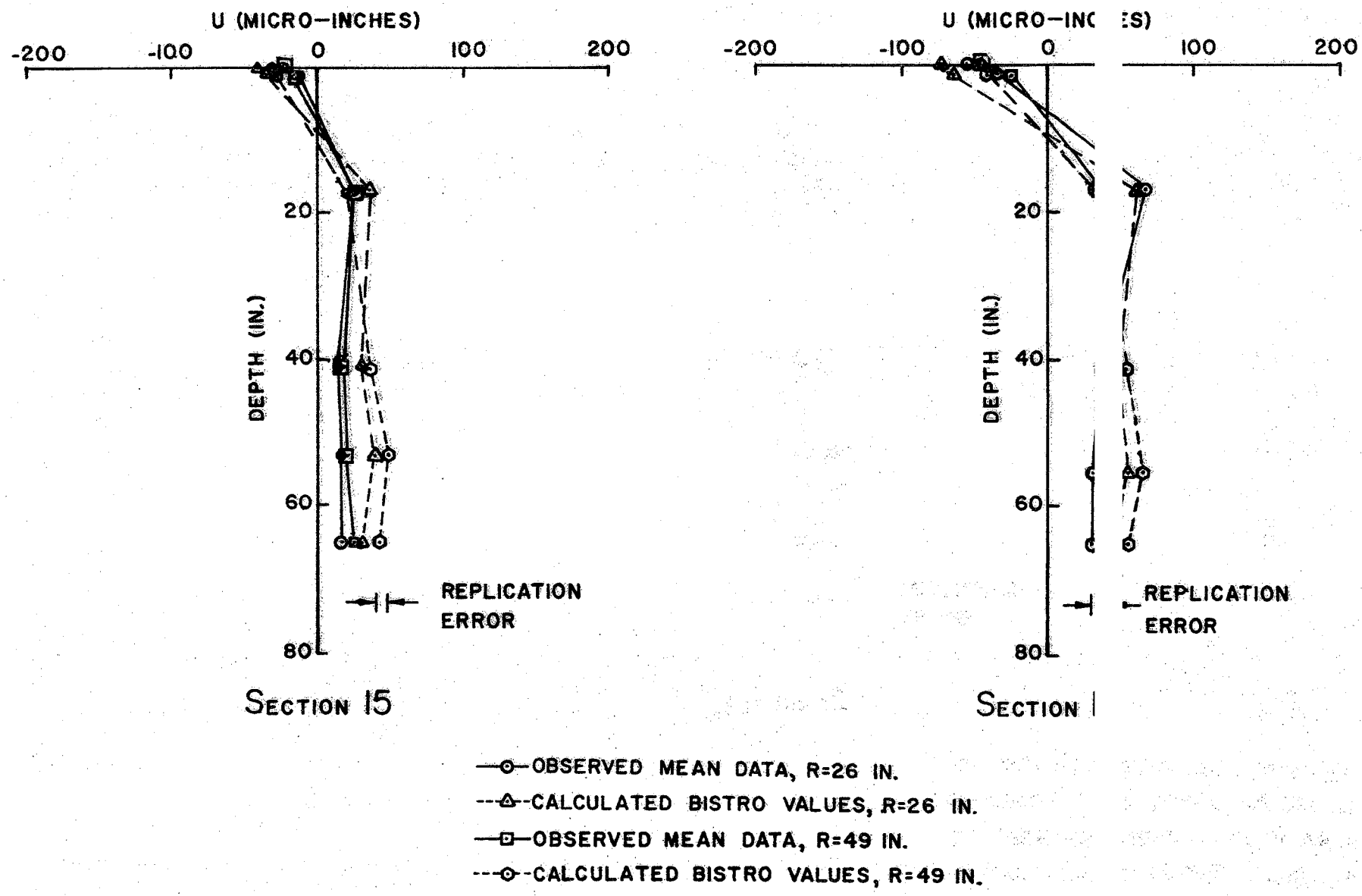

Figure 21: Observed and computed values of u, Sections 15 and 1 plotted versus depth.

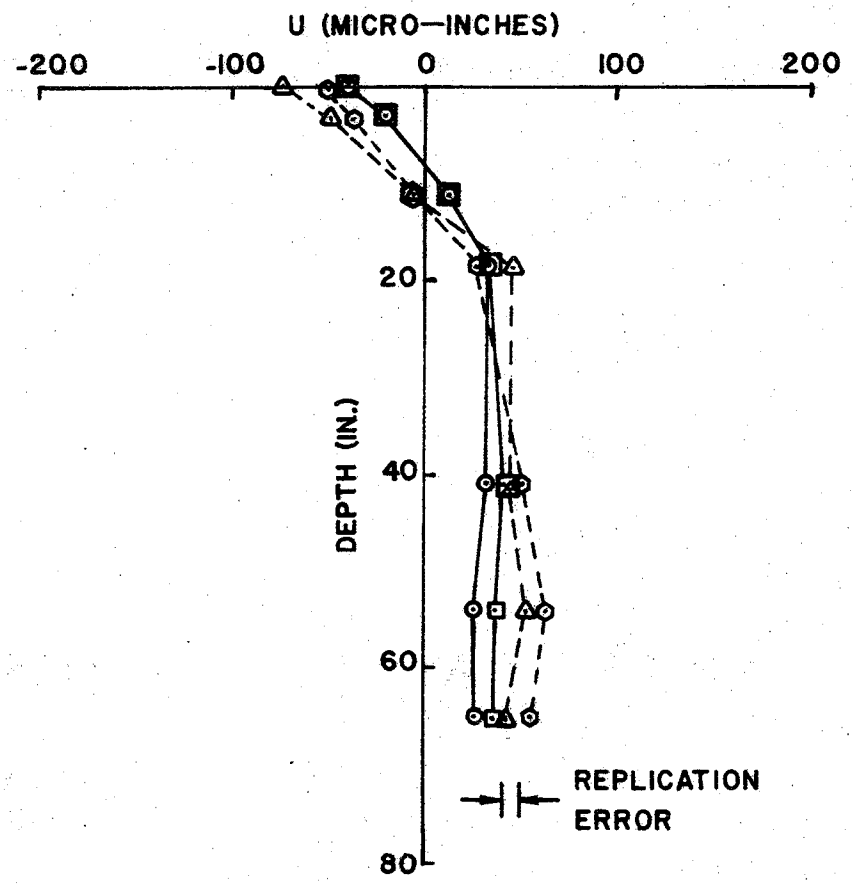

Figure 22: Observed and computed values of u, Section 27 plotted versus depth.

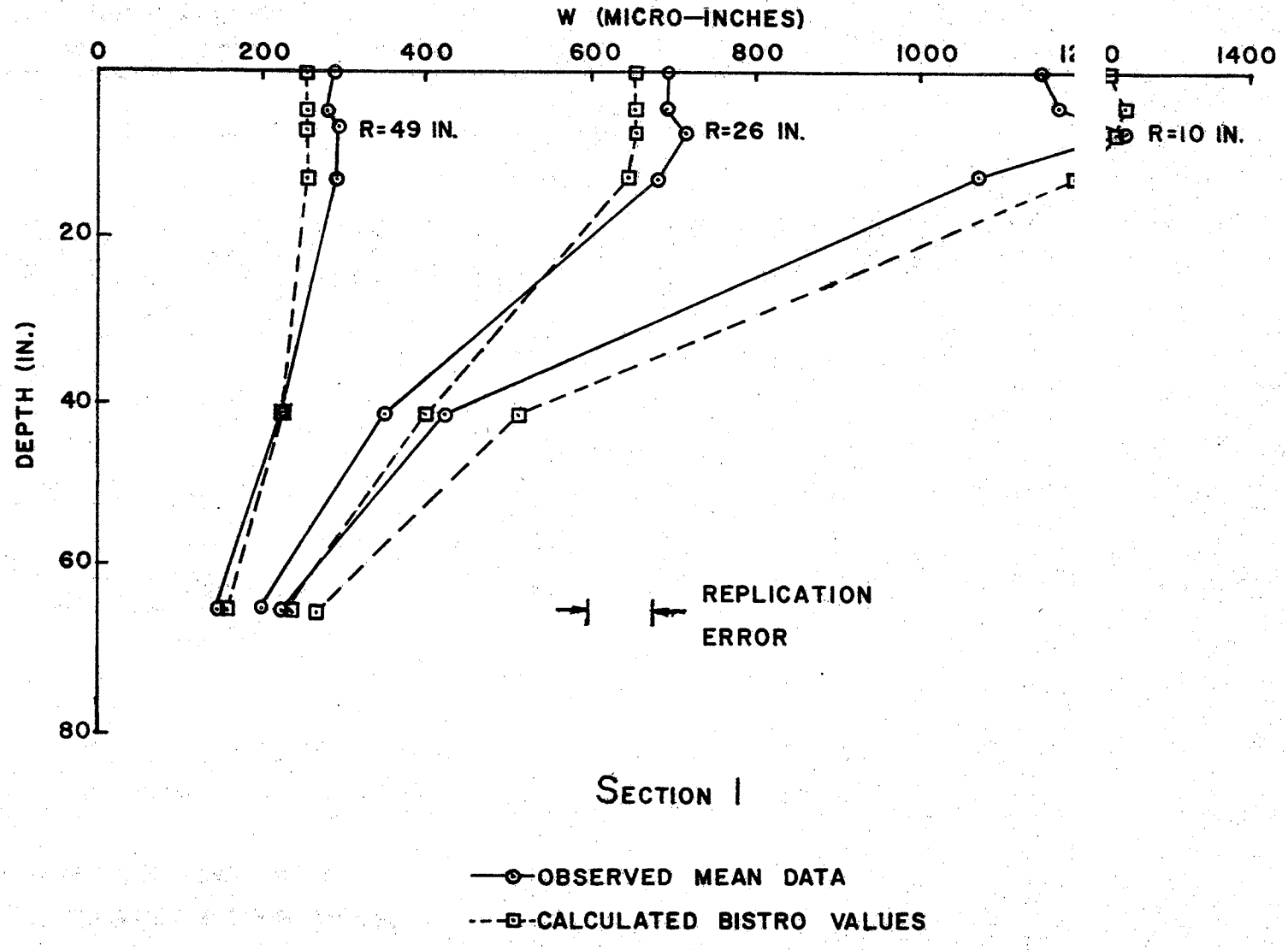

Figure 23: Observed and computed values of w, Section 1, plotted versus depth.

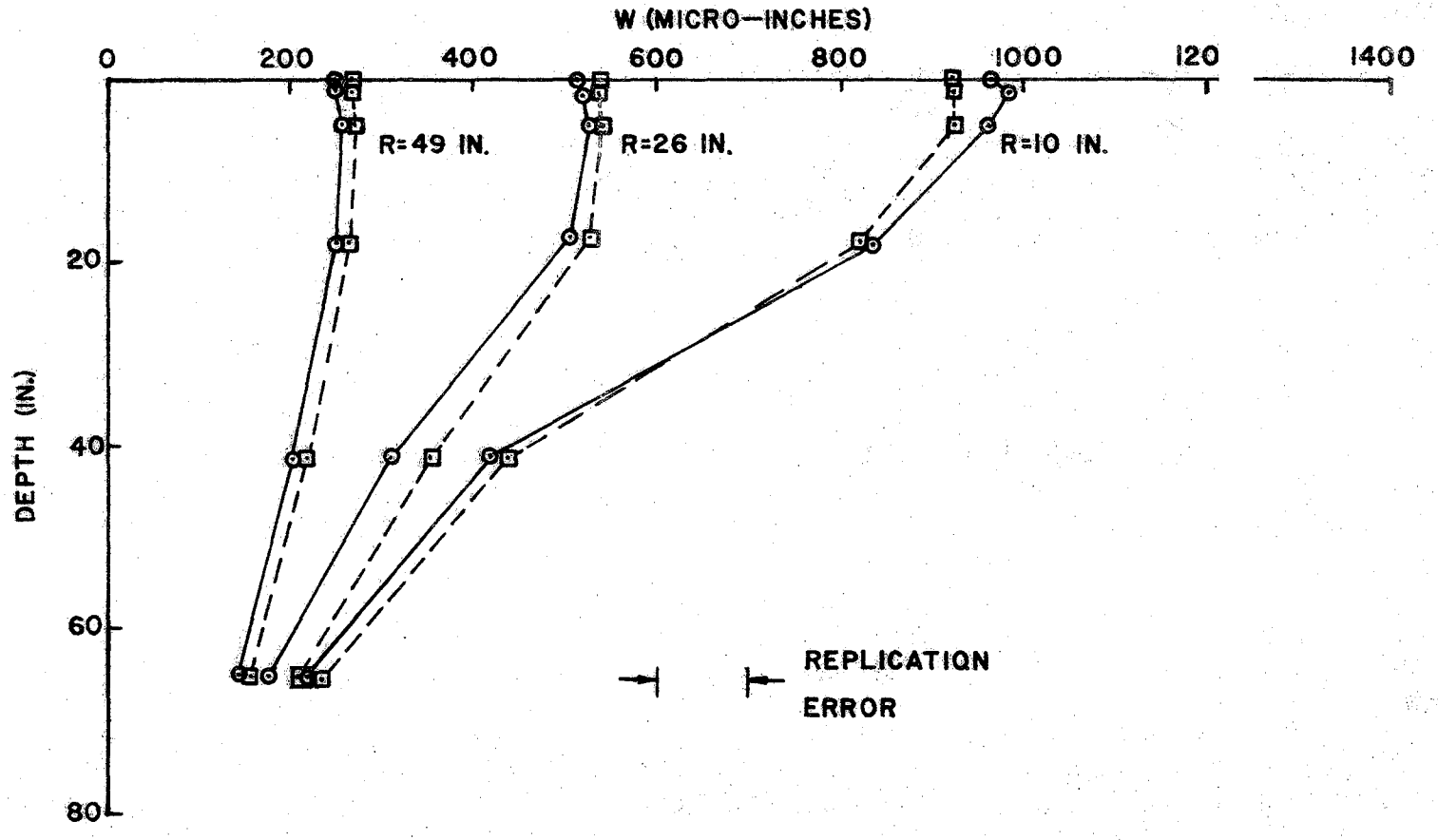

SECTION 3

—⊙—OBSERVED MEAN DATA

---⊡--CALCULATED BISTRO VALUES

Figure 24: Observed and computed values of w, Section 3, plotted versus depth.

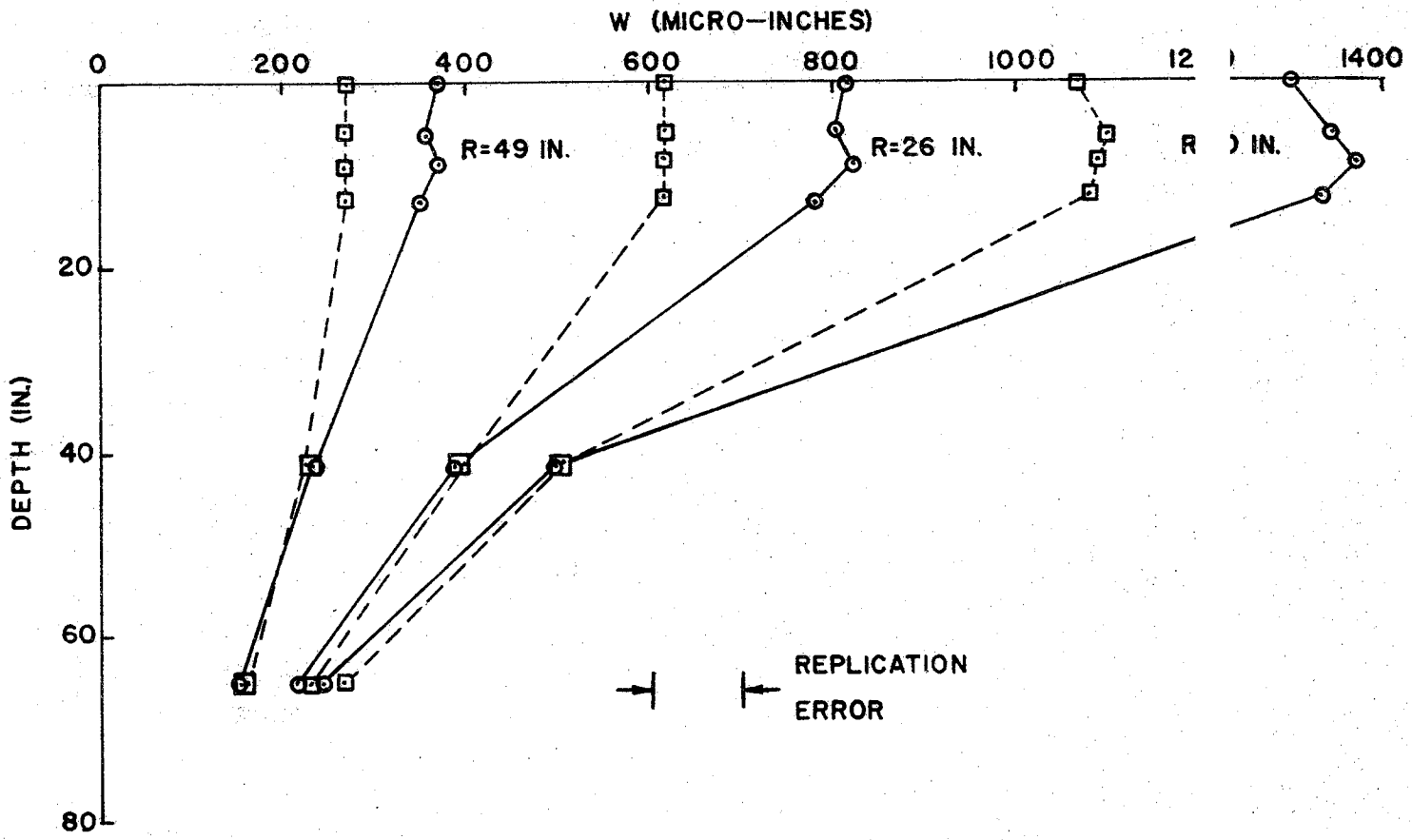

SECTION 5

—o—OBSERVED MEAN DATA

---□--CALCULATED BISTRO VALUES

Figure 25: Observed and computed values of w, Section 5 plotted versus depth.

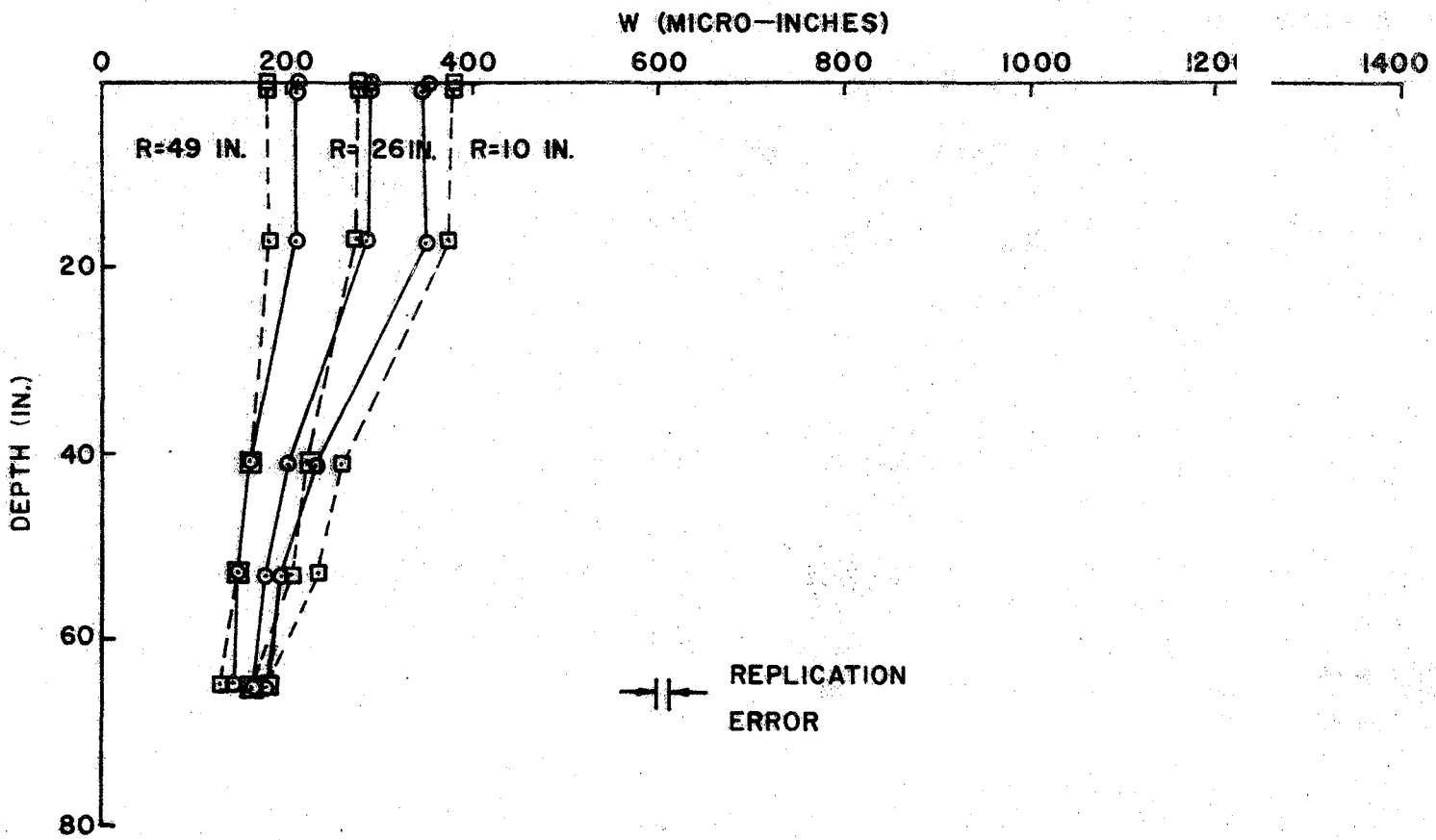

Figure 26: Observed and computed values of w, Section 14, plotted versus depth.

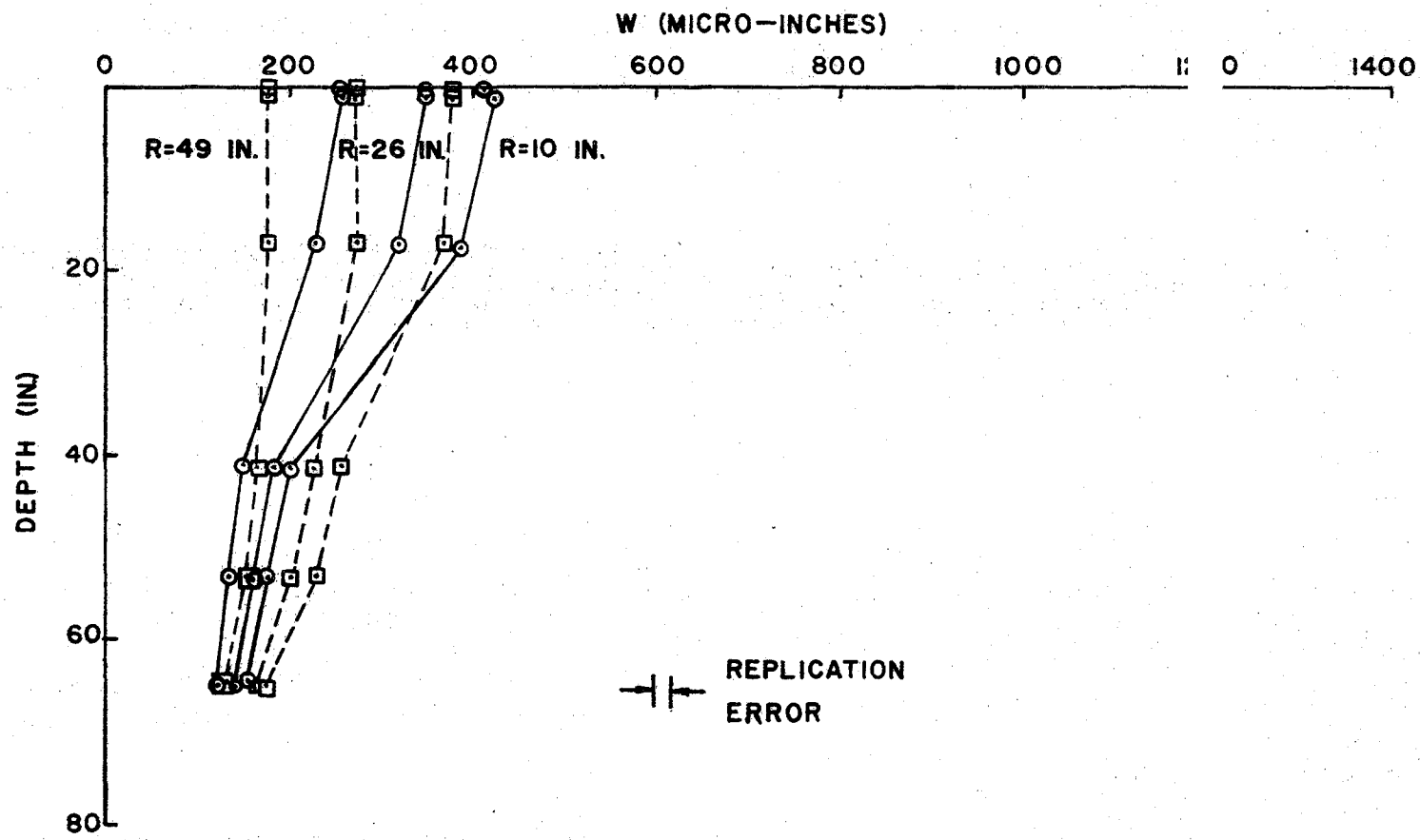

Figure 27: Observed and computed values of w, Section 1
plotted versus depth.

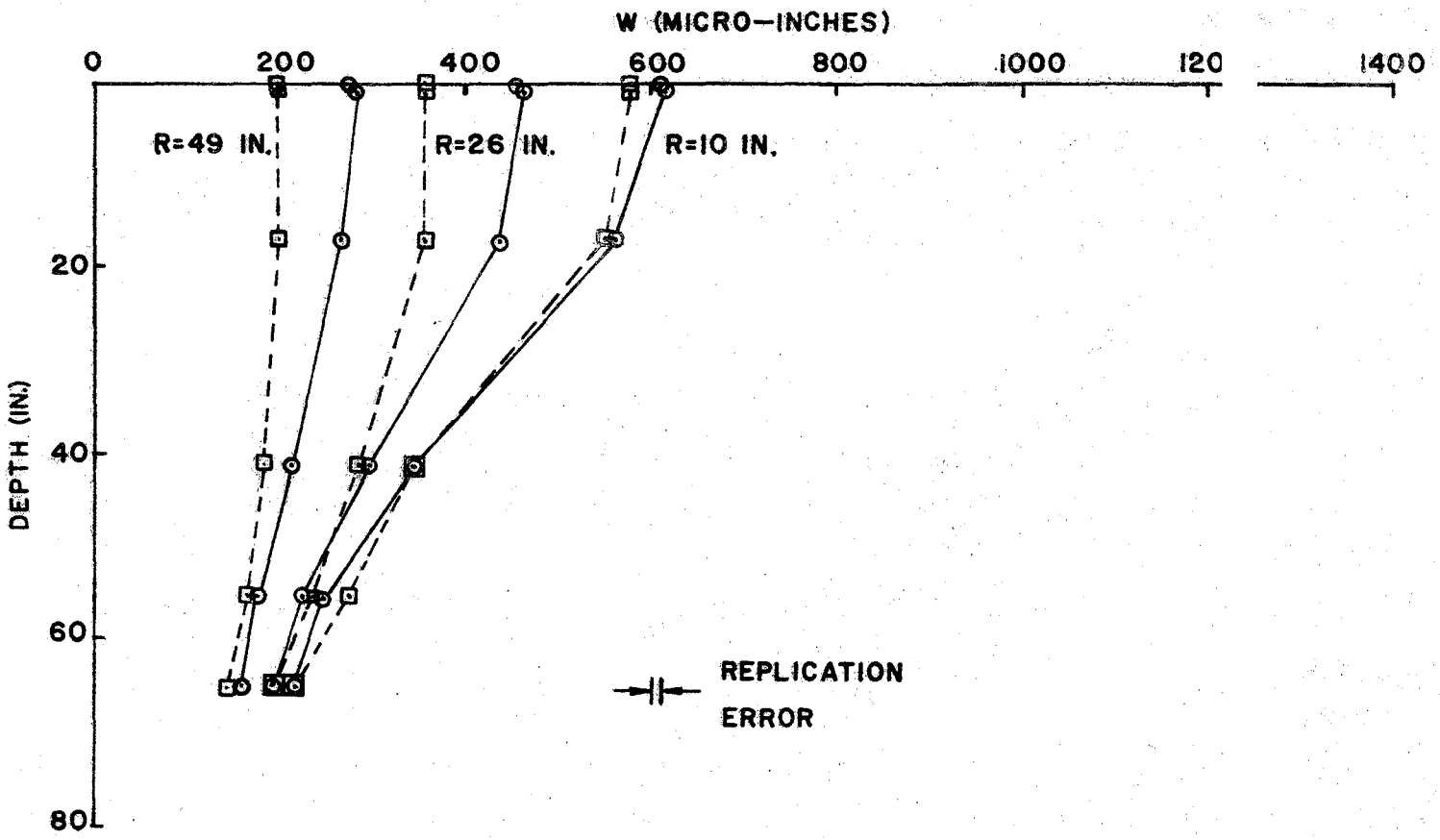

SECTION 18

—⊙—OBSERVED MEAN DATA

---⊡--CALCULATED BISTRO VALUES

Figure 28: Observed and computed values of w, Section 18, plotted versus depth.

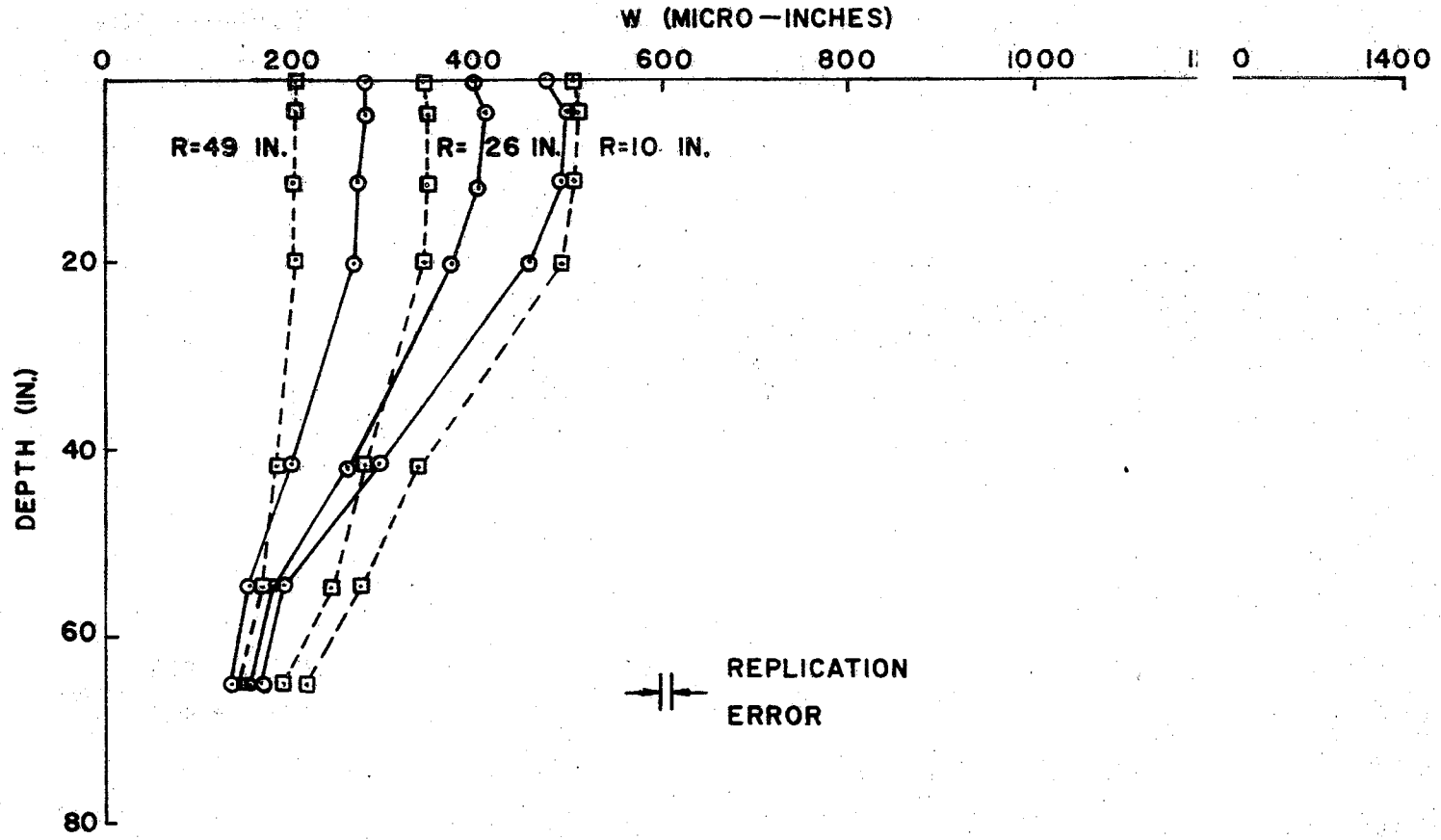

Figure 29: Observed and computed values of w, Section 27, plotted versus depth.

6. FINDINGS AND RECOMMENDATIONS

Findings

The first five findings listed below are based on previously published data, and pertain to the suitability of linear elasticity as a model of the displacement vector in the special case of flexible pavements and their foundations. Findings 6 through 8, stemming from a special study of environmental effects observed at the TTI Pavement Test Facility, are not directly concerned with linear elasticity, but rather with some of the principles of soil mechanisms, a closely allied subject. Finding No. 9, last in the list, is directly addressed to the specific objective of this research.

1. Previously published data from full-scale tests on flexible pavements indicate that the Dynaflect 1000-lb., 8 Hz, sinusoidal load produced a surface deflection of about 45% of the deflection caused by a static load of 1000 lbs., or the same deflection as a dual-wheel load of 1000 lbs. dead weight moving at high speed (roughly 50-60 mph).

2. Finding 1 carries the inference that either the materials supporting the load possessed visco-elastic properties, or the effect on deflections of the inertia of these materials was greater than has usually been assumed.

3. Opinion among a number of pavement researchers leans toward the use of non-linear constitutive equations, derived from laboratory test results, to describe the behavior of flexible pavements under load, thus ruling out the use of linear elasticity for this purpose by these researchers.

4. Results of load-deflection tests made on flexible pavements at the AASHO Road Test a few weeks after construction, but before the first freeze of the winter season, indicated that the load supporting materials behaved, on the average, in a manner in agreement with the assumptions of linear elasticity. Variations from the average behavior were no greater than variations

in the behavior of sections of identical designs located in different traffic loops.

5. Results of load-deflection tests made on flexible pavements at the AASHO Road Test indicated that shortly after a severe freeze-thaw cycle, the supporting materials behaved in a manner consistently contrary to the assumptions of linear elasticity.

6. Free water trapped in the sandy gravel and sandy clay embankments of the TTI Pavement Test Facility shortly after its construction in 1965 caused swelling of the plastic clay embankment, increasing the surface elevation along the center-line of that embankment by an average of 1.7 inches (as of May, 1974), and causing longitudinal cracking in the overlying materials. There was little evidence of volume change in the sandy clay and sandy gravel embankments.

7. Lateral swelling of the plastic clay embankment contributed to the formation and wide opening of the longitudinal cracks in the overlying materials.

8. Surface deflections measured in 1966 on sections supported by the plastic clay and sandy clay embankments were significantly greater than those measured on the same sections in 1972 after drainage of the facility. For sections on the sandy gravel embankment, the 1966 and 1972 surface deflections were not significantly different.

9. Linear elasticity was found to be an acceptable model for the vertical and horizontal components of the displacement vector measured in 1972 within the body of seven selected sections, inasmuch as the combined prediction error in each component was about the same size as the corresponding combined replication error for the seven sections. (This finding is limited to displacements occurring at points in a vertical rectangular plane, $0 \leq r \leq 49$ in. and

$0 \leq z \leq 65$ in., with a vertical load applied to the surface of the pavement at the point $r = z = 0$. For an example of this limitation, see Figure 5.)

Recommendations

1. Observation of the longitudinal cracking that occurred in sections supported by the plastic clay embankment at the TTI Pavement Test Facility suggests that lateral expansion of the embankment may have been a major contributing cause of the cracking. It is recommended that a small research study,involving interviews with THD District personnel, be initiated to determine if there is an association between longitudinal cracking and embankments constructed of swelling clays. If such an association were found to exist, the mechanism involved probably could be clarified by a theoretical study involving the use of an existing finite element computer program. If the mechanism were thoroughly understood, it could likely be introduced into the THD Flexible Pavement System as a predictor of this type of cracking.

If, on the other hand, no association between swelling clay embankments and longitudinal cracking were found in the field, the research could be dropped, with little lost, since the field interviews could be conducted quickly and at small expense.

2. If linear elasticity is actually to be used in the structural subsystem of the THD Flexible Pavement Design System (FPS), two of the major tasks yet to be accomplished are the following: first, a much faster computational procedure must be made available for finding the in situ moduli of typical materials in existing multi-layer pavements from displacement data of the type measured in Study 136; and second, a much faster computational procedure must be made available for use in finding stresses, strains, and displacements at selected points in multi-layer, trial designs in FPS. Both tasks

could be accomplished simultaneously if an extensive table of stresses, strains and displacements for multilayer systems could be computed by a program like BISTRO, and stored for future use in conjunction with two auxiliary computer programs. One of the auxiliary programs would combine a reliable interpolation scheme with an efficient search routine for seeking out moduli consistent with given values of measured displacements and layer thicknesses. The other auxiliary program would combine an interpolation scheme with a search routine for seeking out stresses, strains and displacements consistent with given values of moduli and layer thicknesses.

The building of the table would require much computer time, but once stored, the values would be available for use in all future design problems involving flexible pavements in Texas. The creation of the auxiliary programs should present no great problem, since a start has already been made (12).

It is therefore recommended that a small, relatively inexpensive study be made to determine the scope, cost and general feasibility of producing the basic table and writing the necessary auxiliary programs suggested above. Based on the results of such a study, a rational decision could be made as to whether the work should be undertaken.

REFERENCES

1. F. H. Scrivner, Rudell Peohl, W. M. Moore, and M. B. Phillips, Detecting Seasonal Changes In Load-Carrying Capabilities of Flexible Pavements, NCHRP Report 76, Highway Research Board, Washington, D. C., 1969.

2. The AASHO Road Test - Pavement Research - Report 5, Highway Research Board Special Report 61E, Washington, D. C., 1962.

3. F. H. Scrivner and William M. Moore, An Analysis of Dynamic Displacements Measured Within Pavement Structures, Research Report No. 136-6F, Texas Transportation Institute, 1973.

4. William M. Moore and Gilbert Swift, A Technique for Measuring The Displacement Vector Throughout The Body of a Pavement Structure Subjected to Cyclic Loading, Research Report 136-2, 1971.

5. W. A. Dunlap, A Report on a Mathematical Model Describing the Deformation Characteristics of Granular Materials, Technical Report No. 1, Project 2-8-62-27, Texas Transportation Institute, 1963.

6. W. R. Barker, W. N. Brabston and F. C. Townsend, An Investigation of the Structural Properties of Stabilized Layers in Flexible Pavement Systems, Technical Report No. AFWL-TR-73-21, U. S. Army Engineer Waterways Experiment Station, Vicksburg, Miss., 1973.

7. R. G. Ahlvin, Y. T. Chou and R. L. Hutchinson, The Principle of Superposition in Pavement Analysis, Highway Research Record No. 466, Highway Research Board, Washington, D. C., 1973, pp. 153-162.

8. L. R. Lamotte and R. R. Hocking, Computational Efficiency in the Selection of Regression Variables, Technometrics, Vol. 12, No. 1, Feb. 1970, pp. 83-93.

9. F. H. Scrivner and W. M. Moore, Evaluation of the Stiffness of Individual Layers in a Specially Designed Pavement Facility From Surface Deflections, Research Report 32-8, Texas Transportation Institute, 1966.

10. R. L. Lytton and C. E. Schlieker, Drainage of the TTI Pavement Test Facility, an informal report made to the Texas Highway Department, Texas Transportation Institute, 1972.

11. Frank H. Scrivner, Chester H. Michalak, and William M. Moore, Calculation of the Elastic Moduli of a Two-Layer Pavement System from Measured Surface Deflections, Highway Research Record No. 431, Highway Research Board, Washington, D. C., 1973, p. 18, Table 2; and p. 20.

12. Danny Y. Lu, Chia Shun Shih and Frank H. Scrivner, The Optimization of a Flexible Pavement System Using Linear Elasticity, Research Report 123-17, Texas Highway Department, Center for Highway Research, and Texas Transportation Institute, March 1973, pp. 16-26.

APPENDIX

Table 23 (Basic measured data, Replications A and B).

Table 24 (Mean observed data and BISTRO-computed values).

TABLE 23: BASIC MEASURED DATA, REPLICATIONS A AND B (MICRO- CHES)

Section 1

Displ. Symbol	Replication A (2-28-72) Depth (in.)	Radial Distance (in.) 10.0	26.0	49.0
u	0.0	*	-163	-91
	4.5	*	-36	-21
	8.0	*	45	7
	12.0	*	136	73
	41.0	*	66	85
	65.0	*	37	61
w	0.0	1219	775	359
	4.5	1219	806	359
	8.0	1281	822	369
	12.0	1188	834	387
	41.0	469	394	266
	65.0	256	216	164

Displ. Symbol	Replicatio 3 (8-9-72) Depth (in.)	Radi Distance (in.) 10.0	26.0	49.0
u	0.0	*	-217	-74
	4.1	*	-43	-13
	7.0	*	45	19
	13.0	*	210	87
	41.0	*	105	96
	65.0	*	44	55
w	0.0	1081	613	213
	4.1	1113	581	202
	7.0	1218	605	218
	13.0	952	532	192
	41.0	381	310	177
	65.0	197	190	141

DRILLING LOG DATA

Layer No.	Material	Replication A Depth (in.) From	To	Layer Thickness Measured	Design	Repl Depth (in.) From	To	ation B ayer Thickness easured	Design
1	Asphaltic Concrete	0.0	4.6	4.6	5.0	0.0	4.1	4.1	5.0
2	Limestone + Cement	4.6	8.0	3.4	4.0	4.1	7.0	2.9	4.0
3	Limestone	8.0	12.0	4.0	4.0	7.0	13.0	6.0	4.0
4	Plastic Clay (EMB)	12.0	53.0	41.0	40.0	13.0	56.0	43.0	40.0
5	Plastic Clay (FOUND)	53.0	69.0	16.0		56.0	74.0	18.0	

*Not Measureable

TABLE 23 (CONTINUED)

Section 3

Displ. Symbol	Depth (in.)	Replication A (3-9-72) Radial Distance (in.) 10.0	26.0	49.0
u	0.0	*	-46	-24
	1.0	*	-44	-30
	5.0	*	-9	-15
	17.0	*	178	89
	41.0	*	81	81
	65.0	*	38	53
w	0.0	1162	594	277
	1.0	1162	600	277
	5.0	1141	603	291
	17.0	1016	584	287
	41.0	469	353	228
	65.0	237	192	155

Displ. Symbol	Depth (in.)	Replication (8-11-72) Radia 10.0	Distance (in.) 26.0	49.0
u	0.0	*	-66	-27
	1.2	*	-10	-4
	5.0	*	23	11
	18.0	*	149	91
	41.0	*	83	83
	65.0	*	43	56
w	0.0	758	429	215
	1.2	806	435	211
	5.0	782	448	221
	18.0	661	423	213
	41.0	355	277	177
	65.0	190	166	129

DRILLING LOG DATA

Layer No.	Material	Replication A Depth (in.) From	To	Layer Thickness Measured	Design	Repli Depth (in.) From	To	tion B yer Thickness asured	Design
1	Asphaltic Concrete	0.0	1.0	1.0	1.0	0.0	1.2	1.2	1.0
2	Limestone + Cement	1.0	5.0	4.0	4.0	1.2	5.0	3.8	4.0
3	Limestone	5.0	17.0	12.0	12.0	5.0	18.0	13.0	12.0
4	Plastic Clay (EMB)	17.0	53.0	36.0	36.0	18.0	54.0	36.0	36.0
5	Plastic Clay (FOUND)	53.0	70.0	17.0		54.0	73.0	19.0	

* Not Measurable

TABLE 23 (CONTINUED)

Section 5

Displ. Symbol	Depth (in.)	Replication A (11-30-71) Radial Distance (in.) 10.0	26.0	49.0	Displ. Symbol	Depth (in.)	Replicatic B (8-9-72) Radi 10.C	Distance (in.) 26.0	49.0
u	0.0	*	-102	-72	u	0.0	*	-208	-109
	5.5	*	12	-4		5.5	*	-38	-31
	8.5	*	27	21		9.0	*	22	11
	12.0	*	83	53		13.0	*	130	51
	41.0	*	68	80		41.0	*	107	99
	65.0	*	44	61		65.0	*	49	62
w	0.0	1391	953	462	w	0.0	121C	677	276
	5.5	1453	969	456		5.5	1234	645	256
	8.5	1453	984	478		9.0	129E	661	263
	12.0	1406	925	453		13.0	126E	645	245
	41.0	525	434	287		41.0	471	348	187
	65.0	269	248	183		65.0	21E	187	133

DRILLING LOG DATA

Layer No.	Material	Replication A Depth (in.) From	To	Layer Thickness Measured	Design	Repl Depth (in.) From	To	ation B ayer Thickness leasured	Design
1	Asphaltic Concrete	0.0	5.5	5.5	5.0	0.0	5.5	5.5	5.0
2	Limestone	5.5	8.5	3.0	4.0	5.5	9.0	3.5	4.0
3	Limestone + Cement	8.5	12.0	3.5	4.0	9.0	13.0	4.0	4.0
4	Plastic Clay (EMB.)	12.0	55.0	43.0	40.0	13.0	58.0	45.0	40.0
5	Plastic Clay (FOUND)	55.0	70.0	15.0		58.0	74.0	16.0	

*Not Measureable

TABLE 23 (CONTINUED)

Section 14

Displ. Symbol	Depth (in.)	Replication A (3-21-72) Radial Distance (in.) 10.0	26.0	49.0	Displ. Symbol	Depth (in.)	Replication (8-21-72) Radial 10.0	istance (in.) 26.0	49.0
u	0.0	*	-29	-31	u	0.0	*	-14	-15
	1.1	*	-21	-22		0.7	*	-13	-13
	17.0	*	27	23		17.0	*	41	36
	41.0	*	13	18		41.0	*	21	25
	53.0	*	18	28		52.5	*	25	30
	65.0	*	16	27		65.0	*	19	27
w	0.0	328	278	206	w	0.0	374	311	221
	1.1	334	278	206		0.7	358	303	211
	17.0	319	272	202		17.0	381	306	223
	41.0	219	195	159		41.0	239	211	168
	53.0	197	180	152		52.5	198	182	154
	65.0	175	158	139		65.0	176	165	152

DRILLING LOG DATA

Layer No.	Material	Replication A Depth (in.) From	To	Layer Thickness Measured	Design	Repli Depth (in.) From	To	tion B yer Thickness asured	Design
1	Asphaltic Concrete	0.0	1.1	1.1	1.0	0.0	0.7	0.7	1.0
2	Limestone + Cement	1.1	17.0	15.9	16.0	0.7	17.0	16.3	16.0
3	Sandy Gravel	17.0	53.0	36.0	36.0	17.0	52.5	35.5	36.0
4	Plastic Clay (FOUND)	53.0	69.0	16.0		52.5	76.5	24.0	

*Not Measureable

TABLE 23 (CONTINUED)

Section 15

Displ. Symbol	Depth (in.)	Replication A (3-17-72) Radial Distance (in.) 10.0	26.0	49.0
u	0.0	*	-37	-36
	1.0	*	-22	-24
	17.0	*	18	20
	41.0	*	11	11
	53.5	*	11	14
	65.0	*	11	16
w	0.0	425	366	278
	1.0	431	369	281
	17.0	387	319	236
	41.0	164	150	123
	53.5	147	127	114
	65.0	133	116	103

Displ. Symbol	Depth (in.)	Replicatic B (8-21-72) Radia Distance (in.) 10.0	26.0	49.0
u	0.0	*	-12	-15
	0.8	*	-8	-12
	17.0	*	34	29
	41.0	*	16	21
	53.0	*	19	26
	65.0	*	22	32
w	0.0	398	329	235
	0.8	418	331	239
	17.0	390	323	229
	41.0	239	221	179
	53.0	210	194	161
	65.0	179	168	147

DRILLING LOG DATA

Layer No.	Material	Replication A Depth (in.) From	To	Layer Thickness Measured	Design	Repli Depth (in.) From	To	tion B ayer Thickness leasured	Design
1	Asphaltic Concrete	0.0	1.0	1.0	1.0	0.0	0.8	0.8	1.0
2	Limestone + Cement	1.0	17.0	16.0	16.0	0.8	17.0	16.2	16.0
3	Sandy Gravel	17.0	53.5	36.5	36.0	17.0	53.0	36.0	36.0
4	Plastic Clay (FOUND)	53.5	70.0	16.5		53.0	70.0	17.0	

*Not Measureable

TABLE 23 (CONTINUED)

Section 18

Displ. Symbol	Depth (in.)	Replication A (2-9-72) Radial Distance (in.) 10.0	26.0	49.0
u	0.0	*	-83	-53
	1.0	*	-58	-37
	17.0	*	84	36
	41.0	*	43	39
	55.0	*	33	40
	65.0	*	31	39
w	0.0	697	500	279
	1.0	697	506	280
	17.0	650	500	277
	41.0	391	334	225
	55.0	275	256	184
	65.0	239	212	166

Displ. Symbol	Depth (in.)	Replication (6-18-72) Radial 10.0	istance (in.) 26.0	49.0
u	0.0	*	-32	-32
	0.8	*	-11	-16
	17.0	*	49	40
	41.0	*	33	40
	56.0	*	33	40
	65.0	*	30	40
w	0.0	524	411	282
	0.8	532	419	290
	17.0	476	377	261
	41.0	292	261	202
	56.0	213	202	165
	65.0	192	184	152

DRILLING LOG DATA

Layer No.	Material	Replication A Depth (in.) From	To	Layer Thickness Measured	Design	Repli Depth (in.) From	To	tion B yer Thickness asured	Design
1	Asphaltic Concrete	0.0	1.0	1.0	1.0	0.0	0.8	0.8	1.0
2	Limestone + Lime	1.0	17.0	16.0	16.0	0.8	17.0	16.2	16.0
3	Sandy Clay	17.0	55.0	38.0	36.0	17.0	56.0	39.0	36.0
4	Plastic Clay (FOUND)	55.0	70.0	15.0		56.0	67.0	11.0	

*Not Measureable

TABLE 23 (CONTINUED)

Section 27

Displ. Symbol	Depth (in.)	Replication A (1-13-72) Radial Distance (in.) 10.0	26.0	49.0	Displ. Symbol	Depth (in.)	Replicatic B (7-12-72) Radia Distance (in.) 10.0	26.0	49.0
u	0.0	*	-39	-43	u	0.0	*	-43	-38
	3.3	*	-29	-29		3.3	*	-17	-17
	11.0	*	4	6		11.0	*	22	16
	18.0	*	16	21		19.0	*	50	44
	41.0	*	24	37		41.0	*	42	51
	55.0	*	20	34		53.5	*	31	42
	65.0	*	22	31		65.0	*	30	41
w	0.0	462	381	286	w	0.0	484	416	276
	3.3	475	397	281		3.3	524	421	279
	11.0	491	387	266		11.0	492	427	279
	18.0	459	369	272		19.0	458	387	265
	41.0	281	256	198		41.0	313	277	206
	55.0	189	178	156		53.5	198	190	156
	65.0	162	153	137		65.0	179	166	144

DRILLING LOG DATA

Layer No.	Material	Replication A Depth (in.) From	To	Layer Thickness Measured	Design	Repl Depth (in.) From	To	ation B ayer Thickness easured	Design
1	Aspahltic Concrete	0.0	3.3	3.3	3.0	0.0	3.3	3.3	3.0
2	Limestone + Lime	3.3	11.0	7.7	8.0	3.3	11.0	7.7	8.0
3	Limestone + Cement	11.0	18.0	7.0	8.0	11.0	19.0	8.0	8.0
4	Sandy Clay	18.0	55.0	37.0	34.0	19.0	53.5	34.5	34.0
5	Plastic Clay (FOUND)	55.0	69.0	14.0		53.5	70.0	16.5	

* Not Measurable

TABLE 24: MEAN OBSERVED DATA AND BISTRO-COMPUTED VALUES (MICRO-INCHES), FOR A SINGLE 1000 lb LOAD

Section 1

Displ. Symbol	Depth (in.)	Mean Observed Data: Radial Distance (in.) 10.0	26.0	49.0	Depth (in.)	Calculated Bistro Values: Radial Distance (in.) 10.0	26.0	49.0
u	0.0	*	-189	-82	0.0	*	-147	-61
	4.3	*	-39	-16	4.3	*	-39	-18
	7.5	*	44	12	7.5	*	44	15
	12.5	*	172	79	12.5	*	154	63
	41.0	*	85	90	41.0	*	113	110
	65.0	*	40	57	65.0	*	64	79
w	0.0	1149	693	285	0.0	1230	650	254
	4.3	1165	693	280	4.3	1250	651	253
	7.5	1249	713	293	7.5	1240	651	253
	12.5	1069	682	289	12.5	1190	644	254
	41.0	424	351	221	41.0	517	401	223
	65.0	226	202	152	65.0	267	231	160

Replication Error		Prediction Error	
u-Data	w-Data	u-Data	w-Data
15	78	20	57

* Not Measurable

TABLE 24 (CONTINUED)

Section 3

Displ. Symbol	Depth (in.)	Mean Observed Data: Radial Distance (in.) 10.0	26.0	49.0
u	0.0	*	-55	-25
	1.1	*	-26	-16
	5.0	*	6	-1
	17.5	*	163	89
	41.0	*	81	81
	65.0	*	40	54
w	0.0	959	511	245
	1.1	983	517	243
	5.0	961	525	255
	17.5	838	503	249
	41.0	411	314	202
	65.0	213	178	141

Displ. Symbol	Depth (in.)	Calculated Isotro Values: Radial Distance (in.) 10.0	26.0	49.0
u	0.0	*	-72	-42
	1.1	*	-54	-34
	5.0	*	7	-2
	17.5	*	137	84
	41.0	*	88	94
	65.0	*	51	66
w	0.0	919	536	265
	1.1	922	537	265
	5.0	923	538	265
	17.5	822	523	263
	41.0	431	350	218
	65.0	234	208	154

Replication Error	
u-Data	w-Data
10	98

Prediction Error	
u-Data	w-Data
15	27

* Not Measurable

TABLE 24 (CONTINUED)

Section 5

Displ. Symbol	Depth (in.)	Mean Observed Data: Radial Distance (in.) 10.0	26.0	49.0	Calculated stro Values: Rad 10.(	Distance (in.) 26.0	49.0
u	0.0	*	-154	-90	*	-148	-78
	5.5	*	-13	-17	*	-41	-25
	8.8	*	24	15	*	6	5
	12.5	*	106	51	*	84	40
	41.0	*	87	89	*	103	102
	65.0	*	46	61	*	61	76
w	0.0	1300	814	368	107(	614	268
	5.5	1343	806	355	110(	618	267
	8.8	1375	822	370	109(	616	266
	12.5	1335	784	348	108(	614	266
	41.0	497	390	236	50(	395	224
	65.0	242	217	157	26!	230	160

Replication Error u-Data	w-Data	Predi(on Error u-Dat:	w-Data
20	97	16	157

* Not Measurable

TABLE 24 (CONTINUED)

Section 14

Displ. Symbol	Depth (in.)	Mean Observed Data: Radial Distance (in.) 10.0	26.0	49.0	Displ. Symbol	Depth (in.)	Calculated Radi 10.0	stro Values Distance (in.) 26.0	49.0
u	0.0	*	-21	-22	u	0.0	*	-41	-31
	0.9	*	-16	-17		0.9	*	-36	-28
	17.0	*	33	29		17.0	*	33	20
	41.0	*	16	21		41.0	*	30	35
	52.8	*	21	28		52.8	*	39	49
	65.0	*	17	26		65.0	*	30	41
w	0.0	350	294	213	w	0.0	379	274	179
	0.9	345	290	208		0.9	380	274	179
	17.0	349	288	212		17.0	371	274	180
	41.0	228	202	163		41.0	259	225	164
	52.8	197	180	152		52.8	231	205	154
	65.0	175	161	145		65.0	177	162	130

Replication Error		Predic on Error	
u-Data	w-Data	u-Data	w-Data
5	12	15	23

* Not Measurable

TABLE 24 (CONTINUED)

Section 15

Displ. Symbol	Depth (in.)	Mean Observed DAta: Radial Distance (in.) 10.0	26.0	49.0	Calculated Rad 10.(	Istro Values Distance (in.) 26.0	49.0
u	0.0	*	-24	-25	*	-41	-31
	0.9	*	-14	-17	*	-36	-28
	17.0	*	25	24	*	33	20
	41.0	*	13	15	*	29	35
	53.3	*	14	19	*	39	48
	65.0	*	16	23	*	30	41
w	0.0	411	347	256	378	272	178
	0.9	424	349	259	379	273	178
	17.0	388	320	232	376	272	179
	41.0	201	185	150	258	224	163
	53.3	178	160	137	228	202	153
	65.0	155	141	124	177	162	130

Replication Error		Predic on Error	
u-Data	w-Data	u-Data	w-Data
7	23	17	49

* Not Measurable

TABLE 24 (CONTINUED)

Section 18

Displ. Symbol	Depth (in.)	Mean Observed Data: Radial Distance (in.) 10.0	26.0	49.0
u	0.0	*	-57	-42
	0.9	*	-34	-26
	17.0	*	66	37
	41.0	*	37	39
	55.5	*	31	39
	65.0	*	30	39
w	0.0	610	455	280
	0.9	614	462	284
	17.0	562	438	268
	41.0	341	297	213
	55.5	243	228	174
	65.0	215	197	158

Displ. Symbol	Depth (in.)	Calculated Radi 10.0	stro Values Distance (in.) 26.0	49.0
u	0.0	*	-73	-46
	0.9	*	-64	-41
	17.0	*	61	31
	41.0	*	49	52
	55.5	*	55	65
	65.0	*	44	56
w	0.0	576	358	199
	0.9	578	358	199
	17.0	551	357	199
	41.0	345	284	185
	55.5	276	238	167
	65.0	218	194	145

Replication Error u-Data	w-Data	Predic u-Data	on Error w-Data
12	45	17	45

* Not Measurable

TABLE 24 (CONTINUED)

Section 27

Displ. Symbol	Depth (in.)	Mean Observed Data: Radial Distance (in.) 10.0	26.0	49.0	Calculated Distro Values: Radial Distance (in.) 10.	26.0	49.0
u	0.0	*	-40	-40	*	-73	-53
	3.3	*	-22	-22	*	-50	-38
	11.0	*	12	10	*	-7	-6
	18.5	*	32	32	*	45	27
	41.0	*	32	43	*	45	49
	54.3	*	25	37	*	52	63
	65.0	*	25	35	*	41	54
w	0.0	472	398	280	50	342	204
	3.3	499	408	279	50	344	204
	11.0	491	406	272	50	346	204
	18.5	458	377	268	49	344	204
	41.0	296	266	201	33	280	187
	54.3	193	183	155	27	240	170
	65.0	170	159	140	21	192	145

Replication Error		Predi ion Error	
u-Data	w-Data	u-Dat	w-Data
8	10	18	49

* Not Measurable